

*SUPPORTING INFORMATION FOR*

**Optimization and Characterization of the Antimalarial Activity of *N*-Aryl Acetamides that are Susceptible to Mutations in ROM8 and CSC1**

William Nguyen,<sup>a,b</sup> Coralie Boulet,<sup>c</sup> Madeline G. Dans,<sup>a,b</sup> Katie Loi,<sup>a</sup> Kate E. Jarman,<sup>a,b</sup> Claudia B.G. Barnes,<sup>c</sup> Tomas Yeo,<sup>d,e</sup> Tanaya Sheth,<sup>d,e</sup> Partha Mukherjee,<sup>g</sup> Arnish Chakraborty,<sup>g</sup> Mufuliat T. Famodimu,<sup>h</sup> Michael J. Delves,<sup>h</sup> Harry Pollard,<sup>h</sup> Colin J. Sutherland,<sup>h</sup> Rachael Coyle,<sup>ij</sup> Nicole Sevilleno,<sup>i</sup> Nonlawat Boonyalai,<sup>j</sup> Marcus C. S. Lee,<sup>ij</sup> Tayla Rabie,<sup>k</sup> Lyn-Marié Birkholtz,<sup>k</sup> Delphine Baud,<sup>l</sup> Stephen Brand,<sup>l</sup> Mrittika Chowdury,<sup>m,n</sup> Tania F. de Koning-Ward,<sup>m,n</sup> David A. Fidock,<sup>d,e,f</sup> Paul R. Gilson,<sup>c</sup> and Brad E. Sleebs.<sup>a,b,\*</sup>

<sup>a</sup> The Walter and Eliza Hall Institute of Medical Research, Parkville 3052, Australia.

<sup>b</sup> Department of Medical Biology, The University of Melbourne, Parkville 3010, Australia.

<sup>c</sup> Burnet Institute, Melbourne, Victoria 3004, Australia.

<sup>d</sup> Department of Microbiology & Immunology, Columbia University Irving Medical Center, New York, NY 10032, USA.

<sup>e</sup> Center for Malaria Therapeutics and Antimicrobial Resistance, Columbia University Irving Medical Center, New York, NY 10032, USA.

<sup>f</sup> Division of Infectious Diseases, Department of Medicine, Columbia University Irving Medical Center, New York, NY 10032, USA.

<sup>g</sup> TCG Lifesciences, Kolkata, West Bengal 700091, India.

<sup>h</sup> Department of Infection Biology, London School of Hygiene and Tropical Medicine, London, WC1E 7HT, UK.

<sup>i</sup> Wellcome Sanger Institute, Wellcome Genome Campus, Hinxton CB10 1SA, United Kingdom.

<sup>j</sup> Biological Chemistry and Drug Discovery, Wellcome Centre for Anti-Infectives Research, University of Dundee, Dundee DD1 4HN, United Kingdom.

<sup>k</sup> Department of Biochemistry, Genetics and Microbiology, Institute for Sustainable Malaria Control, University of Pretoria, Pretoria 0028, South Africa.

<sup>l</sup> Medicines for Malaria Venture, Geneva 1215, Switzerland.

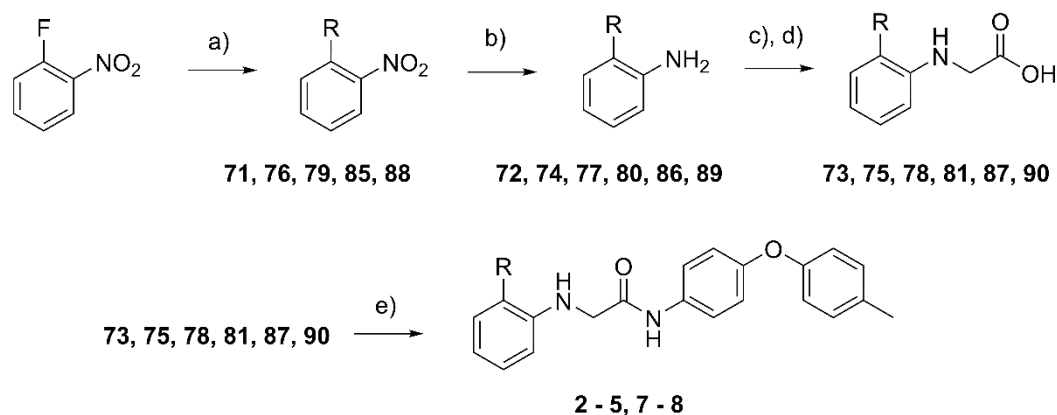
<sup>m</sup> School of Medicine, Deakin University, Waurn Ponds 3216, Australia.

<sup>n</sup> Institute for Mental and Physical Health and Clinical Translation, Deakin University, Geelong 3216, Australia.

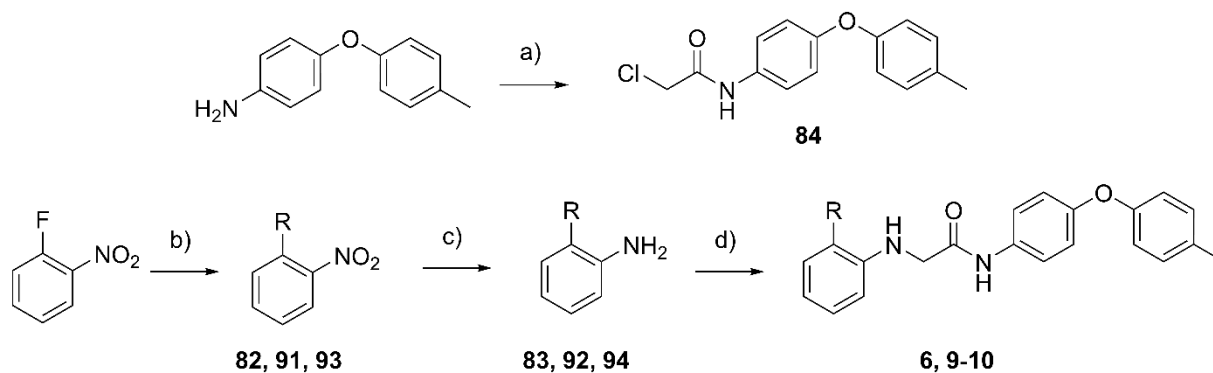
\* Correspondence to: Brad E. Sleebs  
The Walter and Eliza Hall Institute of Medical Research.  
1G Royal Parade, Parkville 3052, Victoria, Australia  
Email: [sleebs@wehi.edu.au](mailto:sleebs@wehi.edu.au)

## INDEX

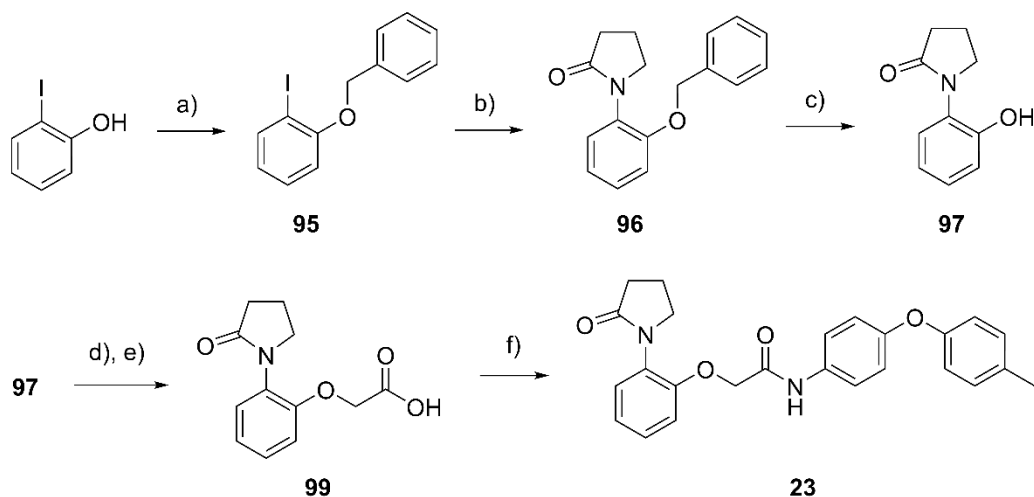
S3	Scheme S1-S11	Synthesis of intermediates and analogs.
S8	Figure S1	Pf LDH dose response curves of selected compounds.
S9	Table S1	Caco-2 analysis.
S10	Table S2	Summary of MIR on analog WEHI-326 ( <b>33</b> ).
S10	Figure S2	IC <sub>50</sub> and IC <sub>90</sub> shifts from MIR study.
S11	Table S3	Whole genome sequencing metrics from MIR study.
S12	Table S4	List of SNPs found by variant caller in samples from MIR study.
S13	Table S5	Homozygous SNPs in samples from MIR study.
S14	Figure S3	AReBar cross-resistance profiling.
S15	Table S6	Parasite barcode population counts from AReBar study.
S16	Figure S4	Mutant CSC1 parasite dose response curves from AReBar study.
S17	Figure S5	MMV020512-resistant parasite activity.
S18	Figure S6	Activity in invasion and egress assay.
S19	Figure S7	<i>P. falciparum</i> NF54 gametocyte assay dose response curves.
S20	Figure S8	Dual gamete formation assay dose response curves.
S21	Figure S9	Standard membrane feeding assay repeat.
S22	Figure S10	<i>P. berghei</i> mouse model.
S23	Figure S11	Mouse plasma exposure for WEHI-326 ( <b>33</b> ).
S23	Table S7	Mouse plasma exposure parameters for WEHI-326 ( <b>33</b> ).
S24	Figure S12	Sequence alignment of <i>P. falciparum</i> 3D7 and <i>P. berghei</i> ANKA ROM8.
S25	Figure S13	Sequence alignment of <i>P. falciparum</i> 3D7 and <i>P. berghei</i> ANKA CSC1.
S26	Figure S14	Hemolysis analysis of WEHI-326 ( <b>33</b> ).
S27		Compound NMR spectra.
S91		HPLC trace of lead compounds



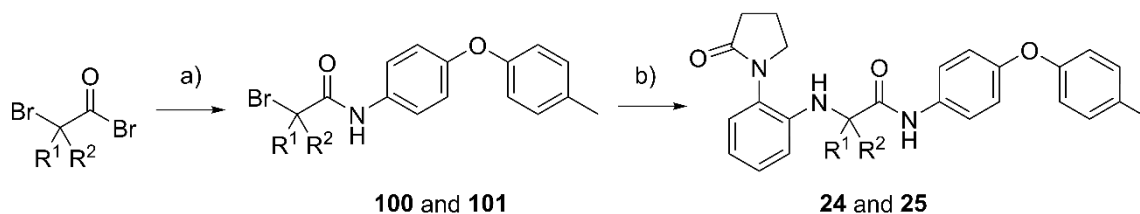
**Scheme S1.** Synthetic route to access *N*-aryl acetamide derivatives **2 - 5, 7 - 8**. *Reagents and conditions:* (a) R = amide, amine or sulfonamide, NaH (or K<sub>2</sub>CO<sub>3</sub>), DMF (or MeCN), heat; (b) Zn, NH<sub>4</sub>Cl, H<sub>2</sub>O/MeOH (1:1), 40 °C; or cat. Pd/C, EtOH, H<sub>2</sub>, 30 °C; (c) ethyl bromoacetate, K<sub>2</sub>CO<sub>3</sub>, MeCN or *tert*-butyl bromoacetate, K<sub>2</sub>CO<sub>3</sub>, MeCN; (d) if ethyl ester, LiOH, EtOH/H<sub>2</sub>O; or if *t*Bu ester, 4M HCl in 1,4-dioxane, 20 °C; (e) HATU, substituted arylamine, DIPEA, DCM, 20 °C. For R groups refer to Table 1.



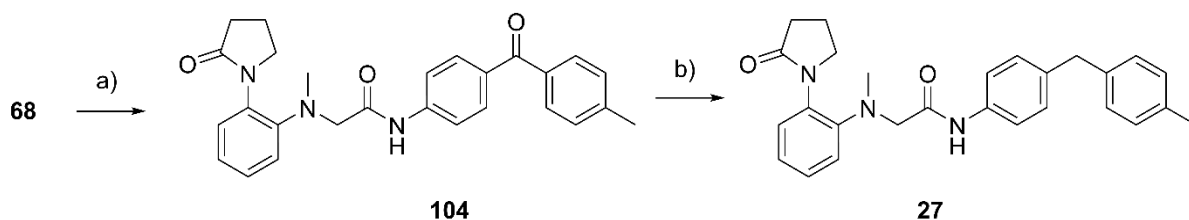
**Scheme S2.** Synthetic route to access *N*-aryl acetamide derivatives **6, 9 - 10**. *Reagents and conditions:* (a) 2-chloroacetyl chloride, DIPEA, 0 °C to 20 °C, DCM; (b) R = amide, amine or sulfonamide, NaH (or K<sub>2</sub>CO<sub>3</sub>), DMF (or MeCN), heat; (c) Zn, NH<sub>4</sub>Cl, H<sub>2</sub>O/MeOH (1:1), 40 °C; or cat. Pd/C, EtOH, H<sub>2</sub>, 30 °C; (d) **84**, KI, DMF, 60 °C. For R groups refer to Table 1.



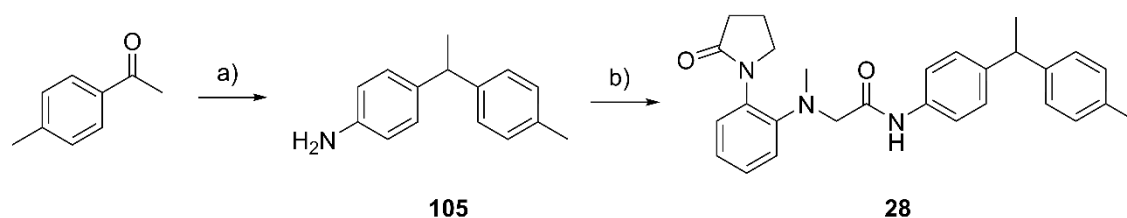
**Scheme S3.** Synthetic route to access **23**. *Reagents and conditions:* (a) bromomethylbenzene,  $\text{K}_2\text{CO}_3$ , acetone,  $56\text{ }^\circ\text{C}$ ; (b) pyrrolidinone, catalytic copper,  $\text{K}_2\text{CO}_3$ ,  $165\text{ }^\circ\text{C}$ ; (c) Pd/C, EtOH,  $\text{H}_2$ ,  $20\text{ }^\circ\text{C}$ ; (d) *tert*-butyl bromoacetate, acetone,  $56\text{ }^\circ\text{C}$ ; (e) 4M HCl in 1,4-dioxane,  $20\text{ }^\circ\text{C}$ ; (f) HATU, 4-(4-methylphenoxy)aniline, DIPEA, DCM,  $20\text{ }^\circ\text{C}$ .



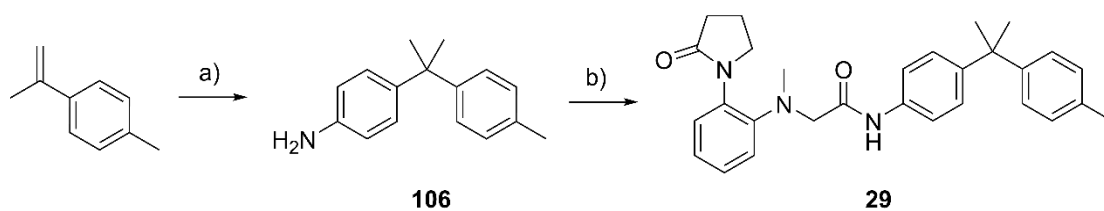
**Scheme S4.** Synthetic route to access **24** and **25**. *Reagents and conditions:* (a) 4-(4-methylphenoxy)aniline, DCM,  $20\text{ }^\circ\text{C}$ ; (b) **103**,  $\text{K}_2\text{CO}_3$ , MeCN,  $90\text{ }^\circ\text{C}$ . For  $\text{R}^1$  and  $\text{R}^2$  groups refer to Table 3.



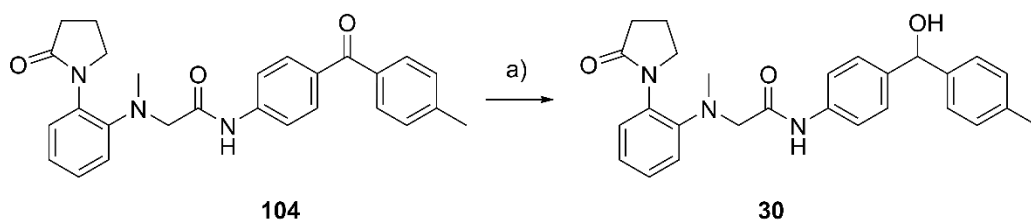
**Scheme S5.** Synthetic route to access **27**. *Reagents and conditions:* (a) HATU, (4-aminophenyl)-(p-tolyl)methanone, DIPEA, DCM, 20 °C; (b) triethylsilane, TFA, 0 °C to 20 °C.



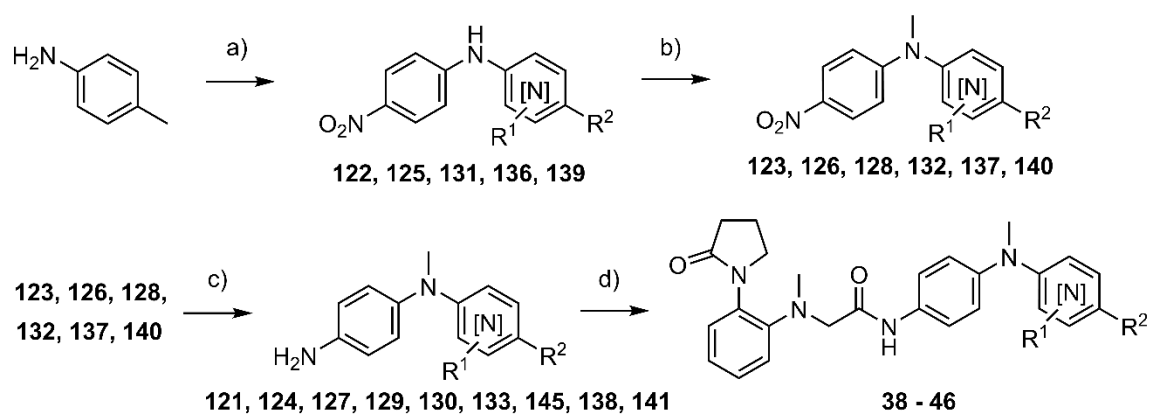
**Scheme S6.** Synthetic route to access **28**. *Reagents and conditions:* (a) p-toluenesulfonyl hydrazide, 1,4-dioxane, 80 °C, then (4-aminophenyl)boronic acid HCl, K<sub>2</sub>CO<sub>3</sub>, 110 °C (b) HATU, **111**, DIPEA, DCM, 20 °C.



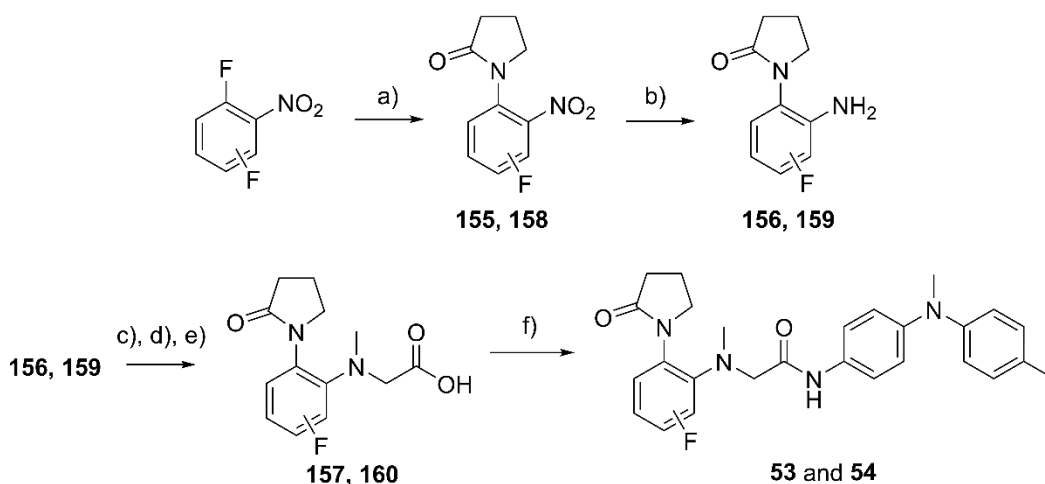
**Scheme S7.** Synthetic route to access **29**. *Reagents and conditions:* (a) aniline, NaOAc, hexafluoroisopropanol, 80 °C (b) HATU, **68**, DIPEA, DCM, 20 °C.



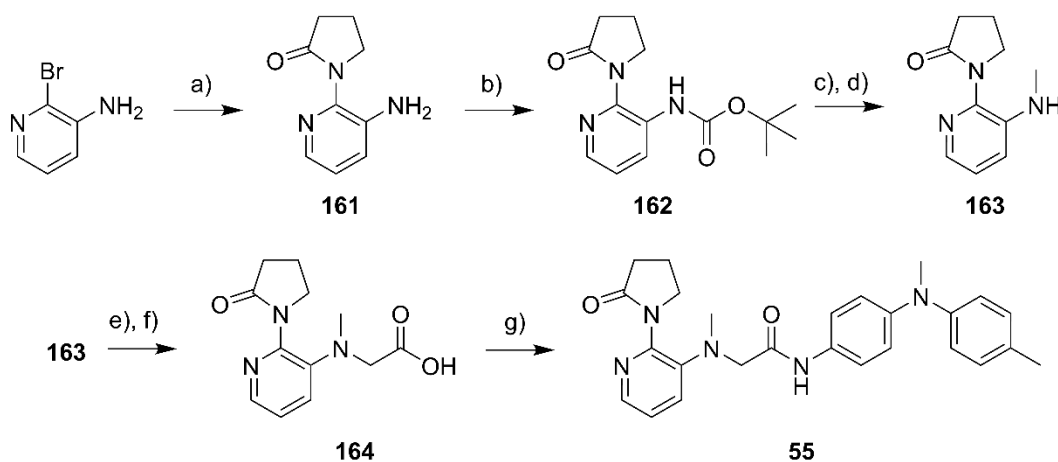
**Scheme S8.** Synthetic route to access **30**. *Reagents and conditions:* (a) NaBH<sub>4</sub>, EtOH, H<sub>2</sub>O, 20 °C.



**Scheme S9.** Synthesis of *N*-substituted biaryl derivatives **38 - 46**. *Reagents and conditions:* (a) 1-fluoro-4-nitrobenzene, K<sub>2</sub>CO<sub>3</sub> DMSO, 130 °C; (b) iodomethane, NaH, DMF, 30 °C; (c) Zn, NH<sub>4</sub>Cl, H<sub>2</sub>O/MeOH (1:1), 40 °C; or cat. Pd/C, EtOH, H<sub>2</sub>, 30 °C; (d) **68**, HATU, DIPEA, DCM, 20 °C. For R groups refer to Table 6.

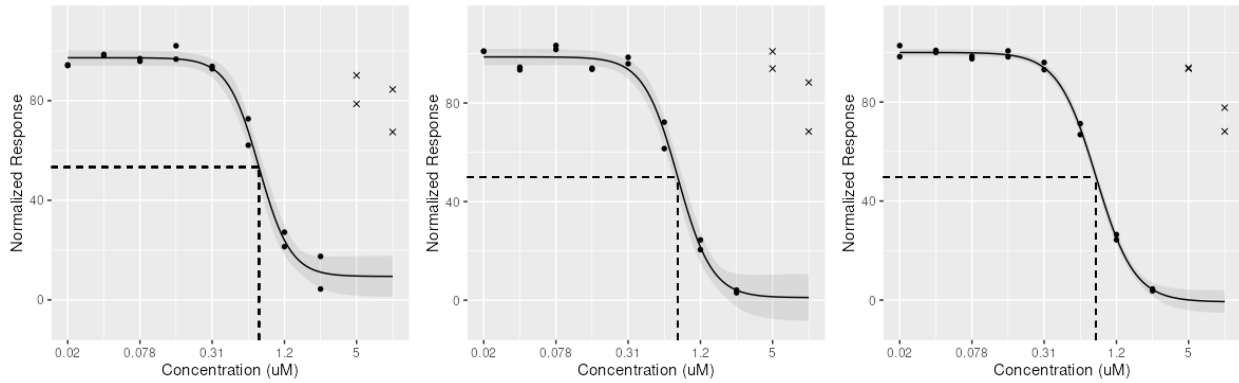


**Scheme S10.** Synthetic route to access **53** and **54**. *Reagents and conditions:* (a) 2-pyrrolidinone,  $K_2CO_3$ , DMF, 80 °C; (b) Zn,  $NH_4Cl$ ,  $H_2O/MeOH$  (1:1), 40 °C; (c) *tert*-butyl bromoacetate,  $K_2CO_3$ , MeCN, 80 °C; (d) MeI,  $K_2CO_3$ , DMF, 35 °C; (e) 4M HCl in 1,4-dioxane, 20 °C; (f) **87**, HATU, DIPEA, DCM, 20 °C. For fluorine position refer to Table 8.

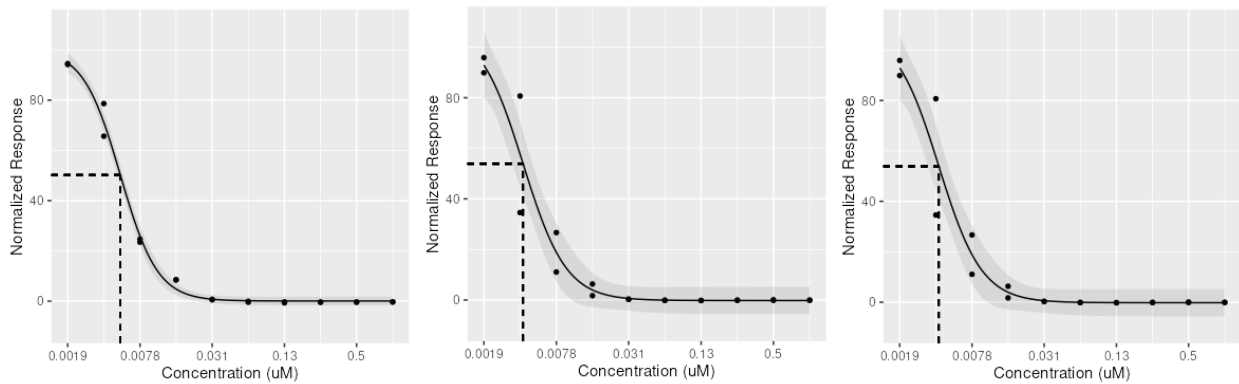


**Scheme S11.** Synthetic route to access **55**. *Reagents and conditions:* (a) 2-bromoaniline, 2-pyrrolidinone, DMEDA, CuI,  $K_2CO_3$ , DMF, 80 °C; (b) Boc anhydride, triethylamine, 1,4-dioxane/ $H_2O$  (3:1); (c) MeI, NaH, THF, 20 °C; (d) TFA/DCM (1:1), 20 °C; (e) ethyl 2-bromoacetate,  $K_2CO_3$ , MeCN, 50 °C; (f) LiOH, EtOH/ $H_2O$ ; (g) **103**, HATU, DIPEA, DCM, 20 °C.

### MMV020512 (1)



### WEHI-326 (33)



### WEHI-328 (60)

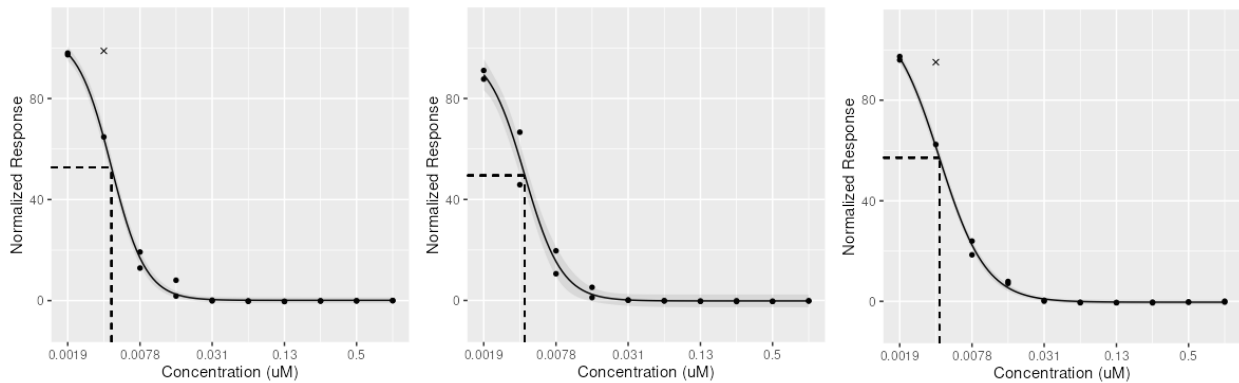


**Figure S1.** Dose response curves of selected compounds against *P. falciparum* 3D7. Each dose response represents the means of one experiment in duplicate measuring the LDH activity of *P. falciparum* 3D7 parasites following exposure to compounds for 72 h.

**Table S1.** Caco-2 permeability of WEHI-326 (**33**).

<b>compound</b>	<b>A to B</b> ( $10^{-6}$ cm/sec)	<b>B to A</b> ( $10^{-6}$ cm/sec)	<b>efflux ratio</b>
WEHI-326 ( <b>33</b> )	1.09	2.52	2.3

**Table S2.** Summary of the MIR on analog WEHI-326 (33).

<b>Parasite Line:</b> Dd2-B2	
<b>IC<sub>50</sub>/IC<sub>90</sub>:</b> 2.74/8.79 nM	
<b>Selection Pressure:</b> 3 × IC <sub>90</sub> (26.98 nM)	
<b>Selection:</b>	3.3 × 10 <sup>6</sup> × 24
<b>Day of recrudescence:</b>	14 (B4), 21 (A3), 32 (A6, B2, C2, D3), 39 (C4, C6), 46 (B3, B5), 50 (D2), 53 (A5)
<b>IC<sub>50</sub> shift:</b> 182 to 843-fold	
<b>MIR:</b> 4.0 × 10 <sup>7</sup>	<b>Log<sub>10</sub> MIR:</b> 7.60

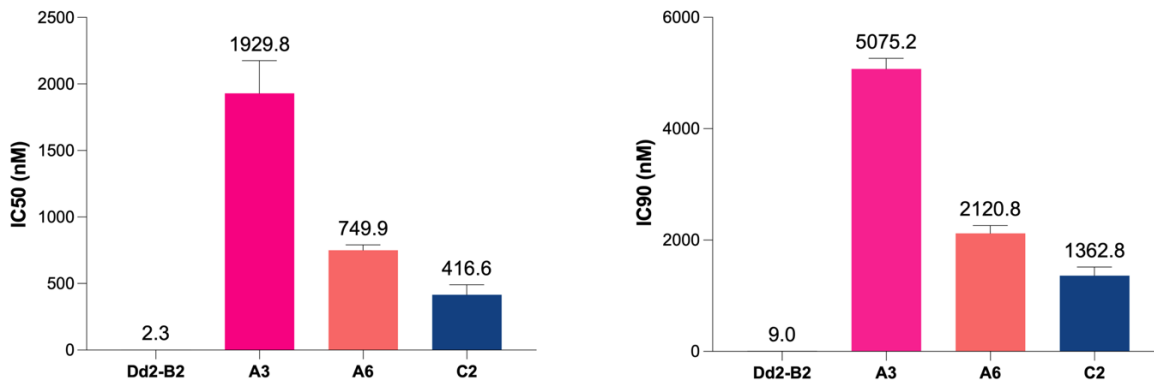


**Figure S2.** WEHI-326 (33) gatekeeper bulk culture IC<sub>50</sub> and IC<sub>90</sub> shifts from the MIR study.

Data shown are mean ± SEM (N, n= 3, 2)

**Table S3.** Whole genome sequencing metrics from the MIR study on WEHI-326 (33).

		Drug treated samples			Parent
Sample names		A3	A6	C2	Dd2_B2
Total reads		5,953,306	4,098,153	6,172,456	4,680,824
# Mapped reads		4,388,383	3,120,966	5,666,787	4,342,594
Duplication rate		34.05%	26.05%	31.92%	31.51%
General error rate		1.54%	1.55%	1.66%	1.71%
Mean mapping quality (Phred)		56.72	56.61	56.6	56.74
Depth of coverage	mean	37.16	27.67	55.43	40.85
	SD	29.63	20.07	52.13	37.53
% of PF genome with > x no. reads	1X	96.04%	95.98%	96.31%	96.07%
	5X	94.41%	94.02%	94.85%	94.20%
	10X	93.11%	91.76%	93.54%	91.81%
	20X	87.72%	76.78%	89.47%	
	30X	71.12%	42.58%	82.55%	71.42%

**Table S4.** List of SNPs found by variant caller in A3, A6 and C2 samples from the MIR study.

CHROM	POS	REF	ALT	AMINO ACID CHANGE	CODON CHANGE	GENE NAME	EFFECT / IMPACT
Pf3D7_05_v3	1154588	C	A	L305I	Cta/Ata	PF3D7_0527900 (ATP-dependent RNA helicase DDX41, putative)	NON SYN CODING / MODERATE
Pf3D7_07_v3	275391	T	C	K1106E	Aaa/Gaa	PF3D7_0705500 (inositol-phosphate phosphatase, putative)	NON SYN CODING / MODERATE
Pf3D7_08_v3	831184	C	A	Q248K	Caa/Aaa	PF3D7_0818200 (14-3-3 protein)	NON SYN CODING / MODERATE
Pf3D7_10_v3	1028876	T	A	K164N	aaA/aaT	PF3D7_1024600 (RAP protein, putative)	NON SYN CODING / MODERATE
Pf3D7_12_v3	2062074	C	A	R823S	Cgt/Agt	PF3D7_1250200 (CSC1-like protein, putative)	NON SYN CODING / MODERATE
Pf3D7_12_v3	2062976	T	C	F957L	Ttc/Ctc	PF3D7_1250200 (CSC1-like protein, putative)	NON SYN CODING / MODERATE
Pf3D7_14_v3	453280	G	A	P534S	Ccc/Tcc	PF3D7_1411200 (rhomboid protease ROM8)	NON SYN CODING / MODERATE

**Table S5.** Homozygous SNPs found in A3, A6 and C2 samples from the MIR study.

GENE NAME	AMINO ACID CHANGE	CODON CHANGE	Drug treated samples		
			A3	A6	C2
PF3D7_0527900	L305I	Cta/Ata	100%	0%	0%
PF3D7_0705500	K1106E	Aaa/Gaa	100%	0%	0%
PF3D7_0818200	Q248K	Caa/Aaa	100%	0%	0%
PF3D7_1024600	K164N	aaA/aaT	0%	0%	100%
PF3D7_1250200	R823S	Cgt/Agt	0%	0%	100%
PF3D7_1250200	F957L	Ttc/Ctc	100%	0%	0%
PF3D7_1411200	P534S	Ccc/Tcc	0%	100%	0%
		<b>IC<sub>50</sub> shift</b>	842.6	327.4	181.9
		<b>IC<sub>90</sub> shift</b>	570.2	235.9	151.5
		<b>N, n</b>	3,2	3,2	3,2

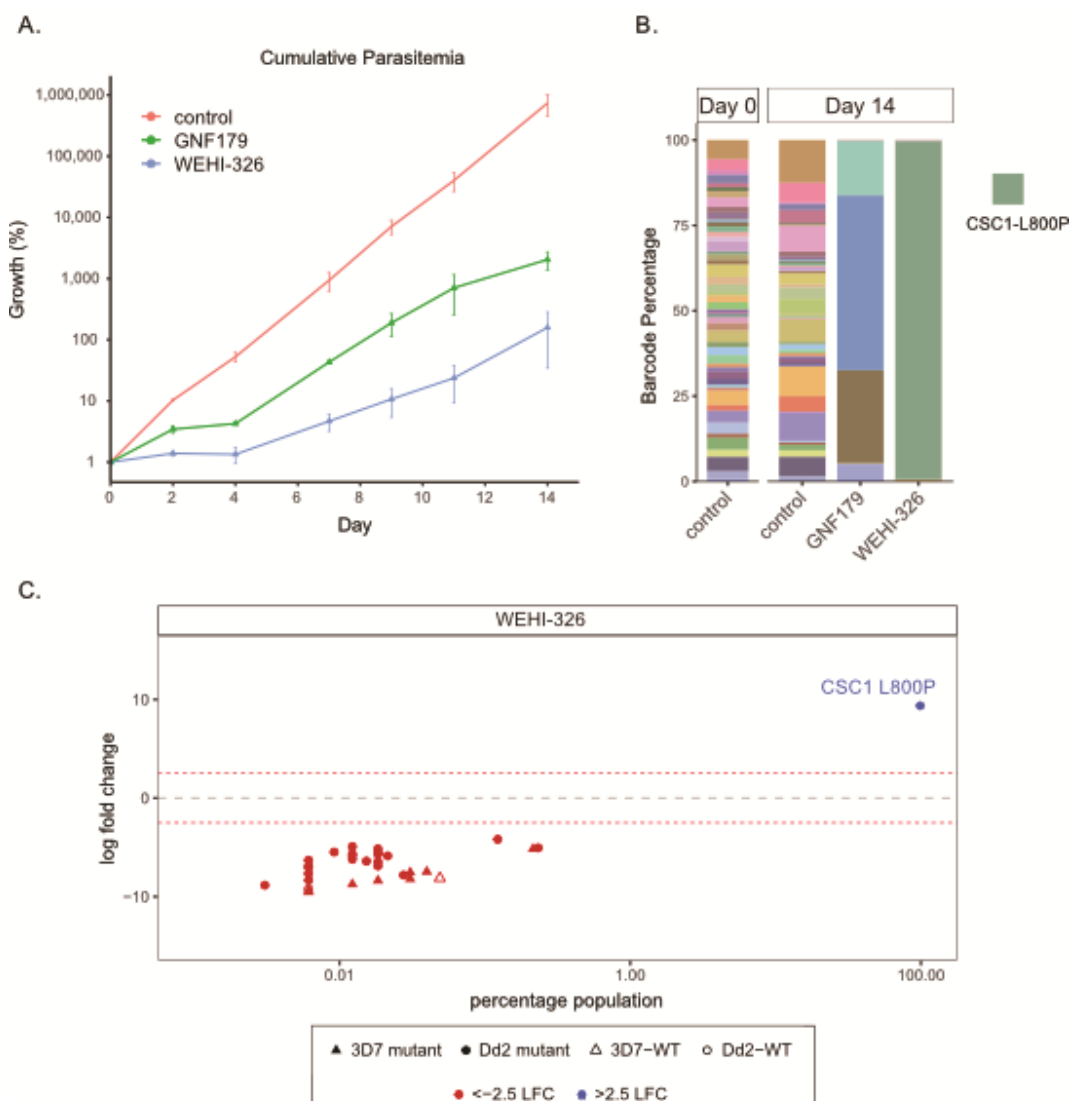


**Figure S3.** AReBar assay cross-resistance profiling of WEHI-326 (**33**). **A.** Growth profile (cumulative parasitemia) for compound WEHI-326 (**33**) ( $3 \times \text{EC}_{50}$ ) and a no drug control against the AReBar pool. Cultures were run in triplicate and parasitaemia was maintained between 0.5-5%. Error bars show standard deviation. **B.** Barcode profile of WEHI-326 (**33**). The proportion of each barcoded line is represented by coloured bars. Shown are average percentage counts of mutant barcode populations from the assay input on day 0, the no drug control harvested on day 14, the GNF179 positive control or WEHI-326 treated cultures at day 14. The CSC1-L800P was enriched to 98.9% of total barcodes in the WEHI-326 cultures (see Table S6). The GNF179 control compound enriched three different barcoded lines with mutations in the expected resistance protein CARL. **C.** Differential analysis showing log<sub>2</sub> fold change (LFC) of each line after treated with WEHI-326 (**33**) when contrasted with day 14 no drug control samples. Plot shows proportion of total population (x-axis) and LFC (y-axis) of individual lines. The data show the expansion (LFC >2.5) of the CSC1 L800P mutant line.

**Table S6.** Barcoded lines used in the AReBar cross-resistance assay. Listed are the 52 barcoded lines in the screening pool. The line name, gene description, gene ID are shown, as well as the proportion (% of total population) at day 0, day 14 (no-drug, GNF179-treated, and WEHI-326(33)-treated). The log<sub>2</sub> fold change compares WEHI-326(33)-treated with the day 14 no-drug control.

Cell name	Input	No drug (day14)	Treated (day14)	LFC	p-value
Dd2 CSC1 L800P	0.933	0.155	98.909	9.365	<.001
Dd2 eEF2 Y186N	2.223	0.058	0.018	-1.652	0.012
Dd2 MCP D195N	1.055	0.043	0.006	-3.087	0.008
Dd2 cytBC1 G33V	1.685	0.148	0.018	-3.231	<.001
Dd2 kelch13 R539T	0.847	0.169	0.012	-4.022	<.001
Dd2 PROT5 M45I	2.106	1.963	0.123	-4.189	<.001
Dd2 CARL I1139K	0.525	0.215	0.012	-4.421	<.001
Dd2 AsnRS R487S	1.871	0.313	0.012	-4.923	<.001
Dd2 MCP P214T	4.077	8.644	0.233	-5.049	<.001
Dd2 DHODH C276Y	2.062	0.556	0.018	-5.157	<.001
3D7 ATPase2 CNV2	2.783	7.580	0.215	-5.162	<.001
Dd2 UDP-GT F37V	0.699	0.060	0.000	-5.402	<.001
Dd2 CARL I1139Kb	0.391	0.353	0.009	-5.478	<.001
Dd2 IleRS L810F	1.103	0.846	0.018	-5.572	<.001
3D7 ACS11 D648Y	1.085	0.502	0.012	-5.61	<.001
Dd2 kelch13 C580Y	1.758	0.892	0.018	-5.67	<.001
Dd2 eEF2 L755F	1.672	0.528	0.012	-5.675	<.001
Dd2 kelch13 C580C	2.084	1.201	0.021	-5.865	<.001
Dd2 CLK3 H259P	1.454	0.757	0.012	-6.205	<.001
Dd2 CARL V1103L	1.155	0.412	0.006	-6.304	<.001
Dd2 ATP4 Q172H	2.106	1.037	0.015	-6.398	<.001
Dd2 HSP90 A41S	2.414	1.555	0.018	-6.473	<.001
Dd2 AcAS T648M	2.418	1.773	0.018	-6.89	<.001
Dd2 PI4K S1320L+L1418F	3.295	0.598	0.006	-6.899	<.001
Dd2 PI4K S743F+H1484Y	1.151	0.673	0.006	-7.024	<.001
3D7 FTb A515T	3.347	6.637	0.040	-7.463	<.001
3D7 MDR2 K840N	1.750	4.748	0.031	-7.549	<.001
Dd2 IleRS E180D	2.449	1.038	0.006	-7.656	<.001
Dd2 QRP1 D1863Y	4.111	5.572	0.028	-7.808	<.001
3D7	5.514	12.433	0.049	-8.131	<.001
3D7 NCR1 A1108T	3.360	8.231	0.031	-8.204	<.001
Dd2 DHFR-TS S216R	2.101	0.454	0.000	-8.336	<.001
Dd2 PROT5 A20V	3.478	1.577	0.006	-8.339	<.001
3D7 ABCI3 R2180P	3.248	5.797	0.018	-8.365	<.001
Dd2 AcAS A597V	1.411	0.494	0.000	-8.43	<.001
Dd2 CPSF Y408S E	1.606	0.478	0.000	-8.468	<.001
Dd2 cytBC1 V284L	1.181	0.571	0.000	-8.654	<.001
3D7 DHFR-TS I403L	0.708	4.277	0.012	-8.738	<.001
Dd2 ATP4 G358S	1.559	1.269	0.003	-8.842	<.001
Dd2 GGPPS S228T	1.450	0.696	0.000	-8.978	<.001
Dd2 IleRS V500A	1.207	0.801	0.000	-9.123	<.001
Dd2	3.625	3.064	0.006	-9.218	<.001
3D7 DHFR-TS G378E	2.379	3.346	0.006	-9.376	<.001
Dd2 CRT M343L	2.852	0.996	0.000	-9.497	<.001
3D7 ACS10 M300I	1.255	3.800	0.006	-9.527	<.001
Dd2 DNApolD ATP4 L927V	2.279	1.070	0.000	-9.572	<.001
Dd2 TyrRS S234C	2.366	1.558	0.000	-10.106	<.001
Dd2 CPSF Y408S S	1.394	0.008	0.000	low counts	-
Dd2 DHODH F227I	1.055	0.013	0.000	low counts	-
Dd2 DHODH I263F	0.278	0.010	0.000	low counts	-
Dd2 DHODH L531F	0.973	0.024	0.006	low counts	-
Dd2 ProRS L482H	0.113	0.007	0.000	low counts	-

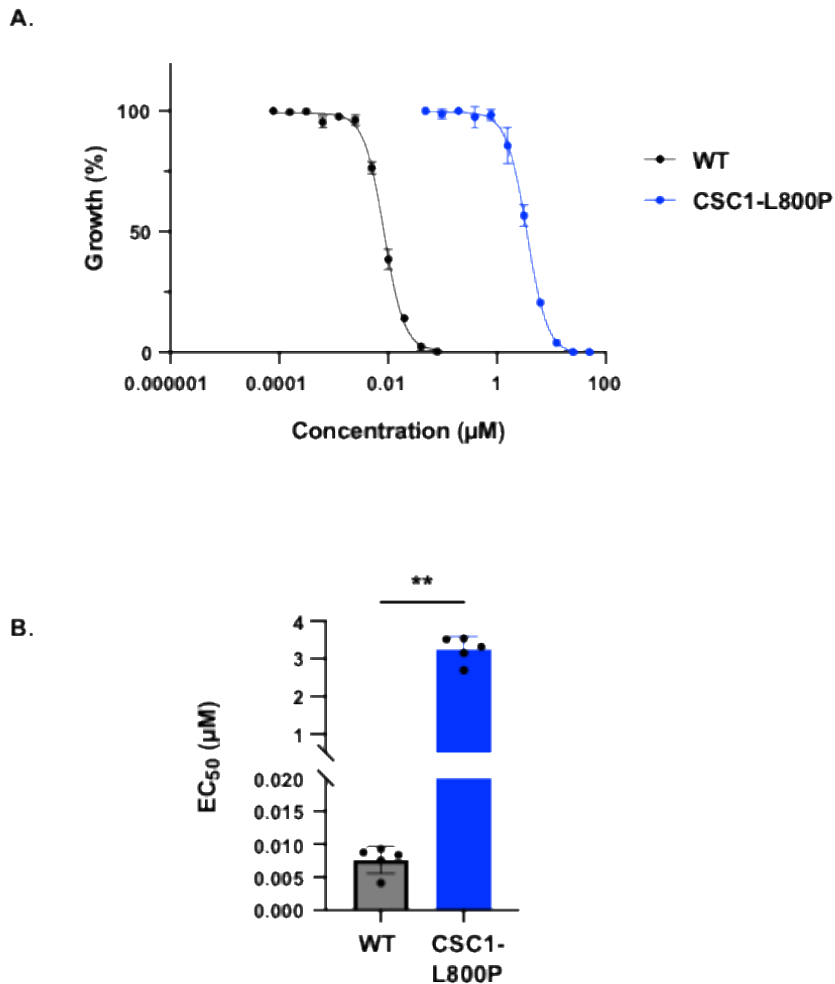


**Figure S4.** Reduced sensitivity of the CSC1-L800P mutant line against WEHI-326 (**55**). A. Representative dose response curves of WEHI-326 (**33**) against the Dd2 wildtype parental line and the isogenic CSC1-L800P mutant line from the AReBar study. Shown is a single biological replicate with technical triplicates. B. EC<sub>50</sub> data for the Dd2 parental line (0.008 µM) and the CSC1-L800P mutant (3.24 µM), with each dot representing a biological replicate and error bars showing standard deviation (\*\* p<0.079).

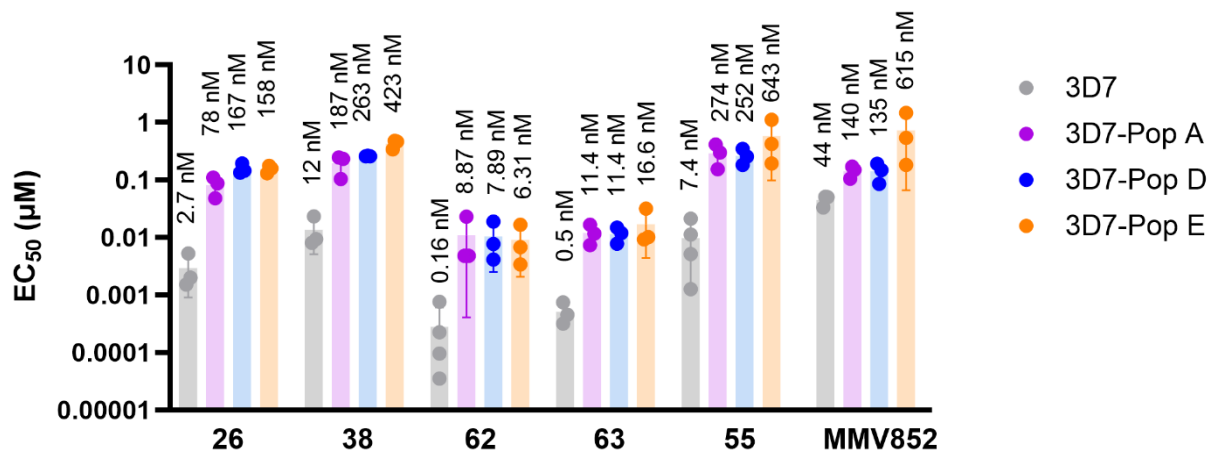


**Figure S5.** EC<sub>50</sub>-fold shifts of selected compounds against MMV020512-resistant *P. falciparum* clones. EC<sub>50</sub> data represent means and SDs for 3 experiments measuring LDH activity of *P. falciparum* 3D7 parasites following exposure to compounds for 72 h. 3D7-Pop A has a T622K mutation in ROM8; 3D7-Pop D has a L954F mutation in CSC1; 3D7-Pop E has a L562R mutation in ROM8. MMV1845852 was used as a putative control CSC1 inhibitor from the MMV Global Health Priority Box.

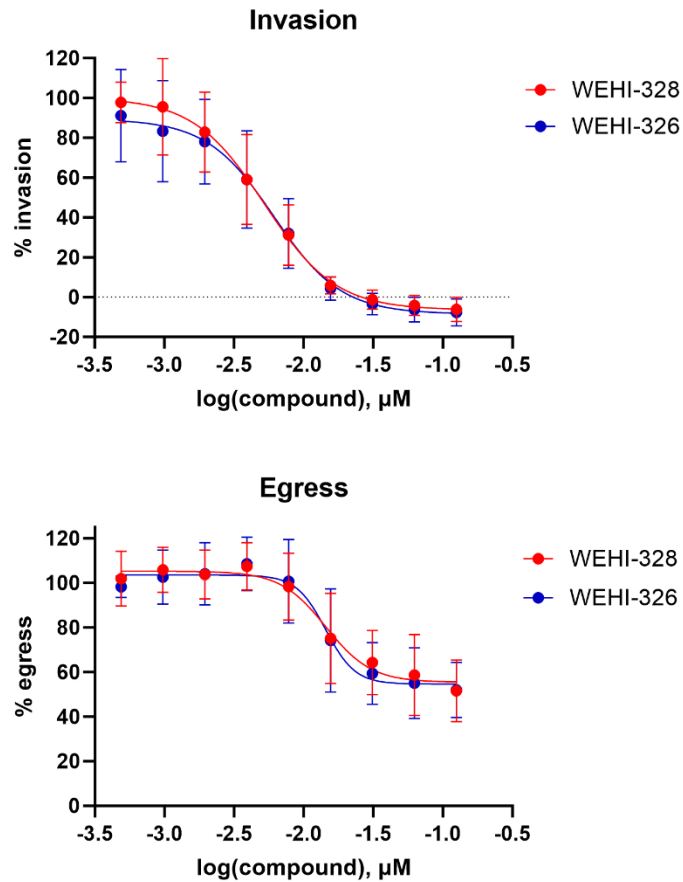


**Figure S6.** Impact of selected compounds on the transition from invasion to ring stage of the asexual stage parasite.  $EC_{50}$  data represents means and SD of  $n=3$  experiments (each conducted in technical duplicate) measuring the bioluminescence of *P. falciparum* parasites expressing nano-Luc following exposure of compound. Late-stage nanoluciferase-expressing schizonts were treated with serially diluted compound for 4 h, during which time merozoite egress and re-invasion occurred. Egress was quantified by measuring the bioluminescent signal intensity of nanoluciferase released into the culture medium during drug treatment. After the 4 h egress and invasion window, drugs were removed and parasites were grown until the following trophozoite stage (24 h), at which stage nanoluciferase is strongly expressed. The bioluminescent signal intensity of trophozoite lysates indicated the success of invasion during the treatment window.

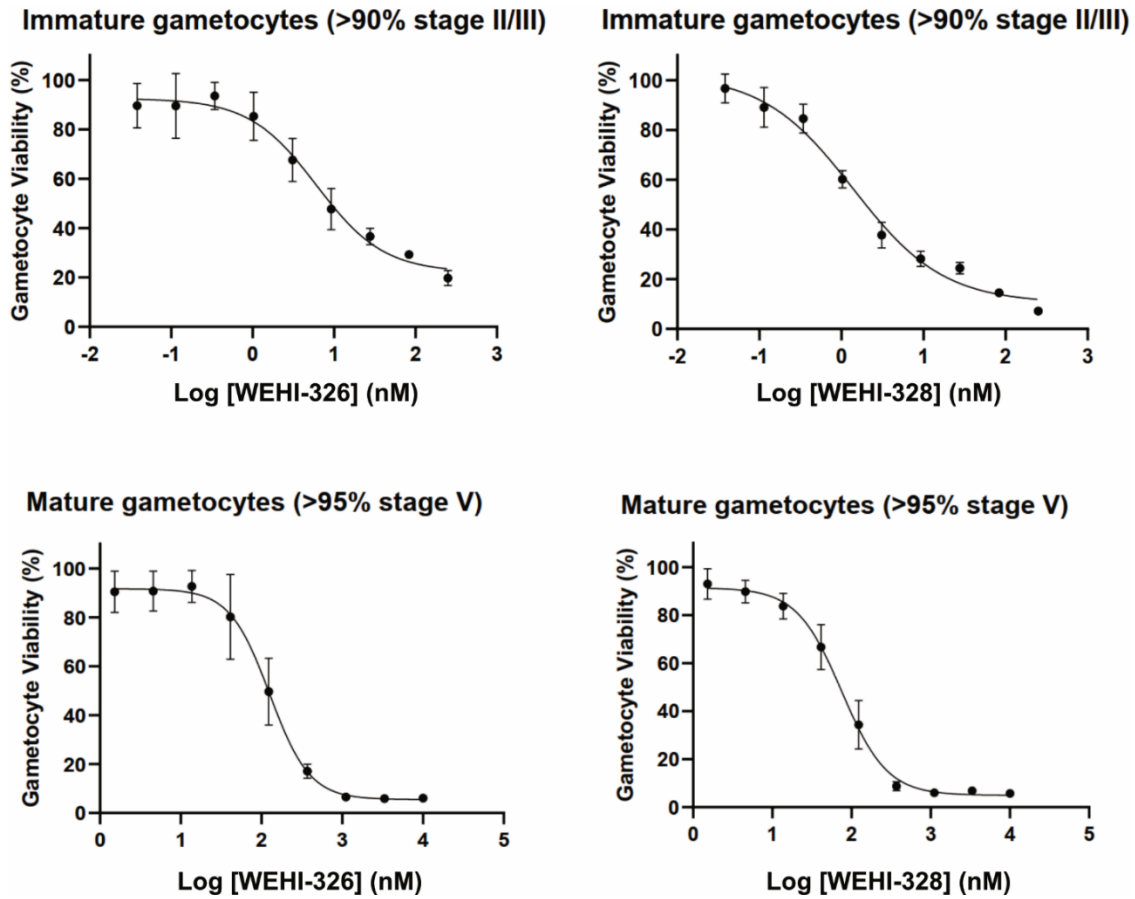


**Figure S7.** Dose response curves of selected compounds against *P. falciparum* NF54 stage II-IV and stage V gametocytes. EC<sub>50</sub> data represents means and  $\pm$ SEM of n=3 experiments measuring the bioluminescence of NF54-Pfs16-GFP-luc or 3D7elo1-pfs16-CBG99 gametocytes following exposure for 48 h.

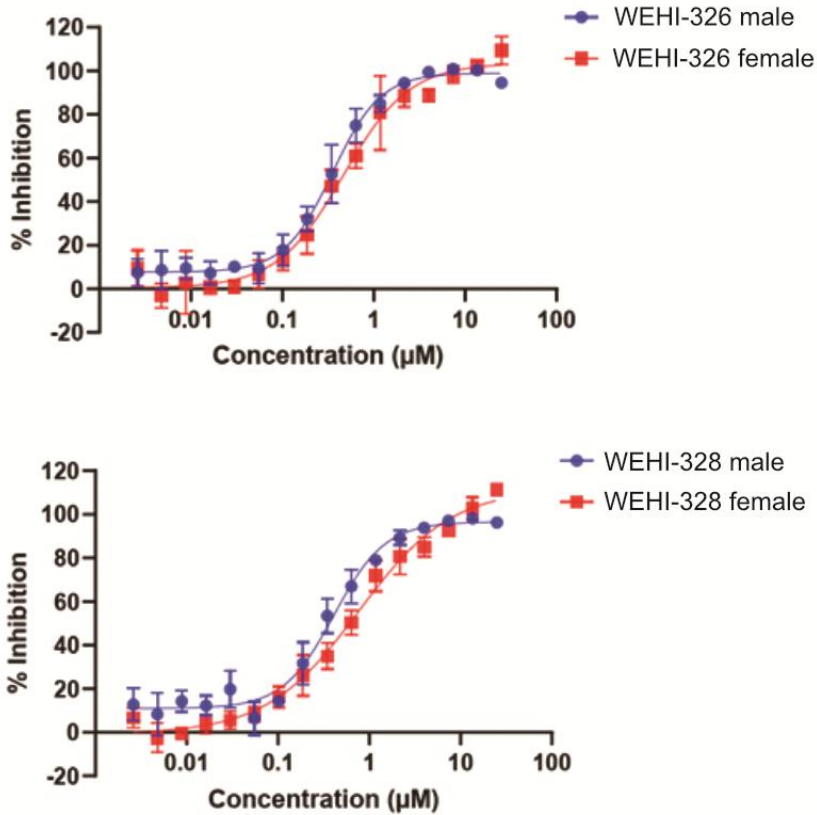


**Figure S8.** Dose response curves of selected compounds against *P. falciparum* NF54 gamete formation. EC<sub>50</sub> data represent means and SDs for four replicate experiments following gametocyte exposure to compounds for 48 h prior to inducing gametogenesis. Male gametogenesis was measured 20 min after induction and female gametogenesis was measured 24 h after induction. The viability of male gametes was quantified by automated microscopy measuring exflagellation and for female gametes measuring fluorescence using an Cy3-labelled  $\alpha$ Pfs25 antibody.

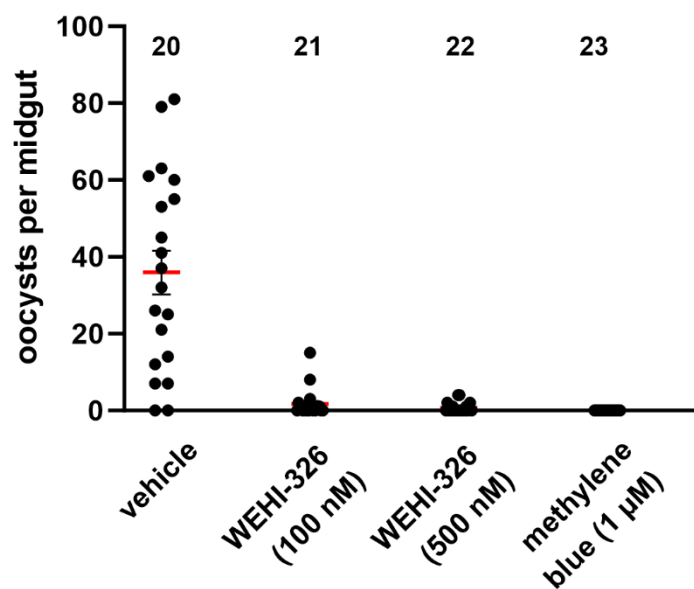


**Figure S9.** Repeat experiment showing the activity of WEHI-326 (**33**) in a standard membrane feeding assay. Oocyst counts and intensity per from midguts dissected from *Anopheles stephensi* mosquitoes 7 days post the blood meal infected with *P. falciparum* NF54 stage V gametocytes treated with compound at the indicated concentration. Numbers indicate the total number of mosquito midguts dissected per treatment group. Red bars indicate average oocyst intensity and error bars represent SEM.

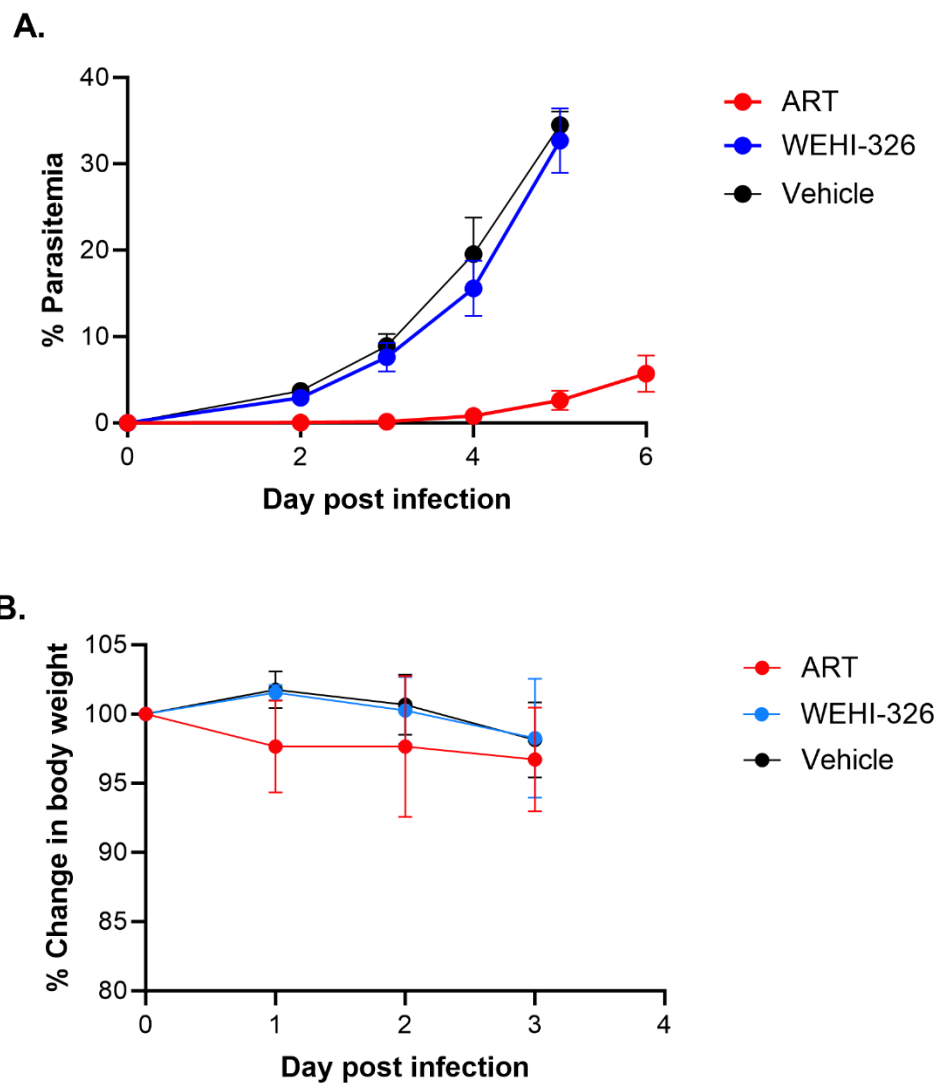


**Figure S10.** Activity of WEHI-326 (**33**) in a *P. berghei* 4 day mouse model. **A.** To infect mice, *P. berghei* ANKA parasites ( $2 \times 10^7$  parasites) were injected into the tail vein. Compounds were administered q.d. 50 mg/kg by oral gavage 4 h after infection (day 0) and then on days 1, 2, and 3. Data are average % parasitemia for  $n = 3$  mice on days 2, 3 and 4 measured by flow cytometry. Error bars represent SEM. Artesunate (ART) was used as a positive control at 30 mg/kg. **B.** % body weight change of mice in the *P. berghei* model.

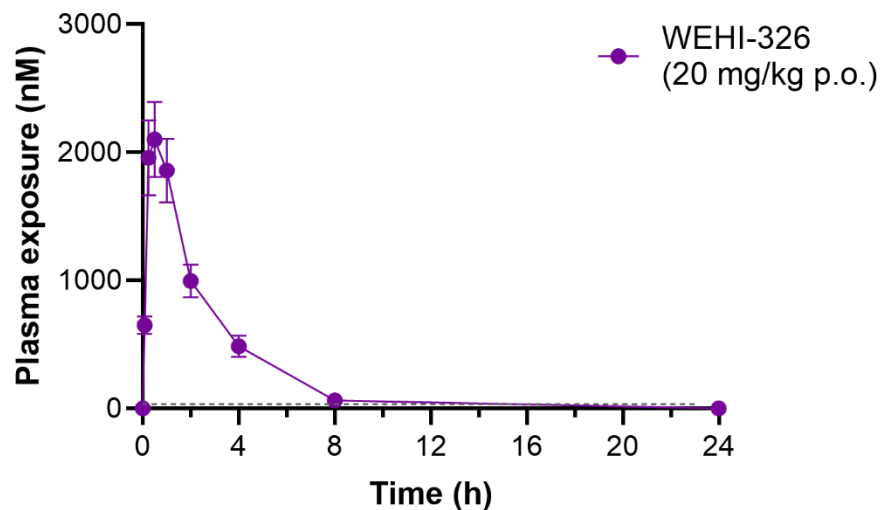


**Figure S11.** Plasma concentrations of WEHI-326 (**33**) in male CD1 mice following oral administration at 20 mg/kg. Data shown is the averages and SEM for n=3 mice. Dotted line indicates WEHI-326 (**55**) EC<sub>50</sub> of 5 nM against *P. falciparum* 3D7 parasites in vitro.

**Table S7.** Exposure parameters for WEHI-326 (**33**) in male Swiss mice following oral administration at 20 mg/kg. Data shown is the averages and SD for n=3 mice.

C <sub>max</sub> (µg/mL)	T <sub>max</sub> (h)	terminal half-life (h)	AUC <sub>0-last</sub> (h*µg/mL)	AUC <sub>0-inf</sub> (h*µg/mL)	Clearance (mL/min/kg)
1.00 (0.24)	0.67 (0.29)	1.48 (0.19)	2.71 (0.63)	2.78 (0.66)	125.4 (33.5)

```

PBANKA_1031300.1-p1 -----ME-----K 3
PF3D7_1411200.1-p1 MVKKKTSVNVKSILETKNKREKKDEDDDEDNKTNKLYNNLYKRNKSIKINILDKNENNGE 60
                                                                ::      :

PBANKA_1031300.1-p1 GNSCSNA--KIFLESEDK---TEKINGSKEYDDDDNLLKKGICS-----N-----T 44
PF3D7_1411200.1-p1 GISLSSEKQKVSFKKKNNNYDINESDGVGDYGDDECEEESEIENEDIINNKNNTNNINNI 120
* * * . * : ::::: : : * : * : * : : . * . *

PBANKA_1031300.1-p1 SMYDQVNEHREVENQ--PSGENEINN---IKNHLL-----KIYNGEVMPSEDNMLL 92
PF3D7_1411200.1-p1 NITNNINNTNNFDNTNNIDNTNNIGNTNNIQINNILERNSKEKSLYKEELTT---NIQN 176
. : * : * : . : : * . . * : * * : * : : * : : * : * : * :

PBANKA_1031300.1-p1 SSNNTIILLKCV-----NN---KGVVRNGSKNSKSNYKKEKYKR-SHTKKEKFKFVNS 142
PF3D7_1411200.1-p1 GENNTVQVFNFKKYDYNPDRKTRDDLNDNENSCSSFTRRGKYNKTKTIKSNKLLKLTN 236
. : * : * : : : : : : : : : : : : * : * : * : . * : * : * : . :

PBANKA_1031300.1-p1 AGEDLLSDSRDYPSLKVNYKINKKNHYEKTKKMGFPQMAMNDKNER--ISSICTDNAKF 200
PF3D7_1411200.1-p1 THENLLSDHHDYTSLVKVNKINKKSNYDKTKRPFSLITFNEKQNRVNRSSVCTDNAKF 296
. : * : * : * : * * * * * * * * * * * * * * * * * * * * * * * * * * * *

PBANKA_1031300.1-p1 INFLEKHEGKNAH-YKNRKRNNLRQKQK--NVQKKEGNLKTINNYILDIDHRNMSSAN 256
PF3D7_1411200.1-p1 LSFLNDYERKTYLIKNRKRFNEKIKKIQTNIKKREKYDTAETLNNYIVNIDEDNKYEEN 356
. : * : * : : : : * * * * * : : : : : : : * . . * : * * * : * : * . *

PBANKA_1031300.1-p1 MGSNNIHKSKTSLKYHTHDEQ-AEQAYLSELQIAESERSVKDKNRLKNYSNTIKEENKII 315
PF3D7_1411200.1-p1 LPSEKIPKIDTTPRKHFPPMKTDTCMFYKDRDDIQKSEERLKNYATLVEEQKFL 416
. : * : * * . * : : * : : . . . : . : : * : * : * : * : * : * : * :

PBANKA_1031300.1-p1 KQKDKIKAL-LSRTRRCFLFRKKTLRKRKEKIIIFLNHNYTPENGKFNDFHYKTIHKDD 374
PF3D7_1411200.1-p1 RDKSKSKDIEKHKKKKCFLLPKKKLRKRKEKIIIFLNHNSAYKNGPFNDFHYKTVYKND 476
. : * . * * : : : * : * : * * * * * * * * * * * * * * * * * * * * * *

PBANKA_1031300.1-p1 LENLEEEKIYLHNNKNGTIIKIIYRIFPQFSIFSLILFVTFIQVWVFIIILISVKSDFELT 434
PF3D7_1411200.1-p1 LENLDEEKLVIDYSKDNTFKKAIHRIFPQFSIFSLTLVYVTFIQVWVIFILLISVKSDFELT 536
* * * : * : * : . : . * . * : * : * * * * * * * * * * * * * * * * * * * * * *

PBANKA_1031300.1-p1 PSNDSLKNFGSNFPYQIFKKAQVYRLFTALFLHSNHNHCANTYVQLTVGFLELYGTY 494
PF3D7_1411200.1-p1 PSNDSLKNFGSNFPHNIFKNAEFYRLFTSLFLHSNHNHCANTYVQLTVGFLELYGTY 596
* * * * * * * * * * * * * * * * * * * * * * * * * * * * * * * * * * * * * * * *

PBANKA_1031300.1-p1 VVFLVYVFTGIYGIILSSPLTYCYSTTESSSSSSGIIGIFFSEILMMTNFNVDTISISVH 554
PF3D7_1411200.1-p1 VVFLVYVFTGIYGIILSSPLTYCYSTTESSSSSSGIIGIFFSEILMMTNFNVDKISISVH 656
* * * * * * * * * * * * * * * * * * * * * * * * * * * * * * * * * * * * * * * *

PBANKA_1031300.1-p1 LFCFFLLLLFLKFSNLNTISINISYSHFFGFLGGFLIGIILKRNQLKYFLKNNLLIQILSLI 614
PF3D7_1411200.1-p1 LFCFFLLLLFLKFSNLNTVSIINISYSHFFGFLGGFLIGIILKRNQLKYFLRNFLIQILCFV 716
* * * * * * * * * * * * * * * * * * * * * * * * * * * * * * * * * * * * * * *

PBANKA_1031300.1-p1 FLIVSLATAIFVSTSVMQDCPY 636
PF3D7_1411200.1-p1 FLVISLGAAIFISTYVVQNCPN 738
* : * : * : * : * * * * * * * *

```

**Figure S12.** Sequence alignment of *P. falciparum* 3D7 and *P. berghei* ANKA ROM8. *N*-Aryl acetamide resistant mutations are highlighted as follows: L526R in cyan; T622K in yellow; P534S in green.



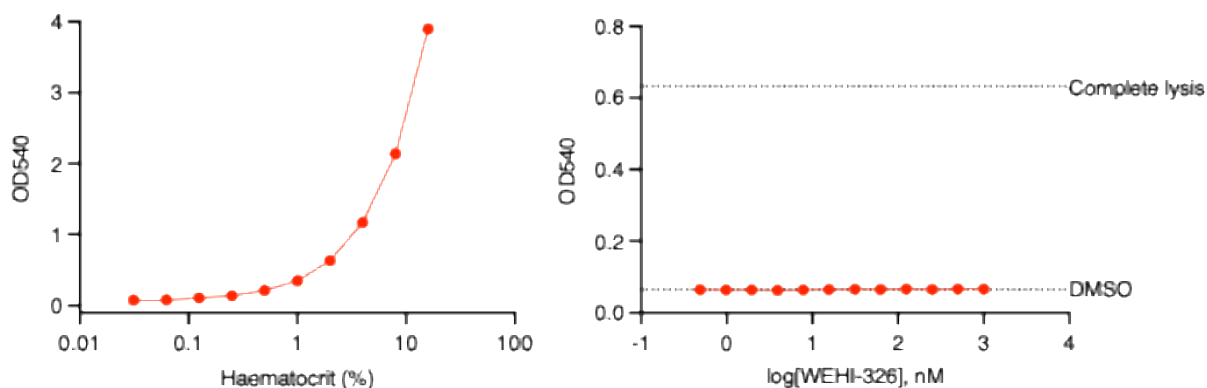
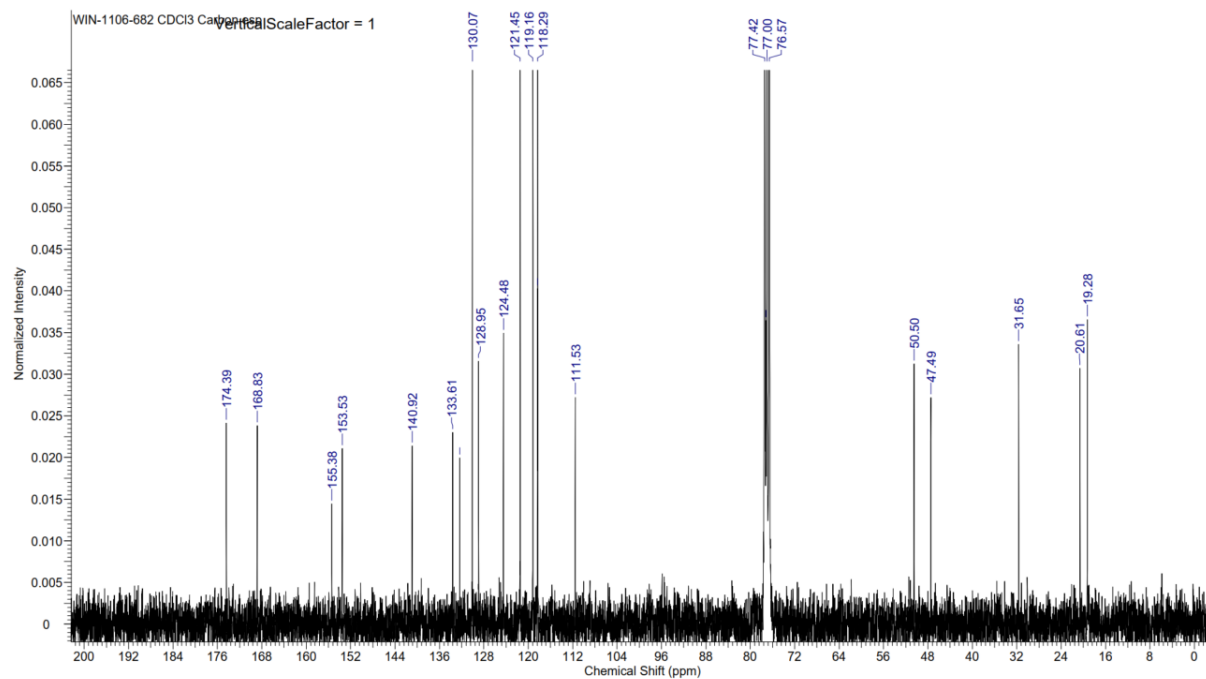
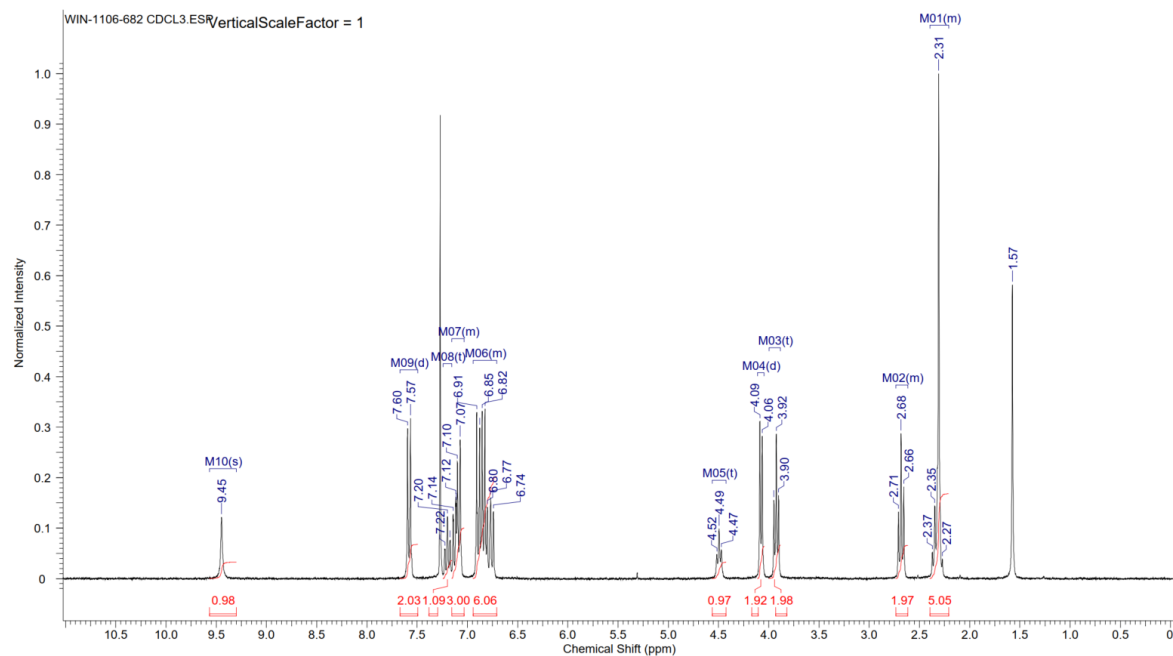
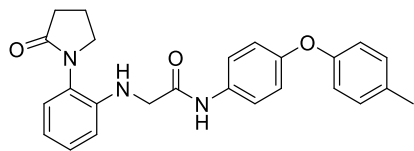


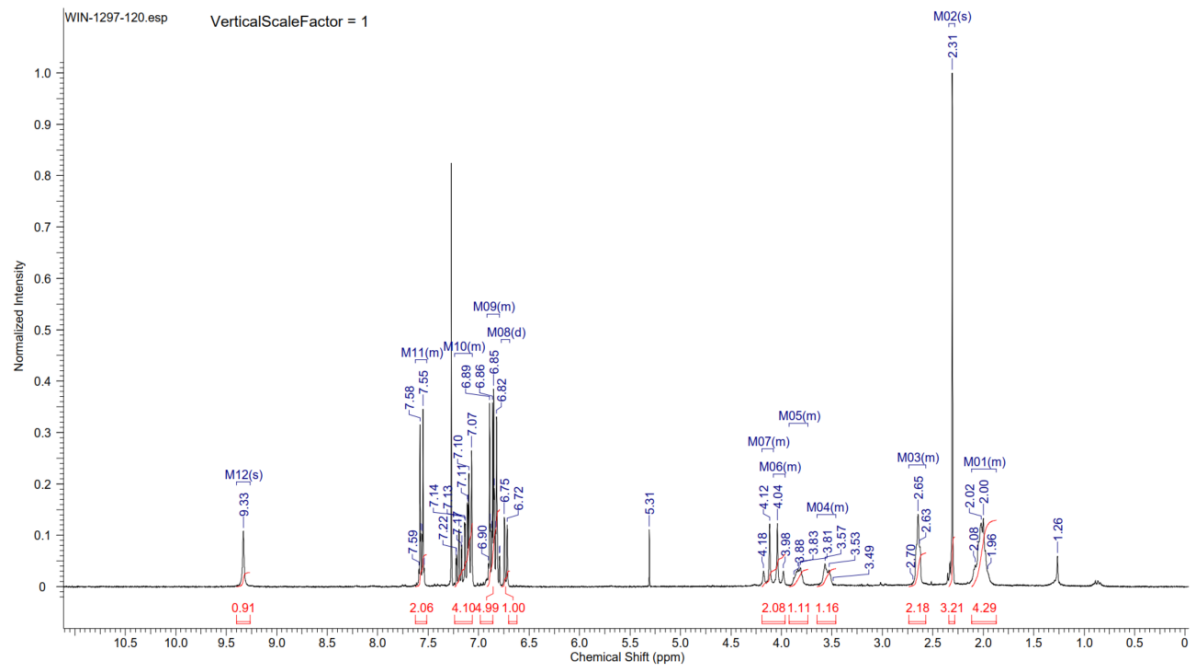
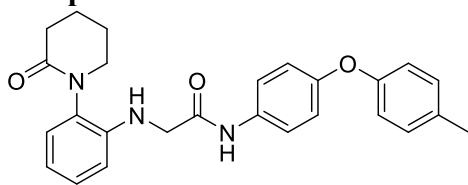
**Figure S14.** WEHI-326 (**33**) does not induce lysis of hemoglobin release from uninfected red blood cells. Left panel. Serially diluted uninfected red blood cells were subjected to freeze-thaw lysis and hemoglobin was quantified by measuring the absorbance at 540 nm (OD540). Right panel. Uninfected red blood cells at 2% hematocrit were treated with WEHI-326 for 4 h. WEHI-326-induced hemolysis was then quantified by measuring the OD540 of hemoglobin released into the medium. “DMSO” indicates the OD540 of samples treated with the DMSO vehicle control. “Complete lysis” indicates the OD540 of freeze-thaw lysed, 2% haematocrit uninfected red blood cells (obtained from the left panel). Points represent the mean of technical duplicates.

# Compound spectra

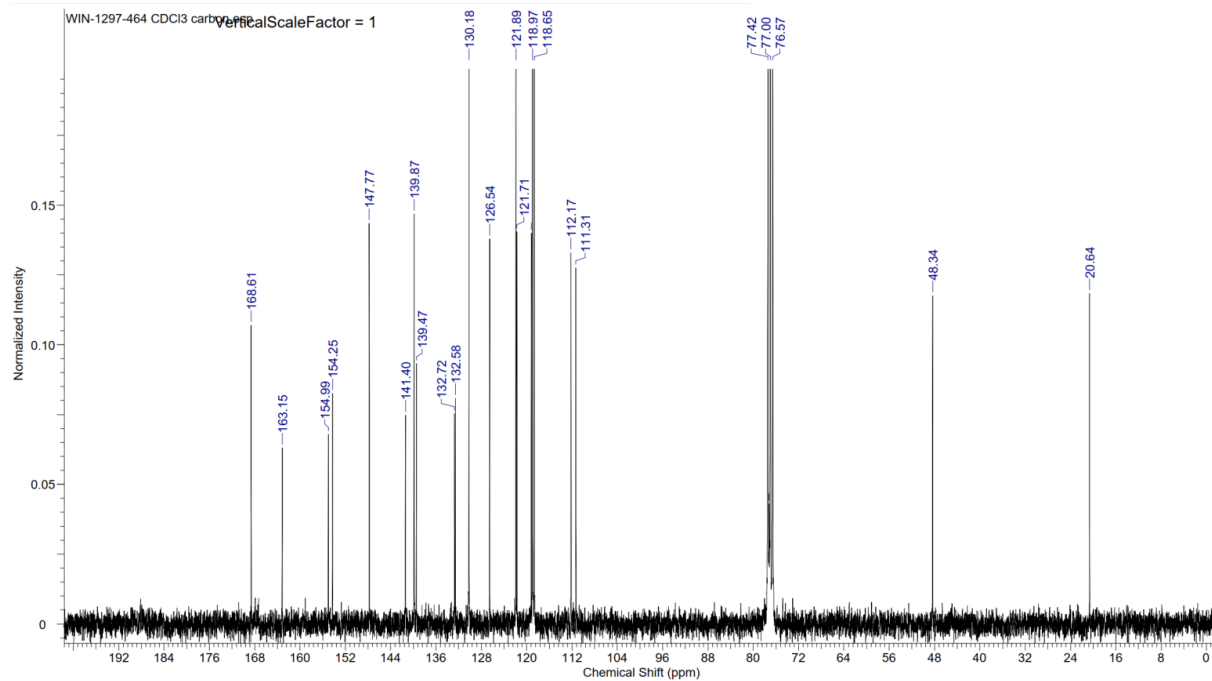
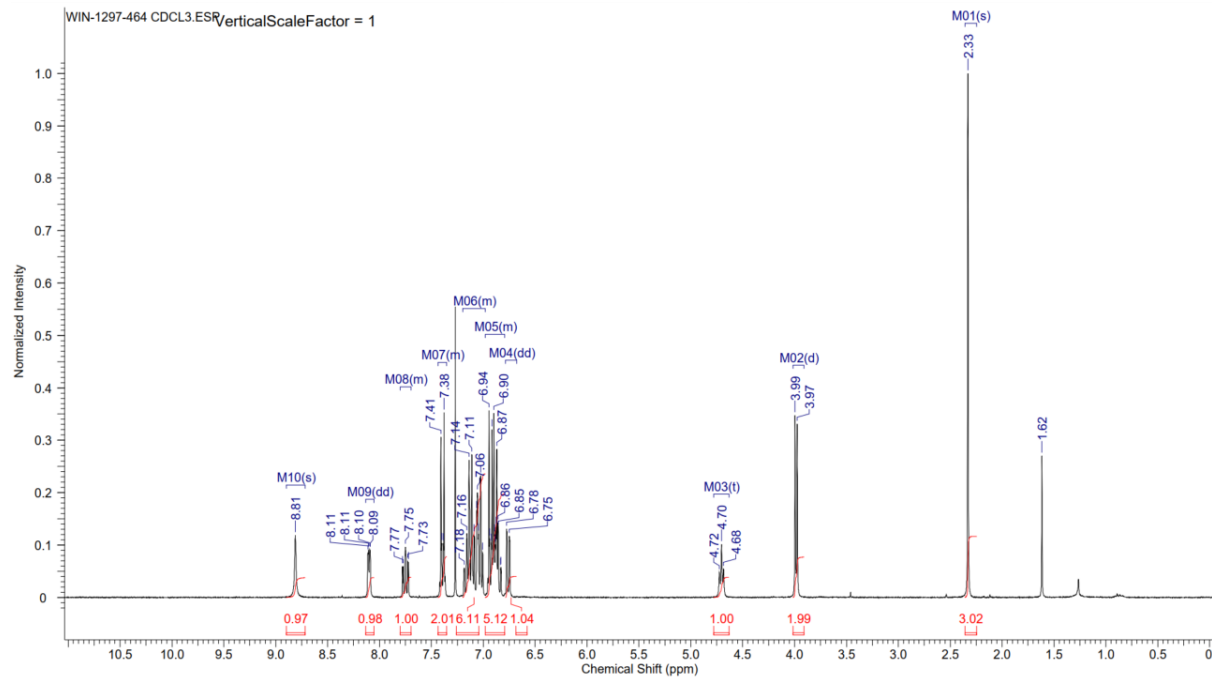
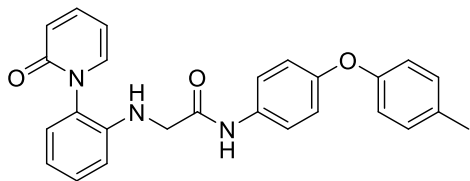
## Compound 1



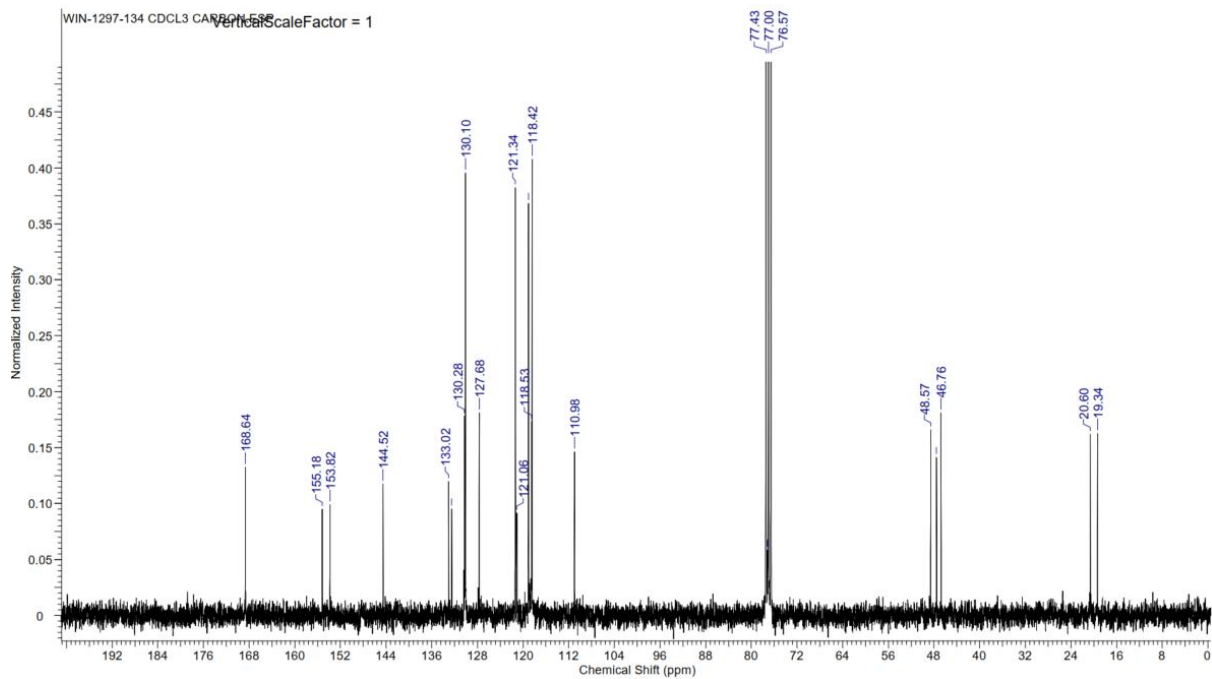
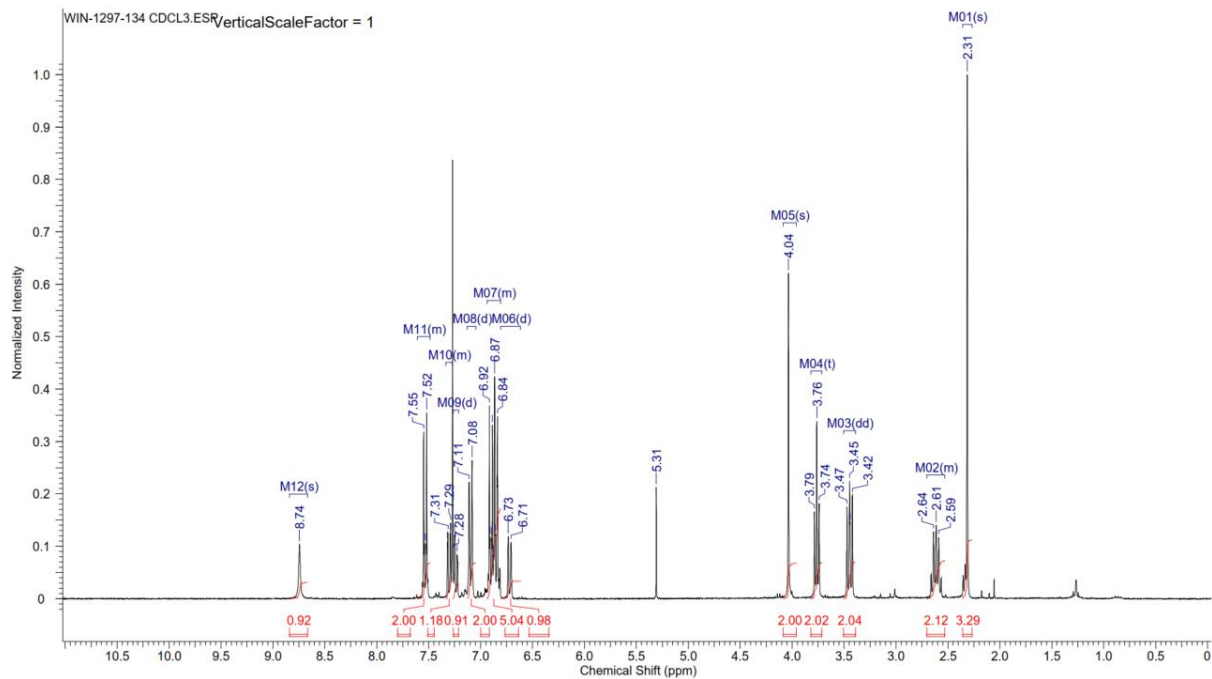
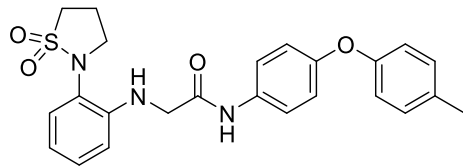
# Compound 2



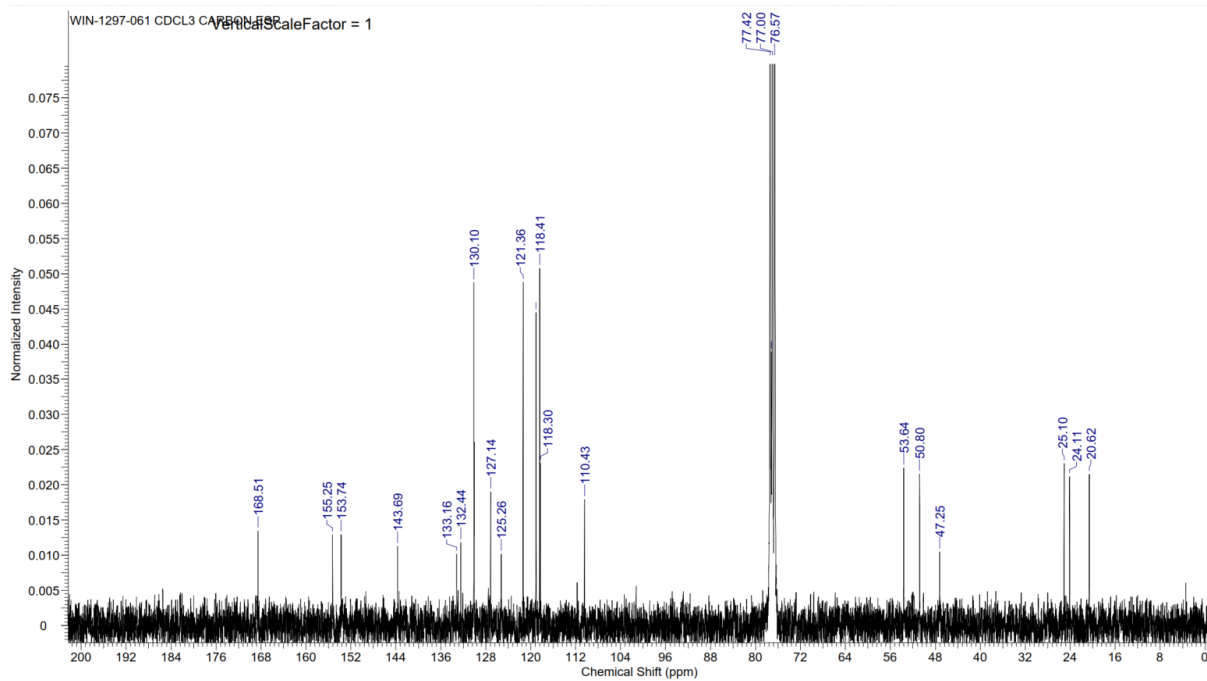
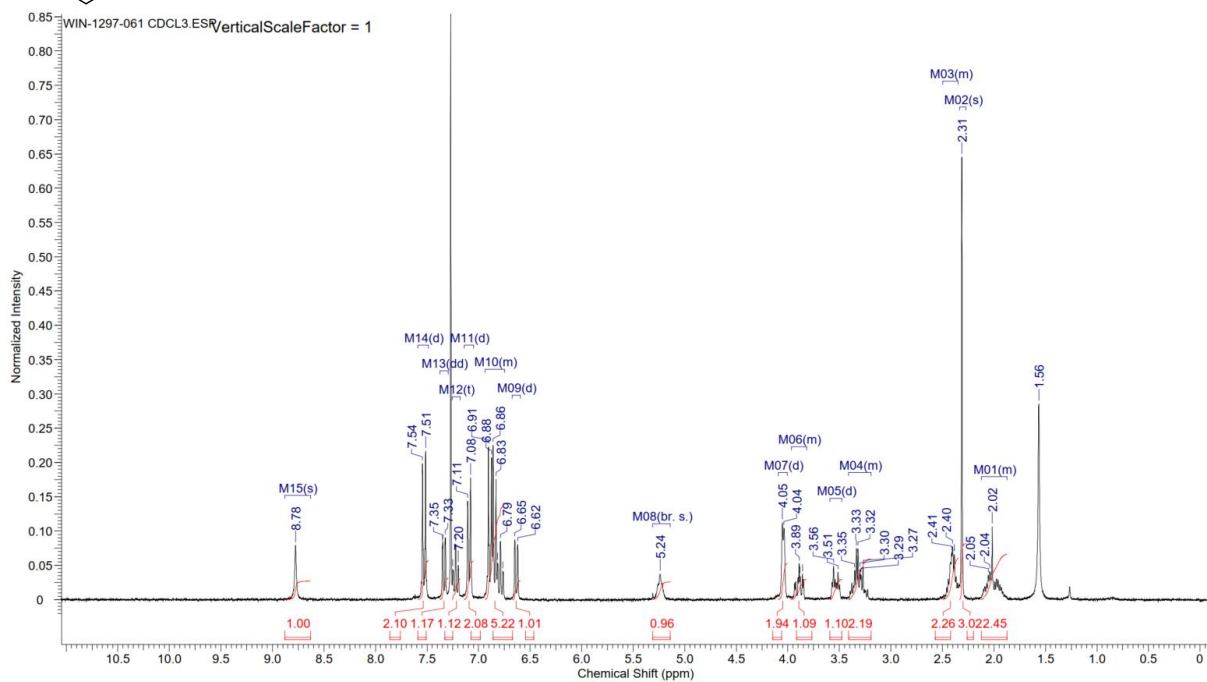
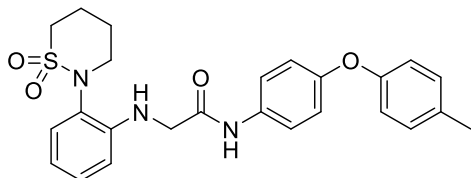
# Compound 3



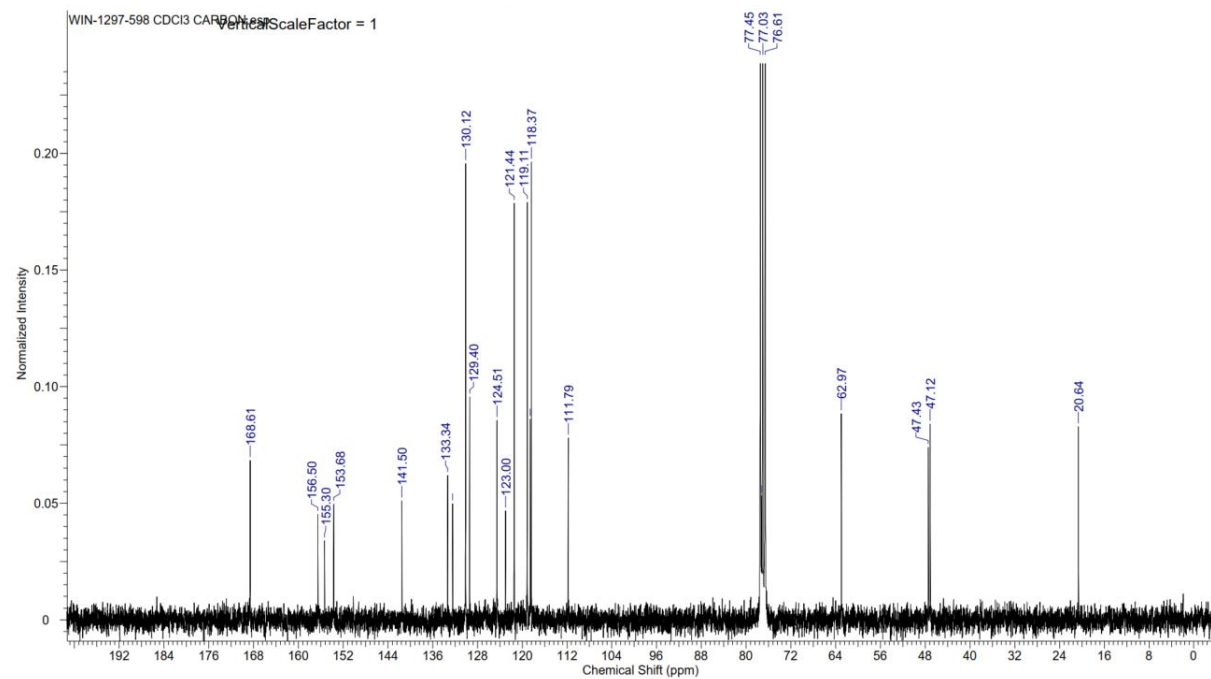
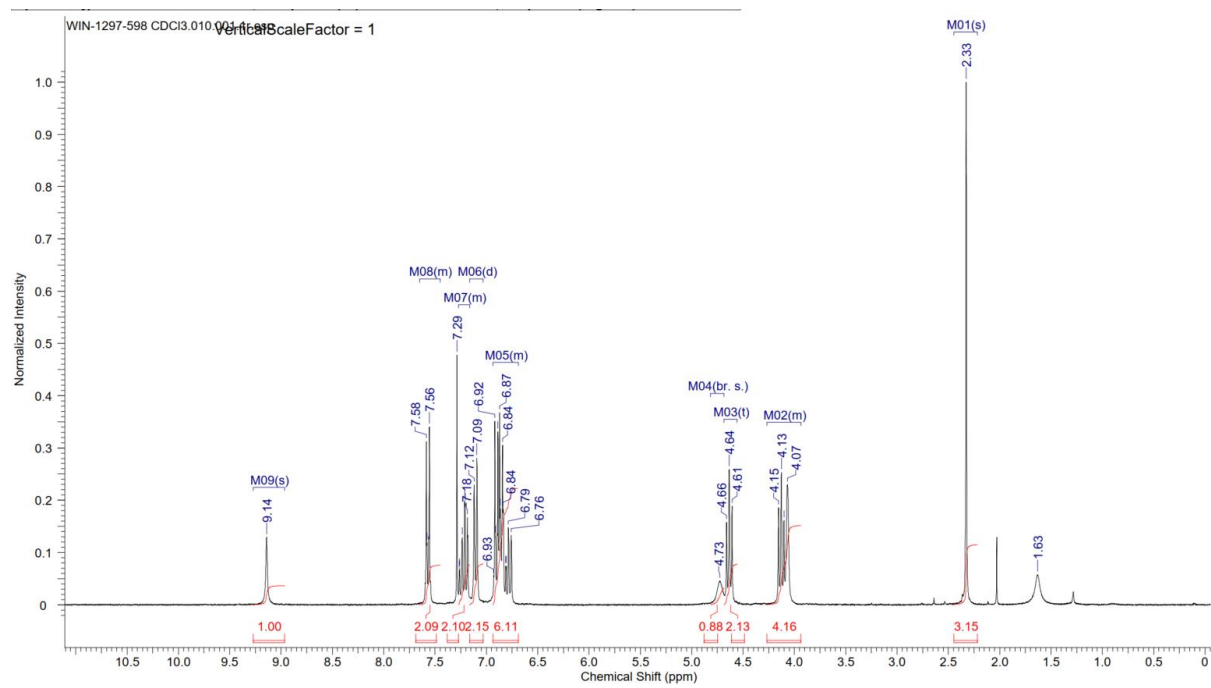
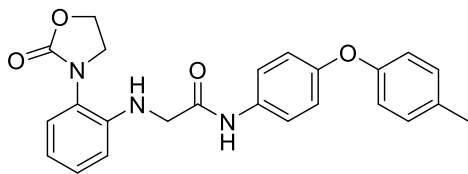
# Compound 4



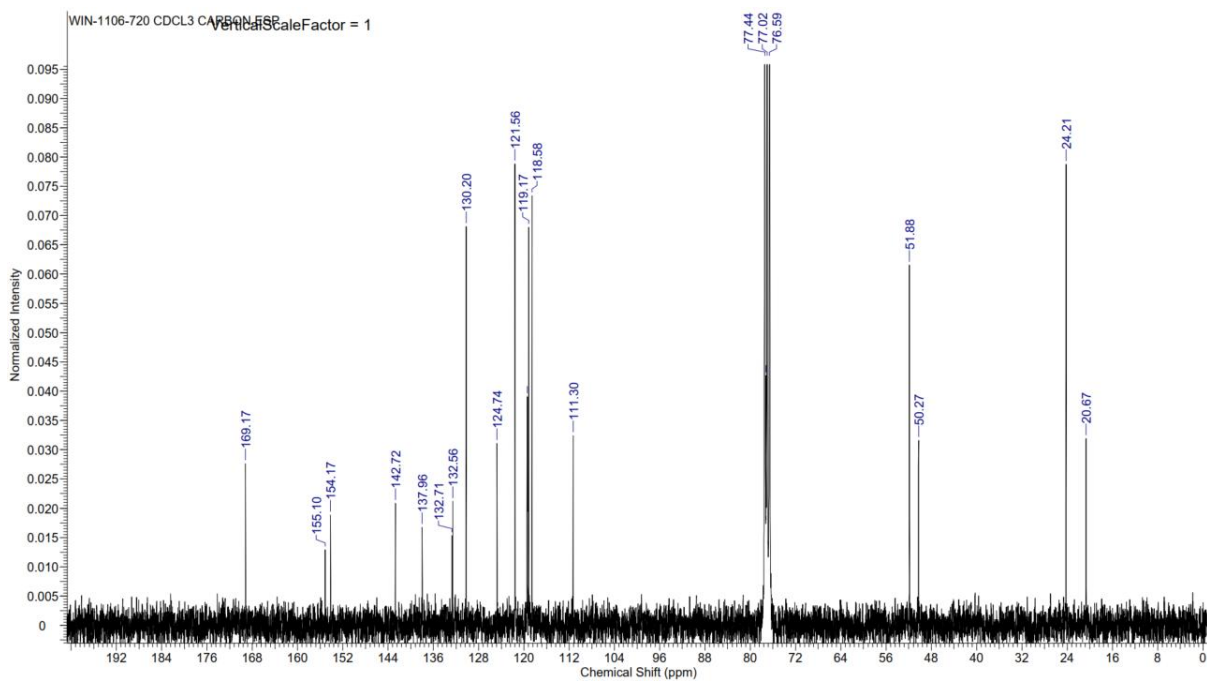
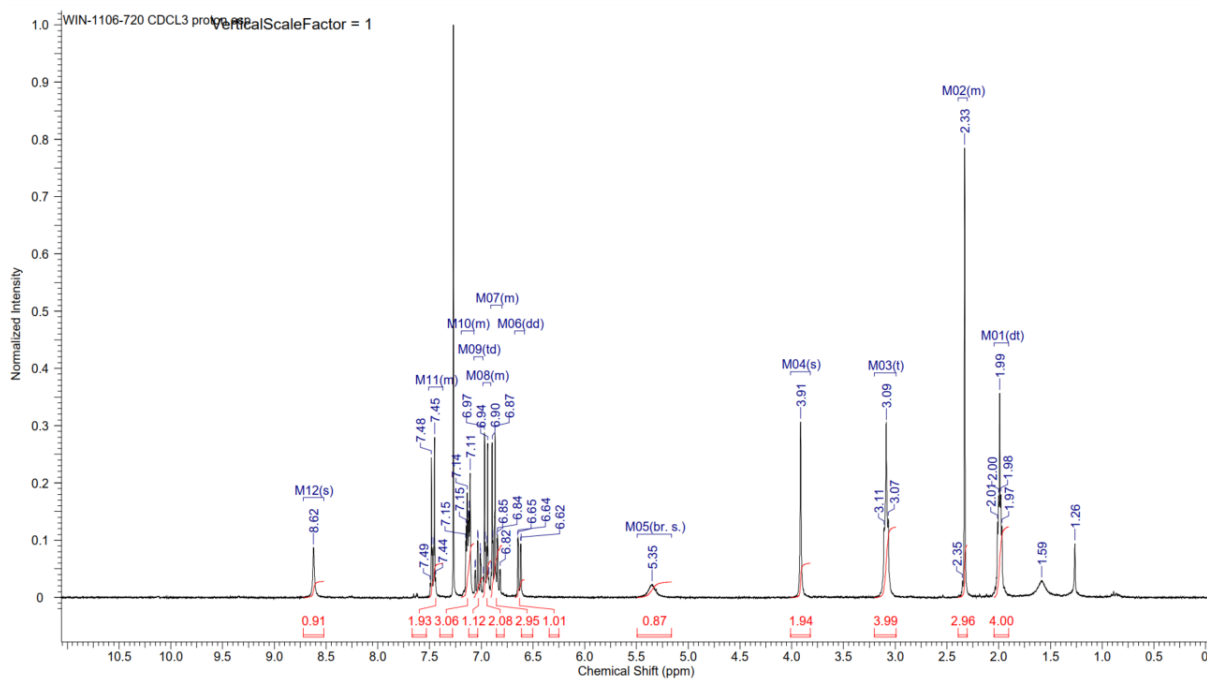
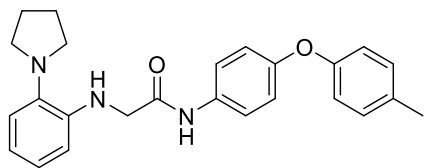
# Compound 5



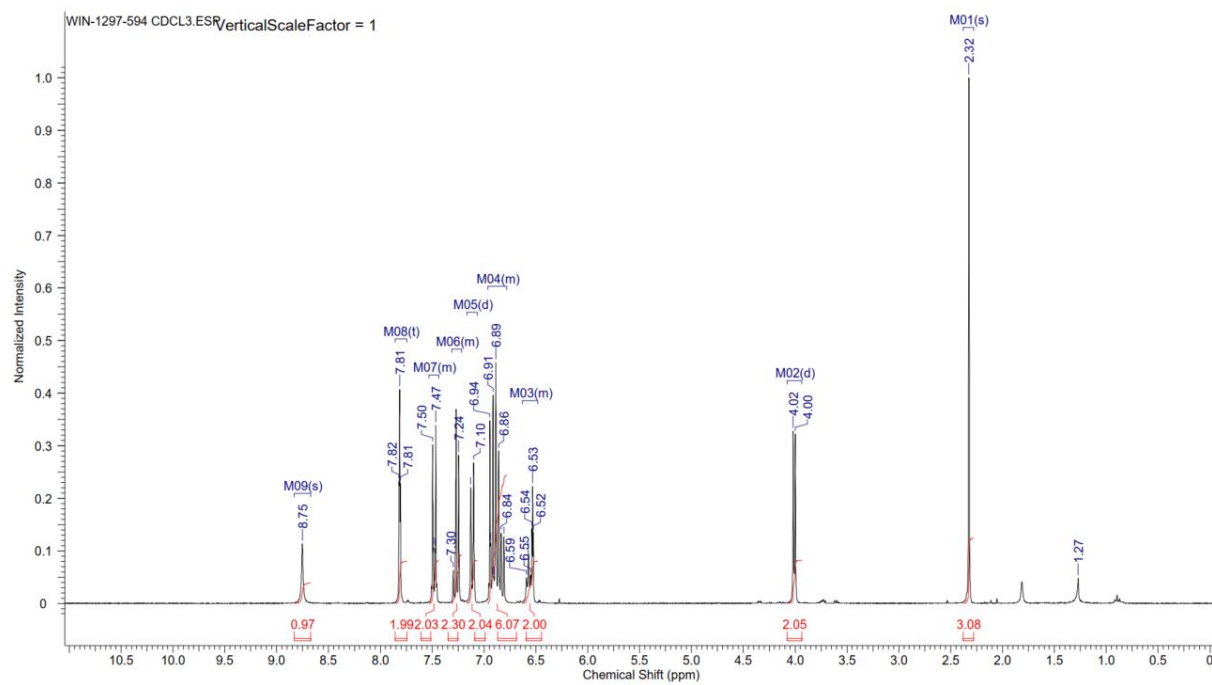
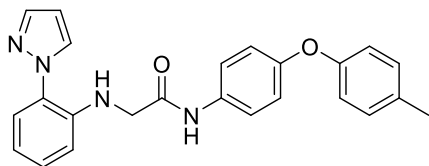
# Compound 6



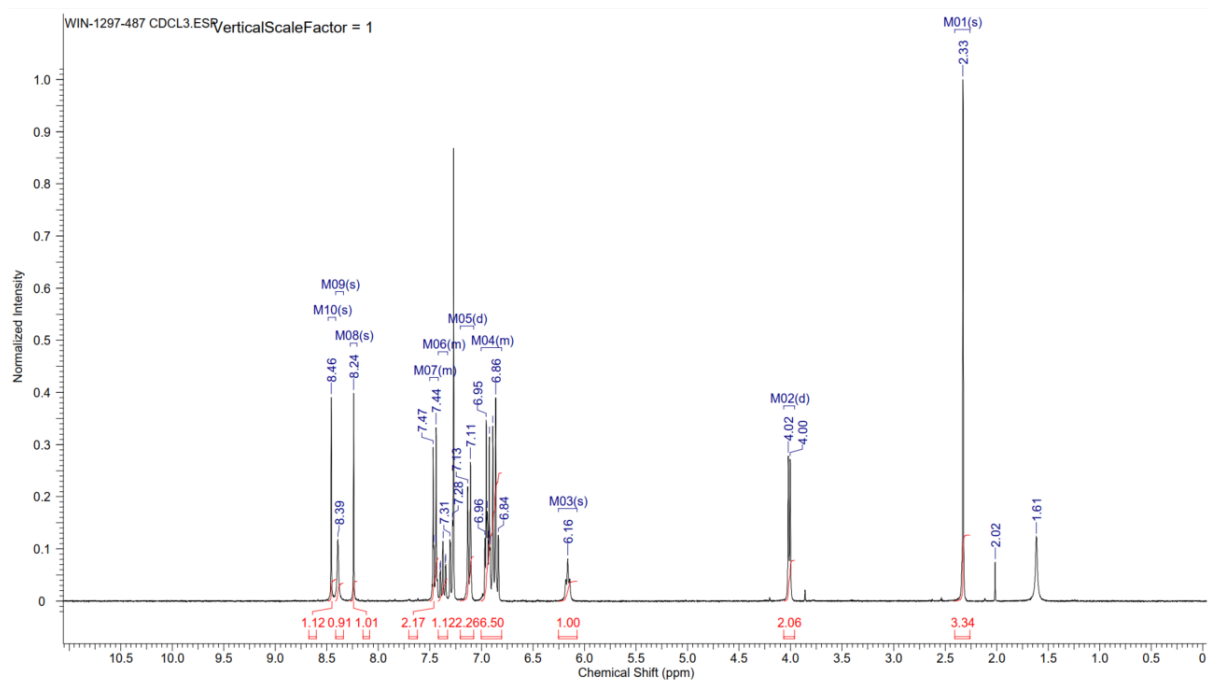
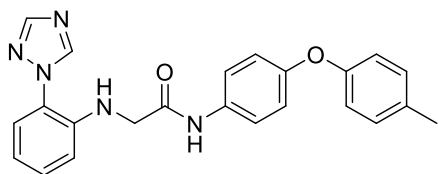
# Compound 7



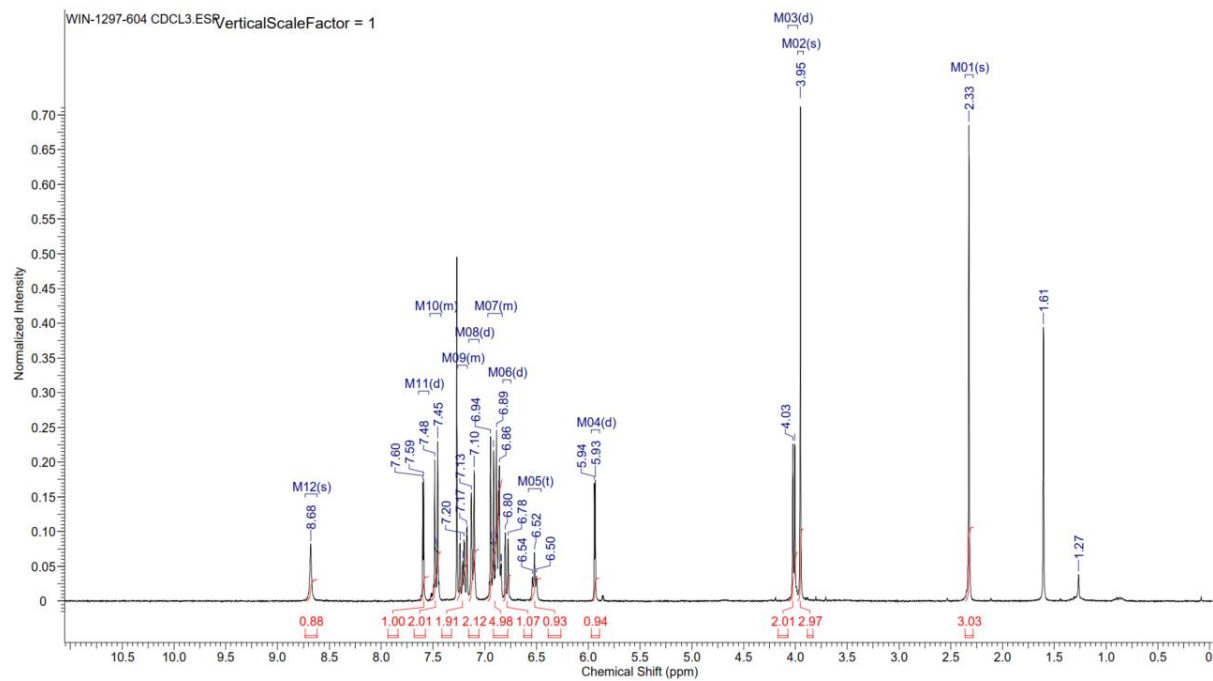
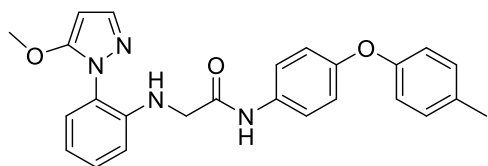
# Compound 8



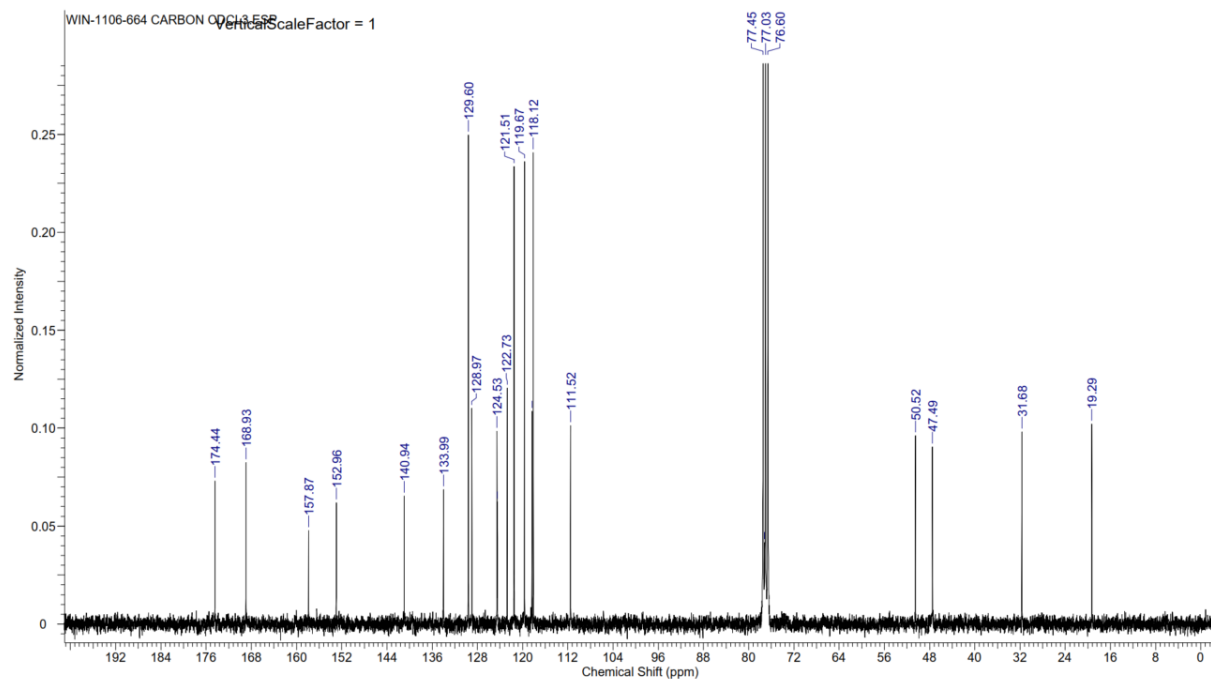
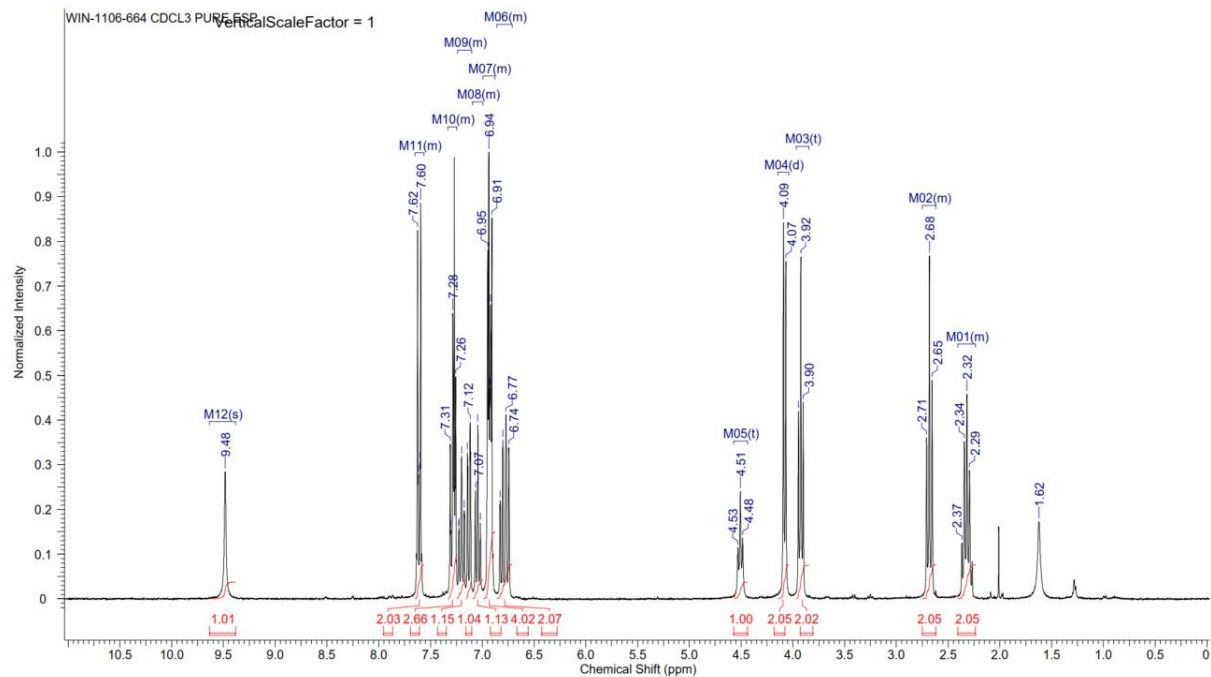
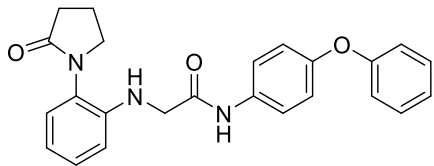
# Compound 9



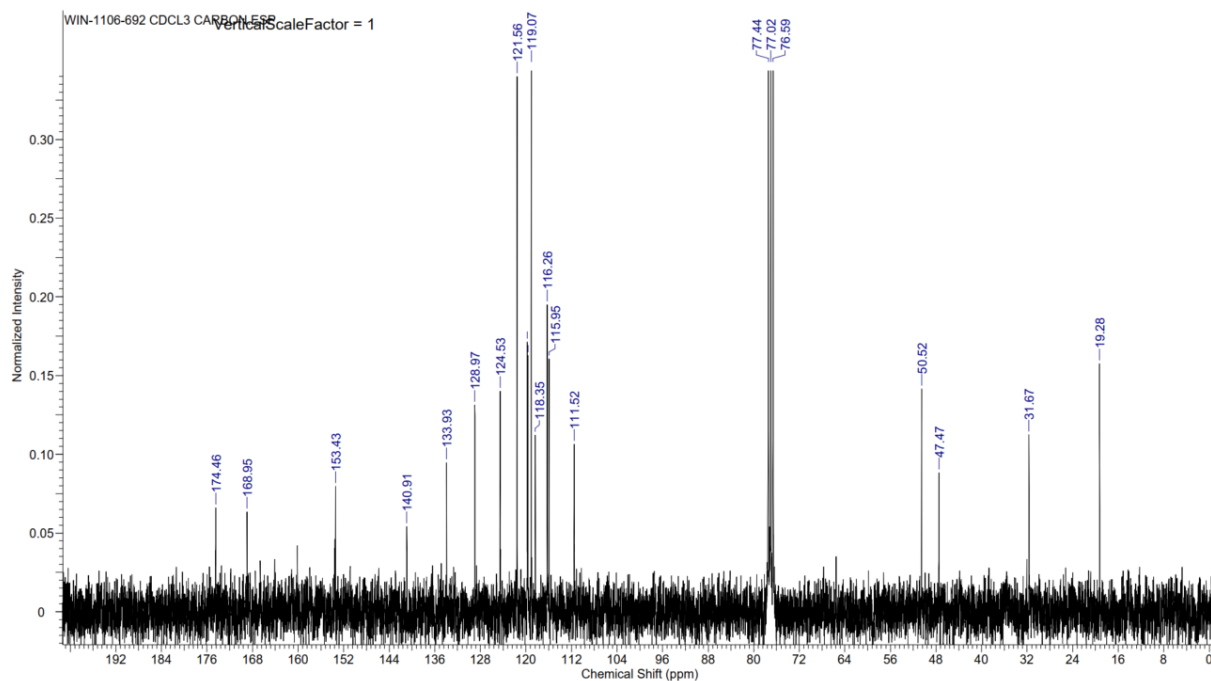
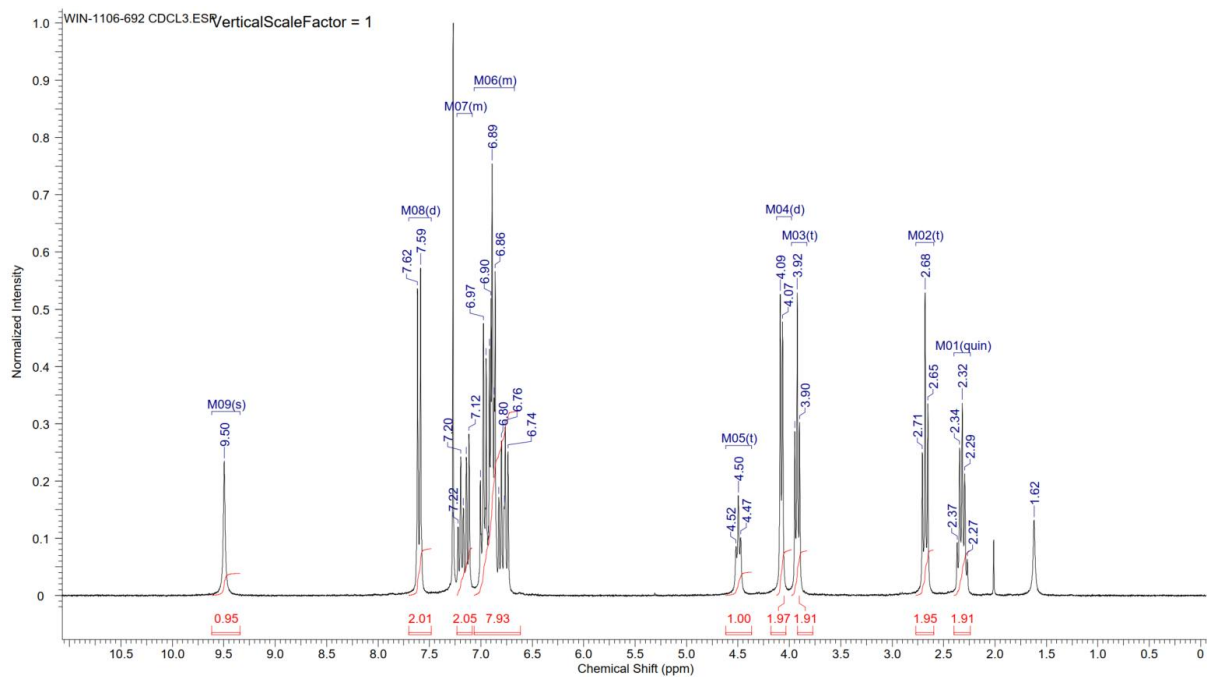
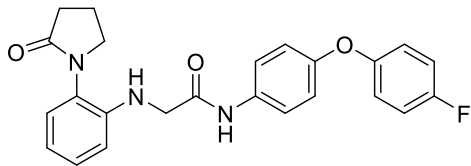
# Compound 10



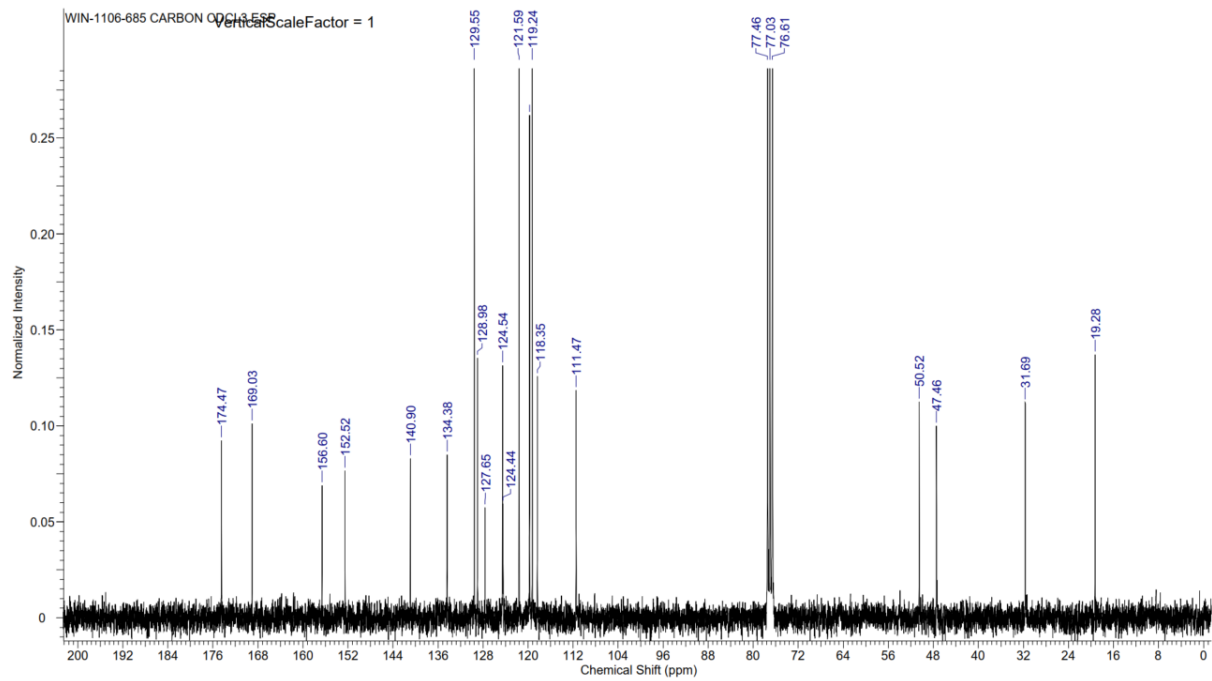
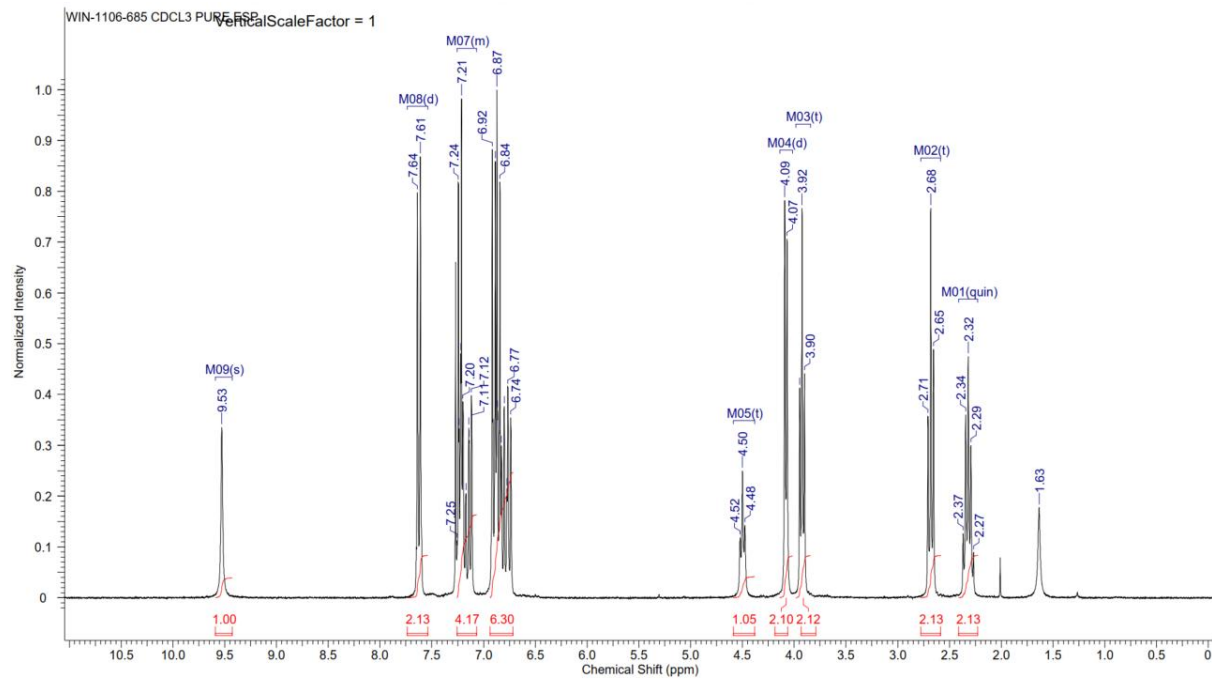
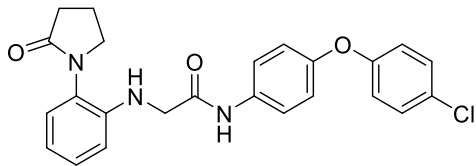
# Compound 11



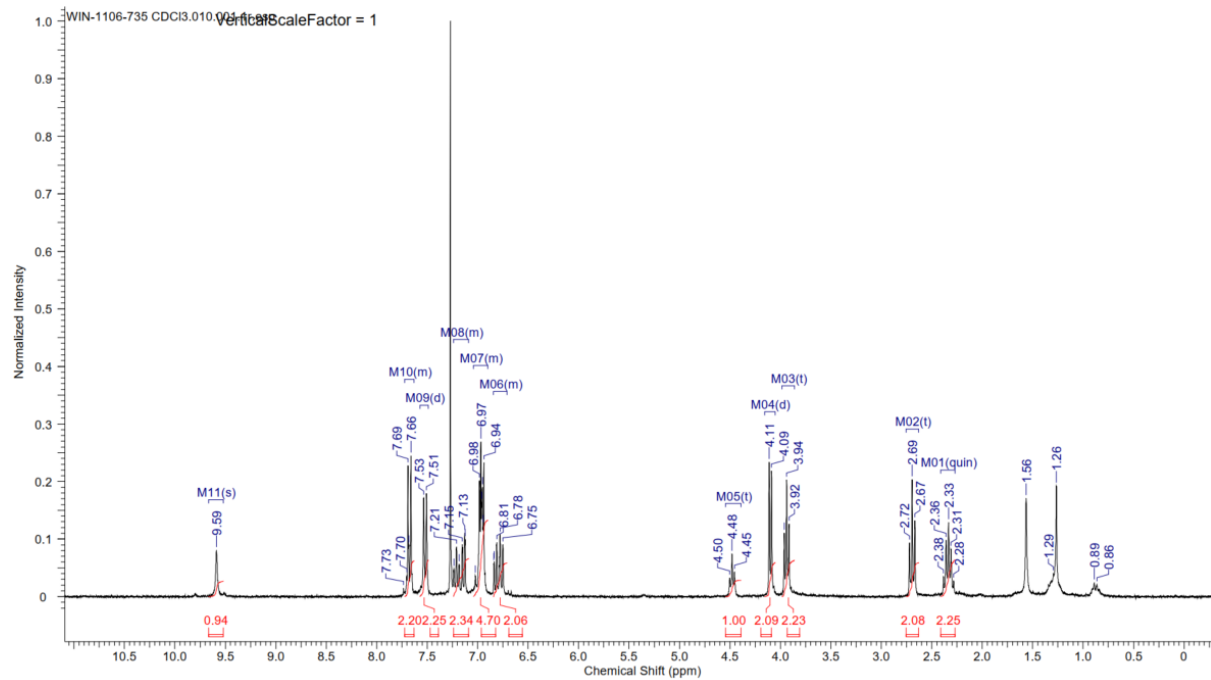
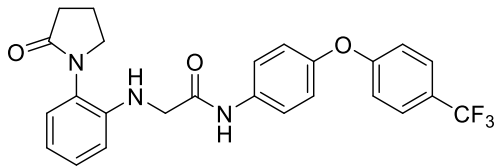
# Compound 12



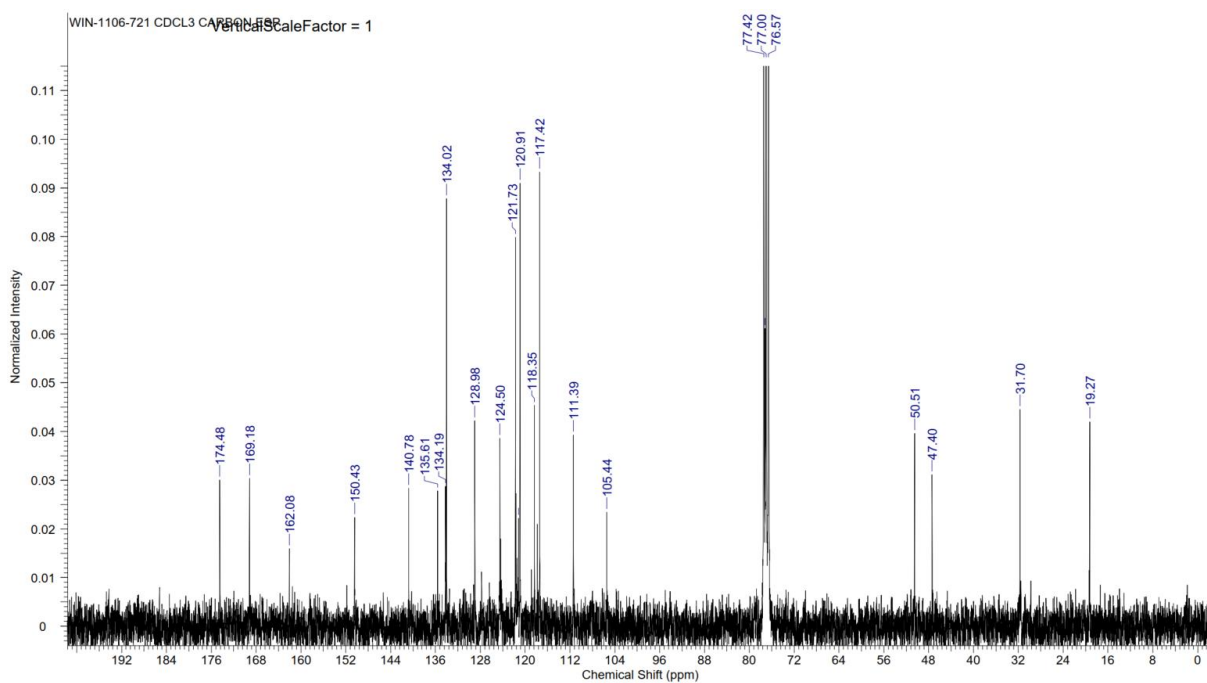
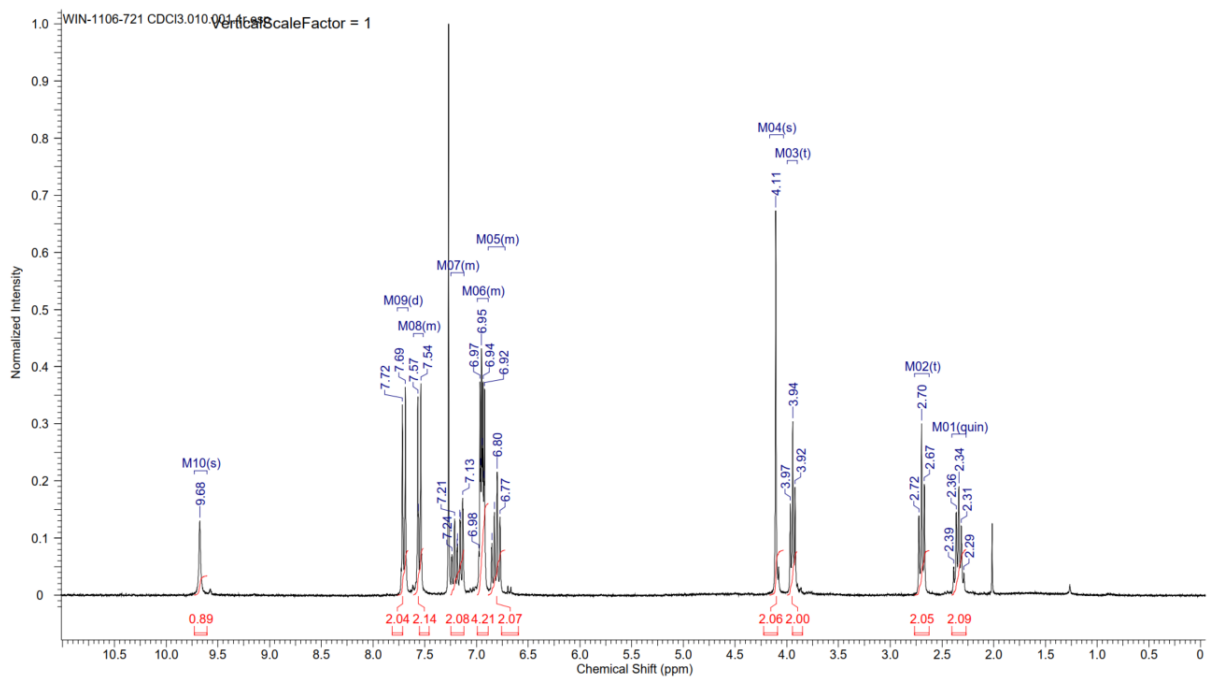
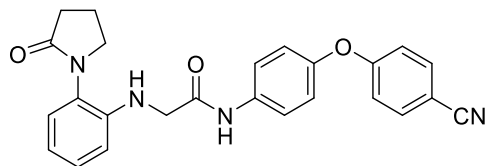
# Compound 13



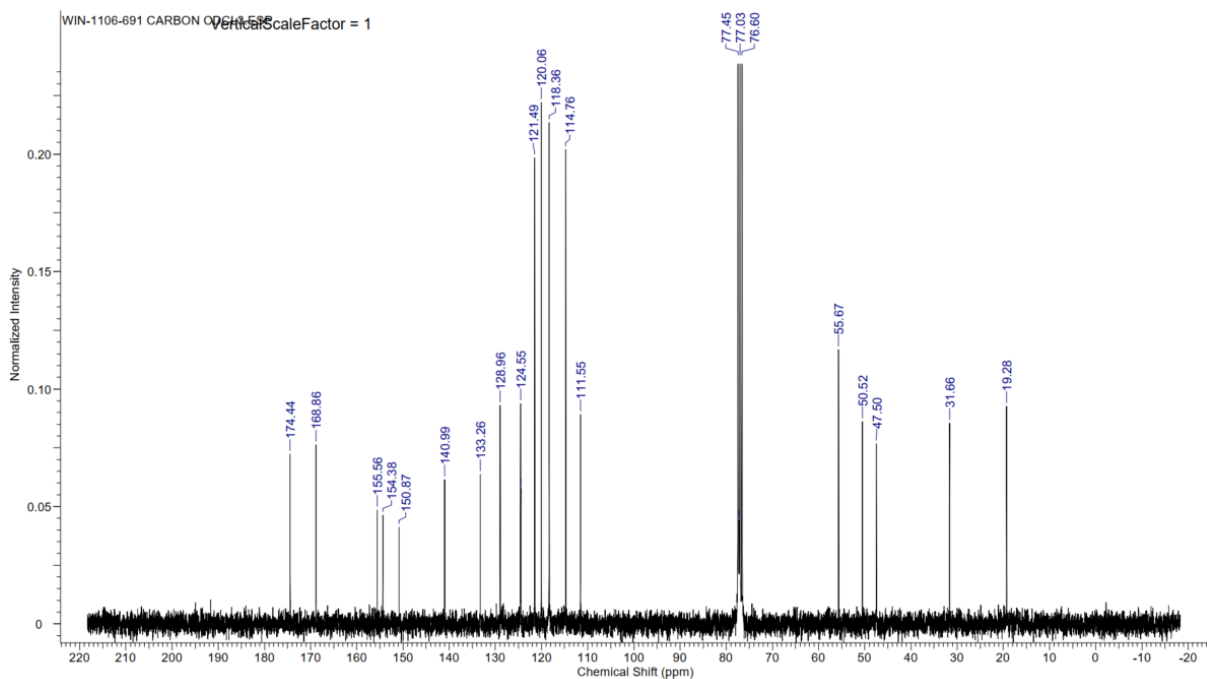
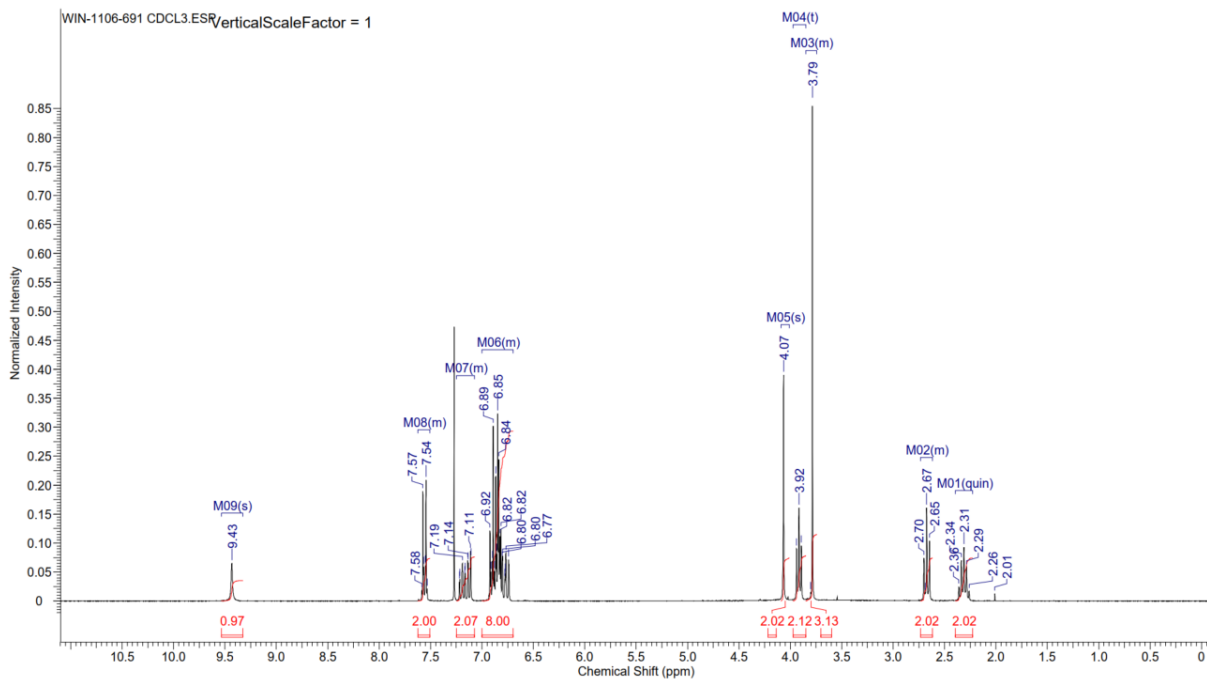
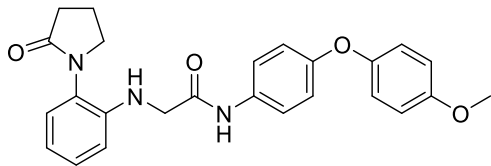
# Compound 14



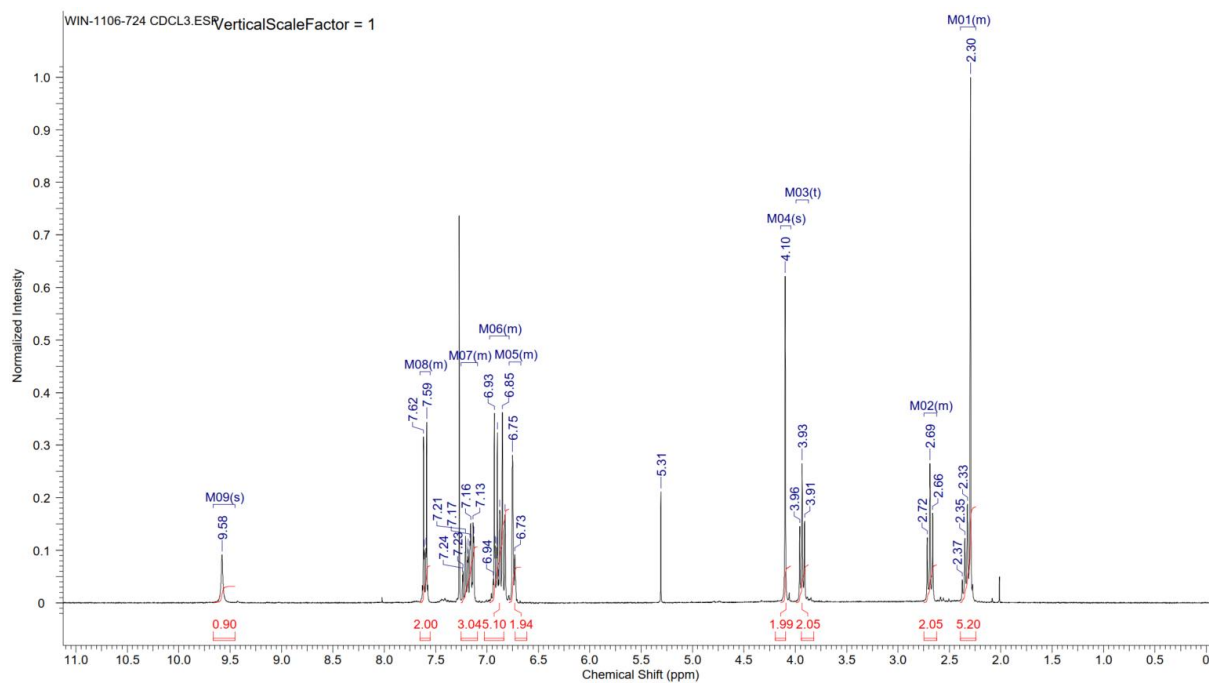
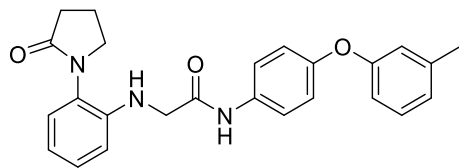
# Compound 15



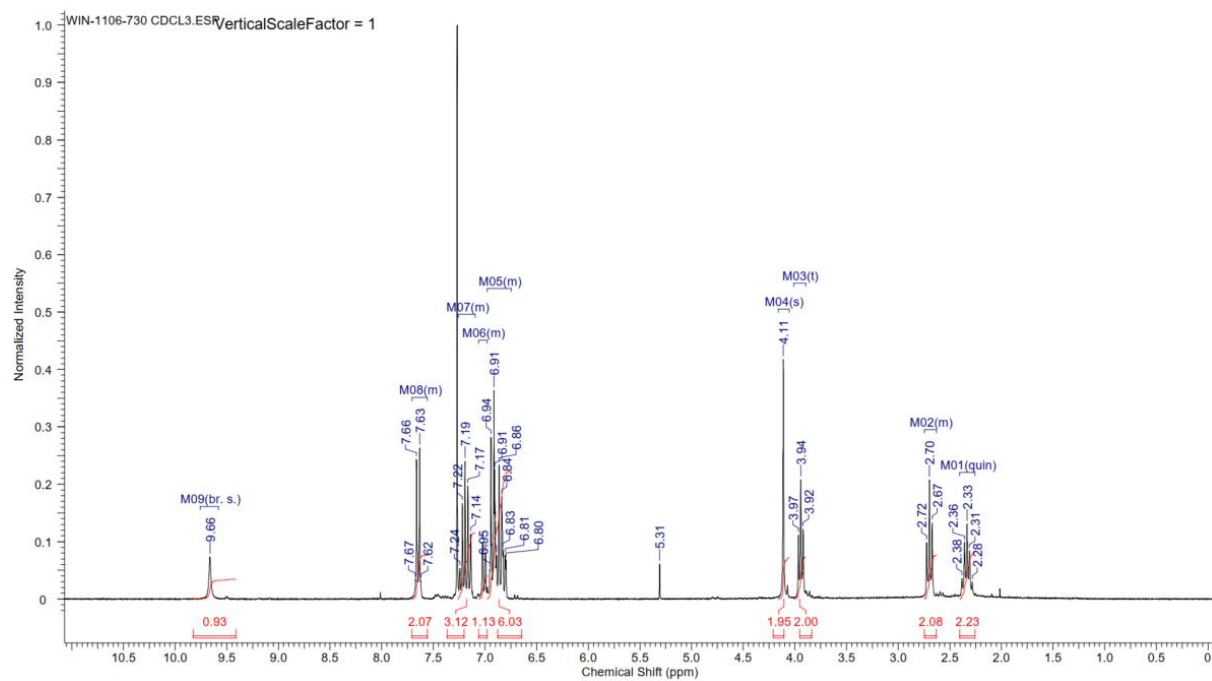
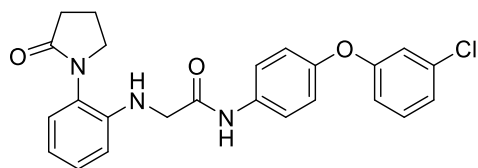
# Compound 16



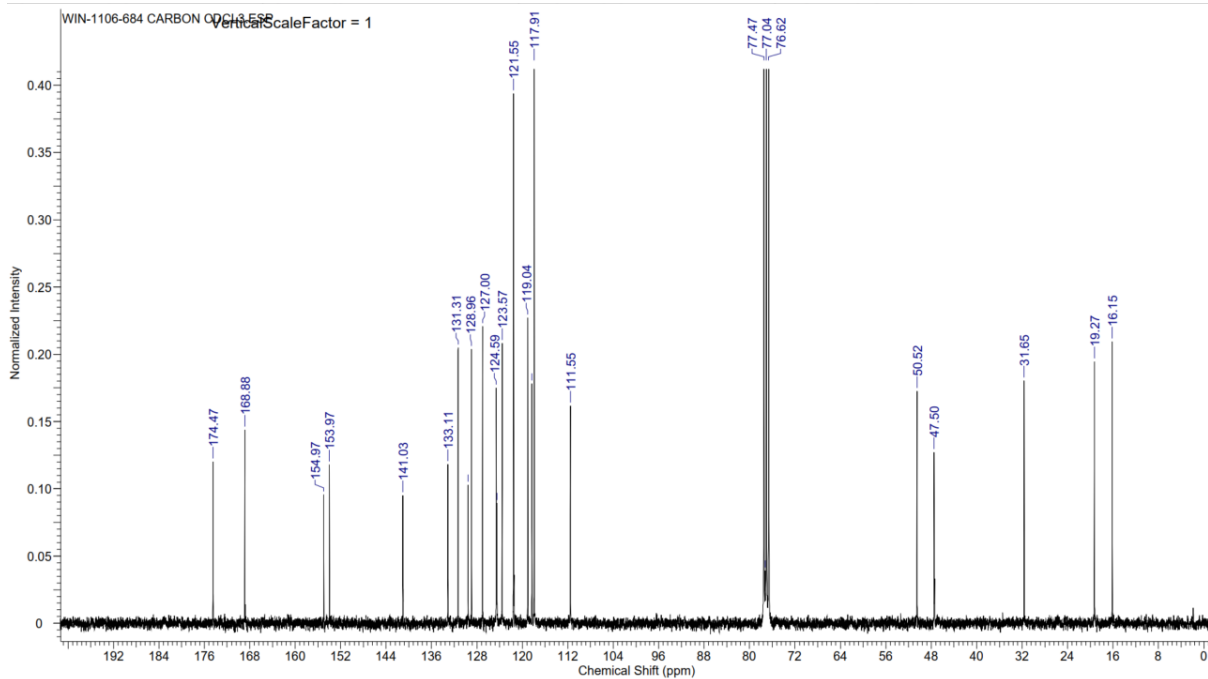
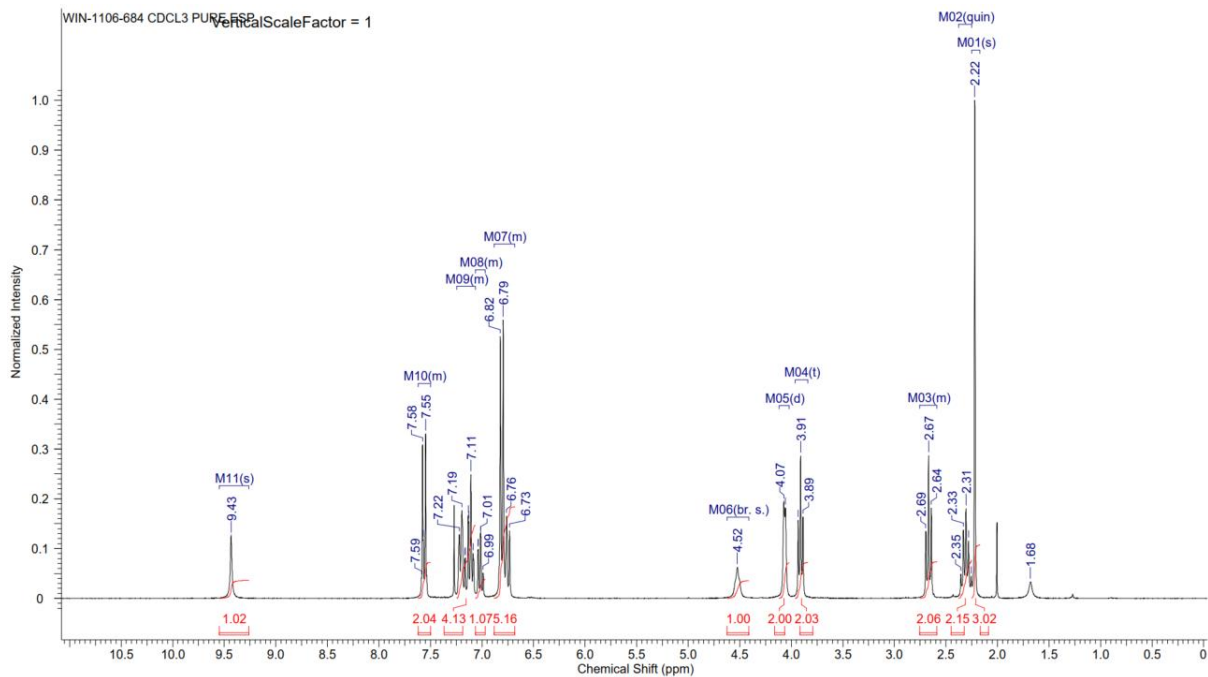
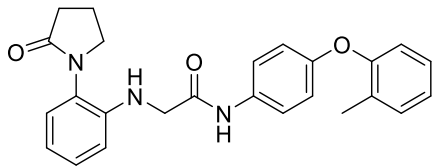
# Compound 17



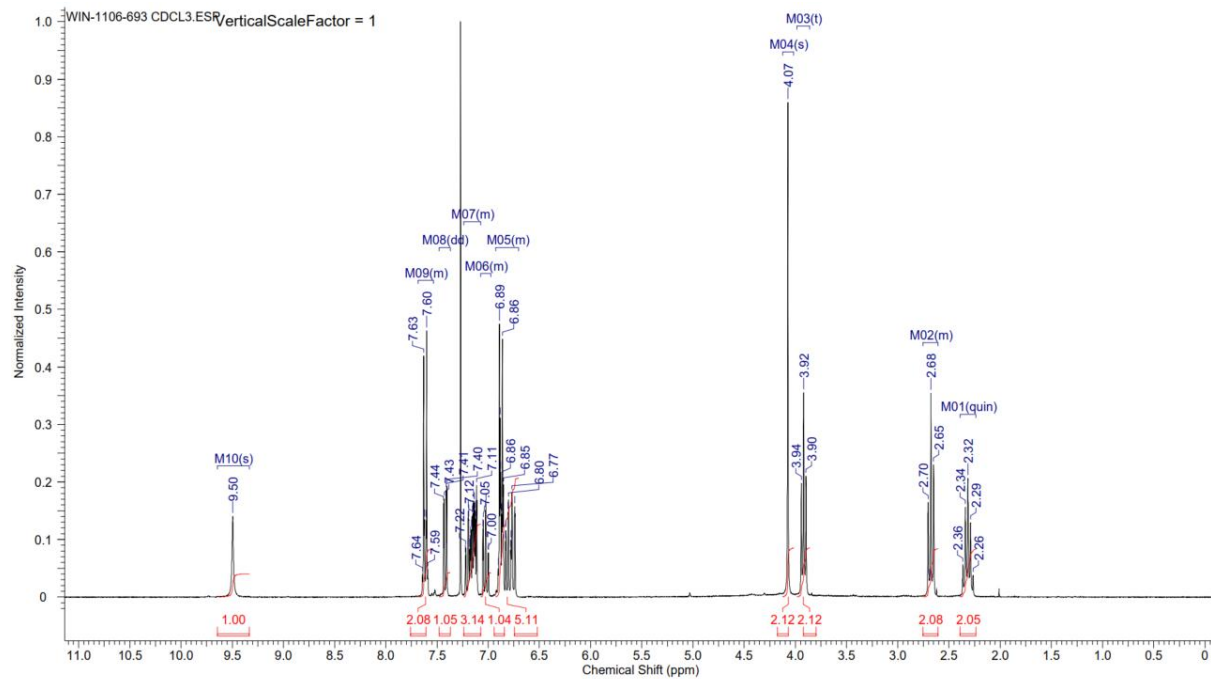
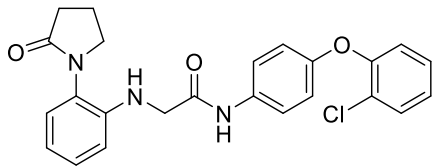
# Compound 18



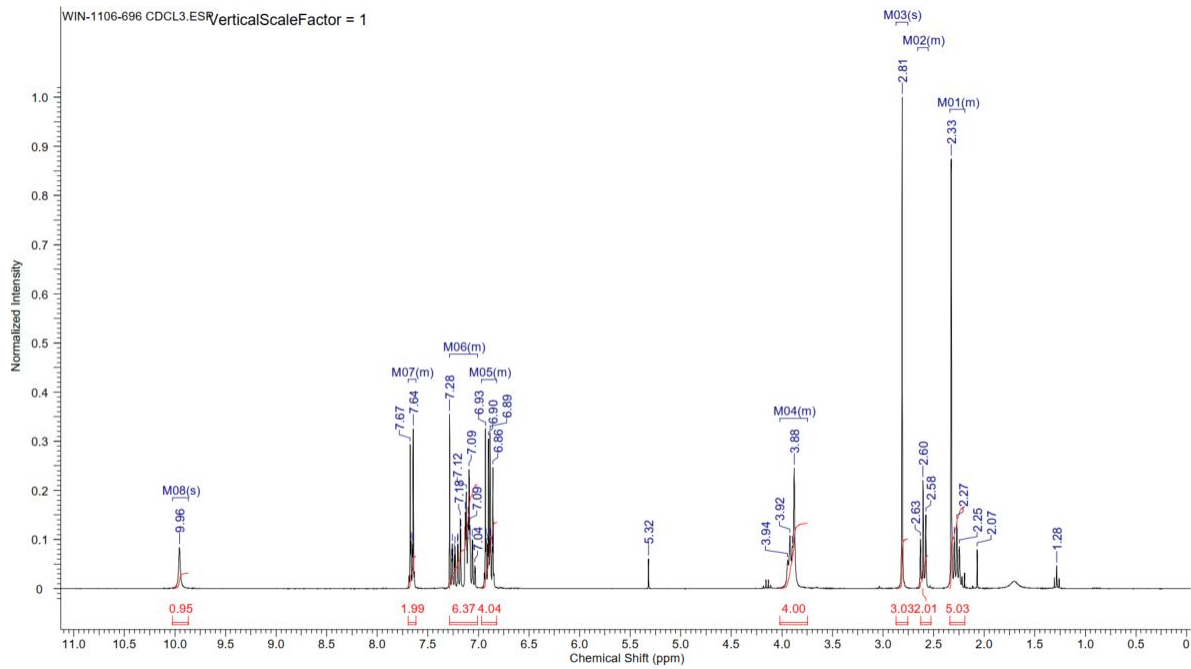
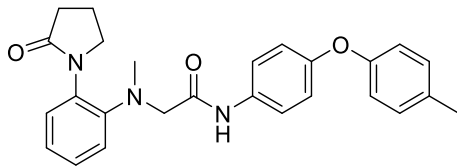
# Compound 19



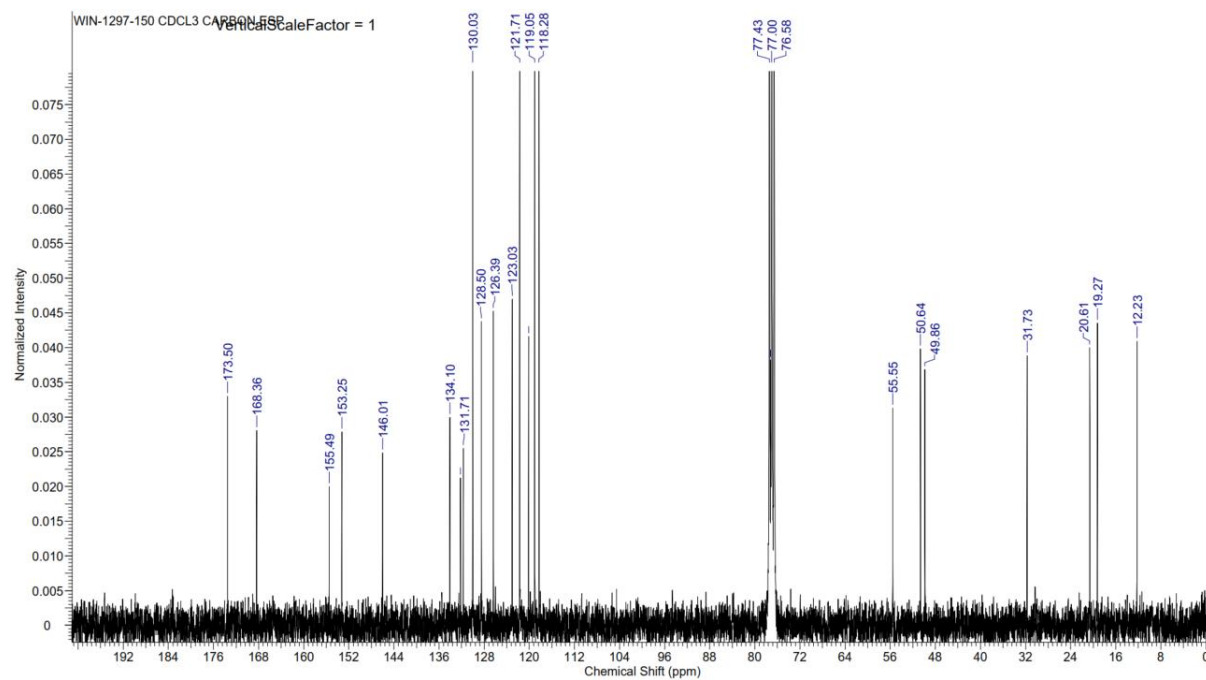
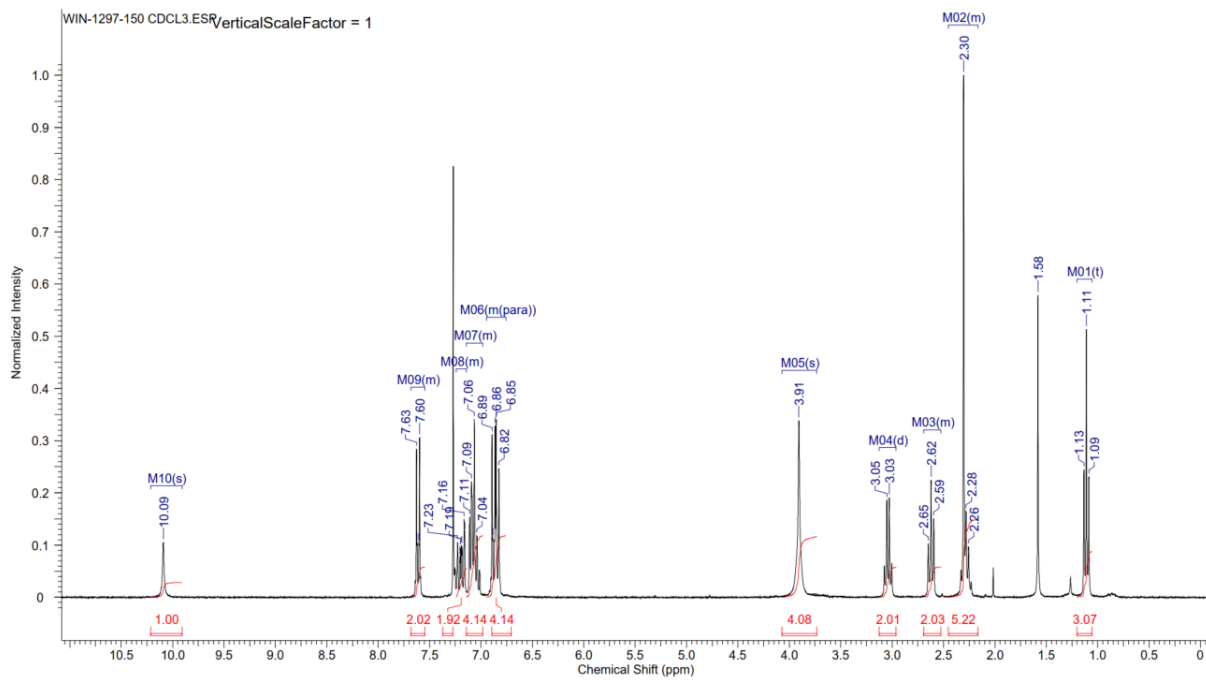
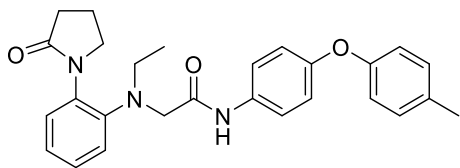
# Compound 20



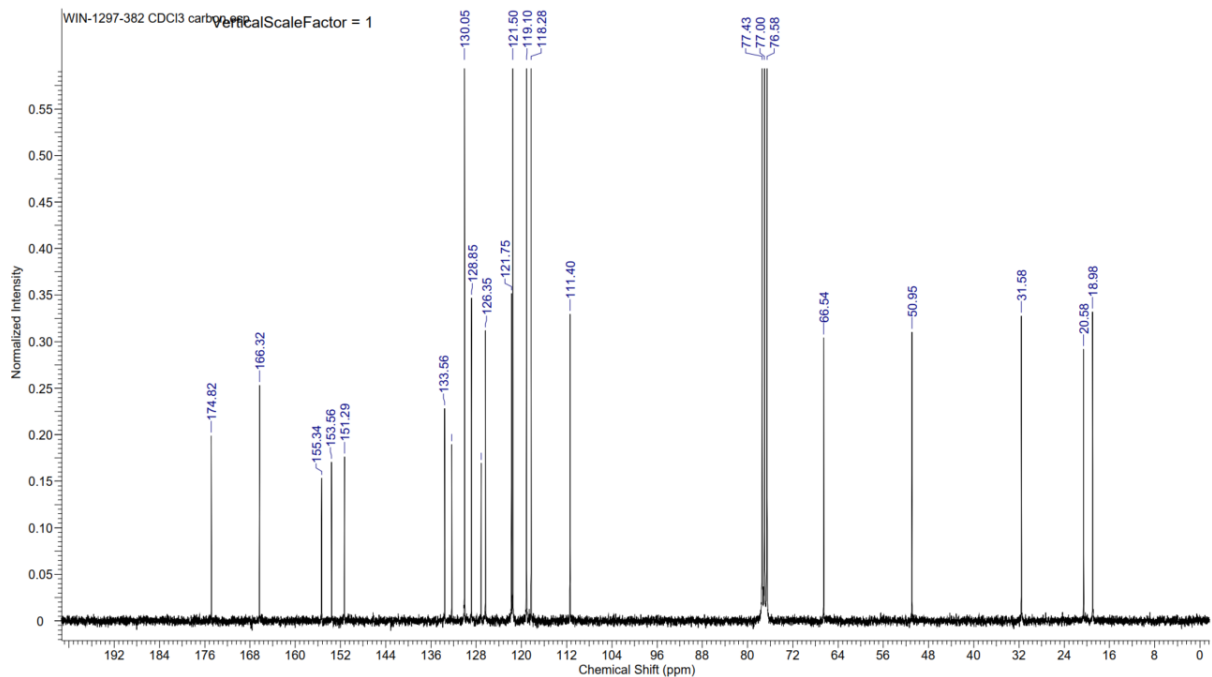
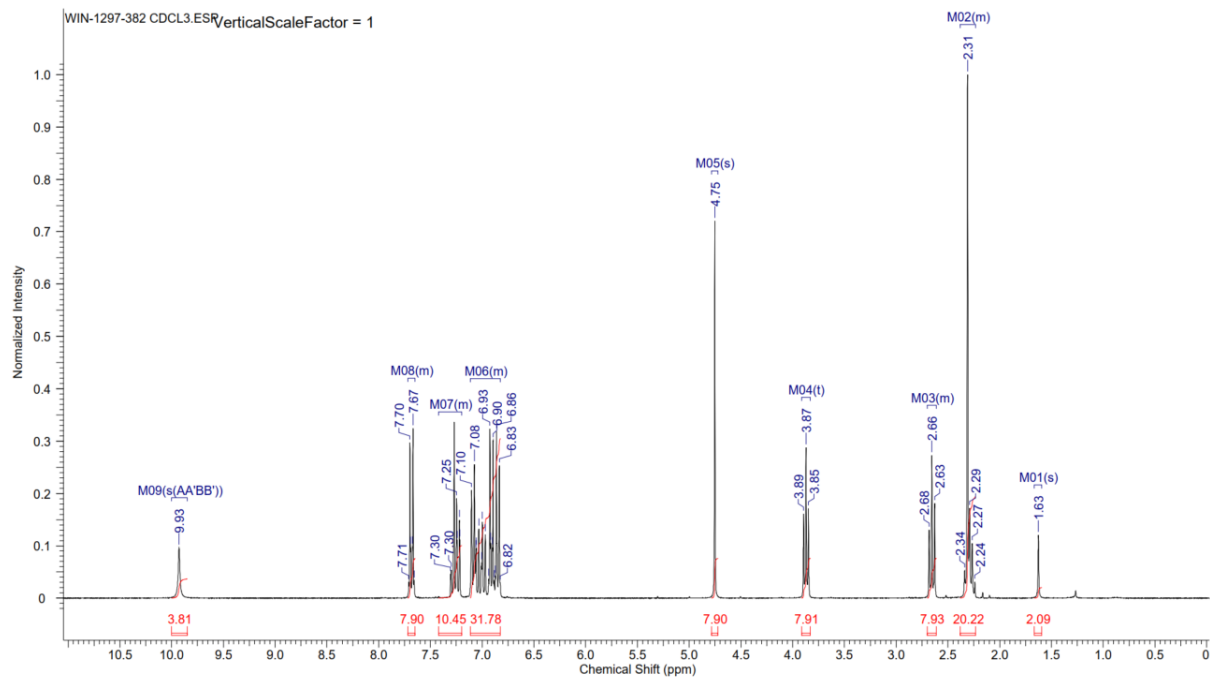
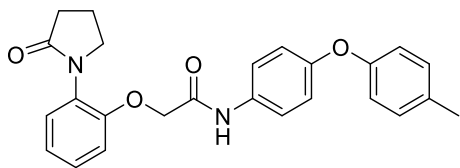
# Compound 21



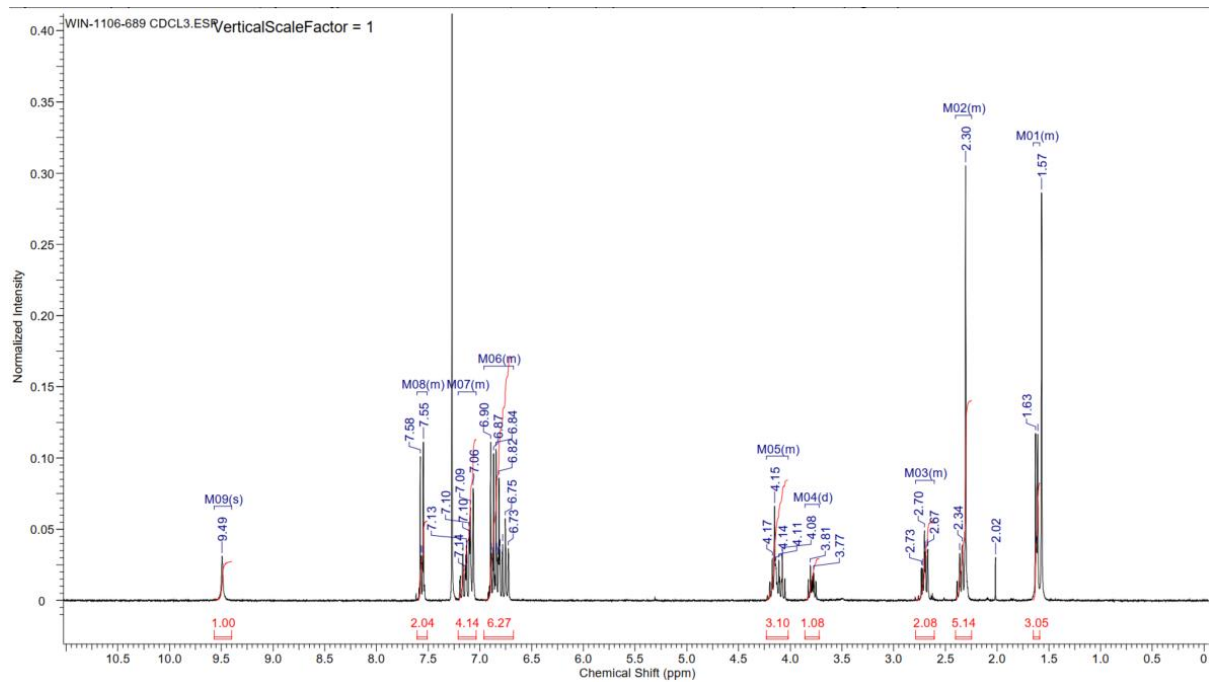
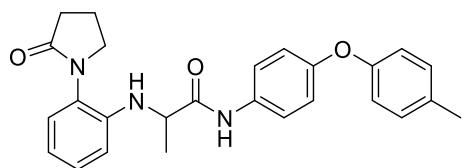
# Compound 22



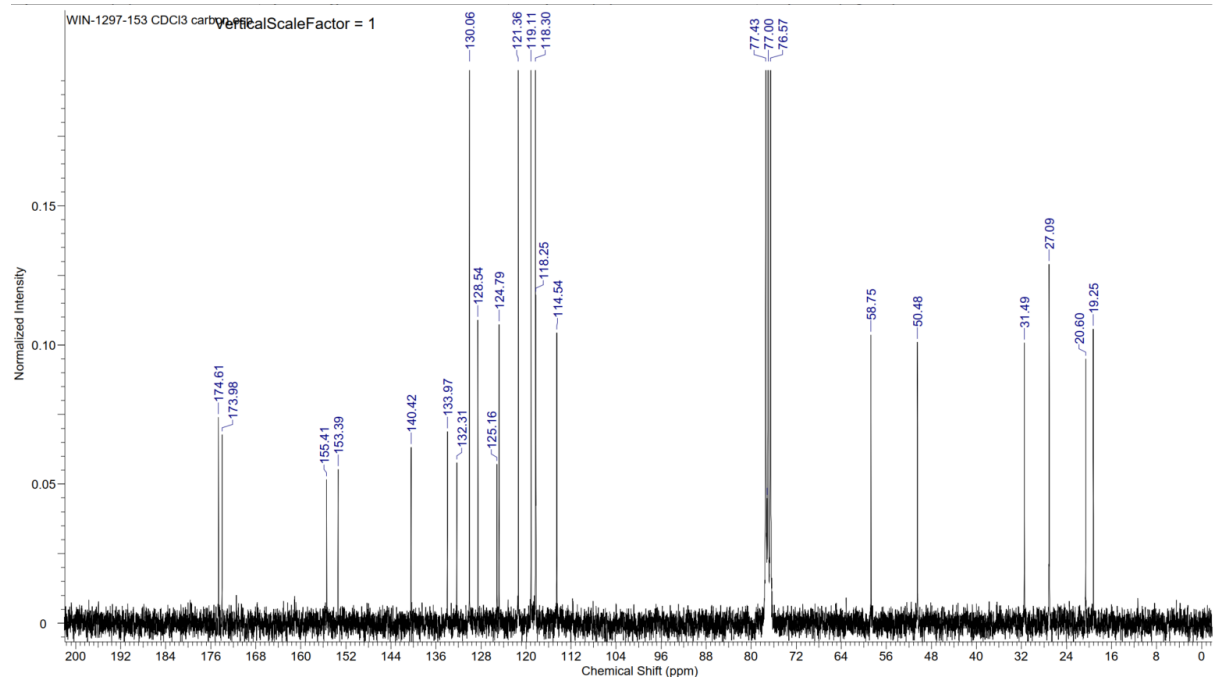
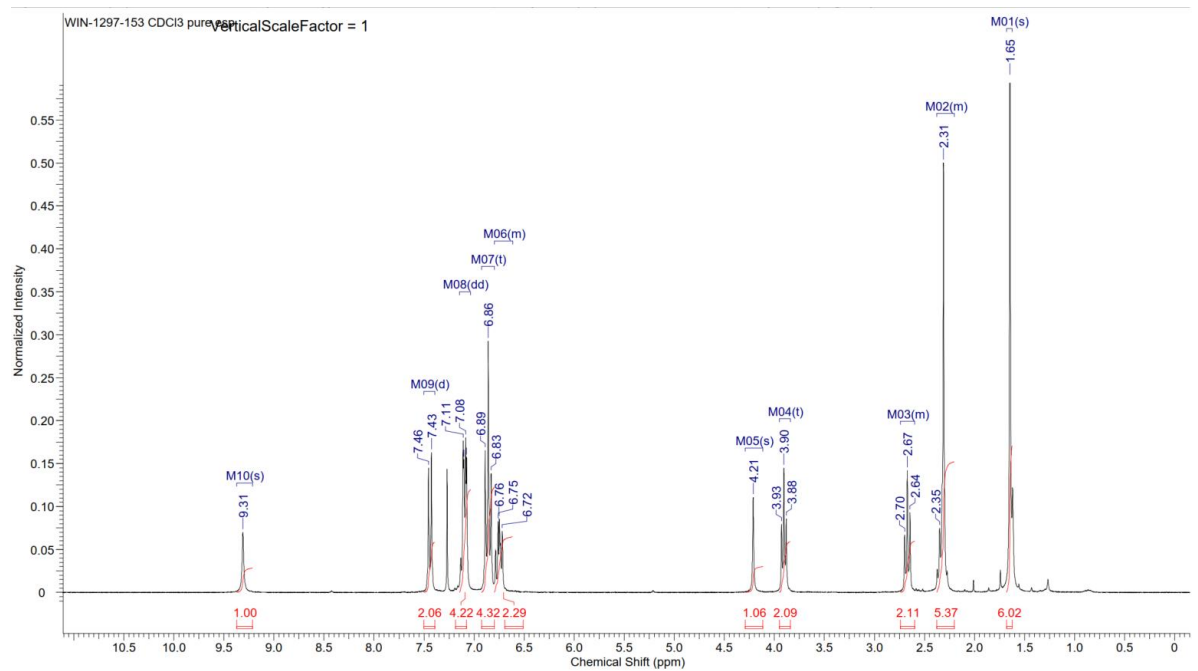
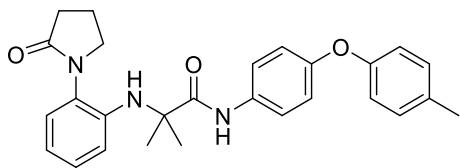
# Compound 23



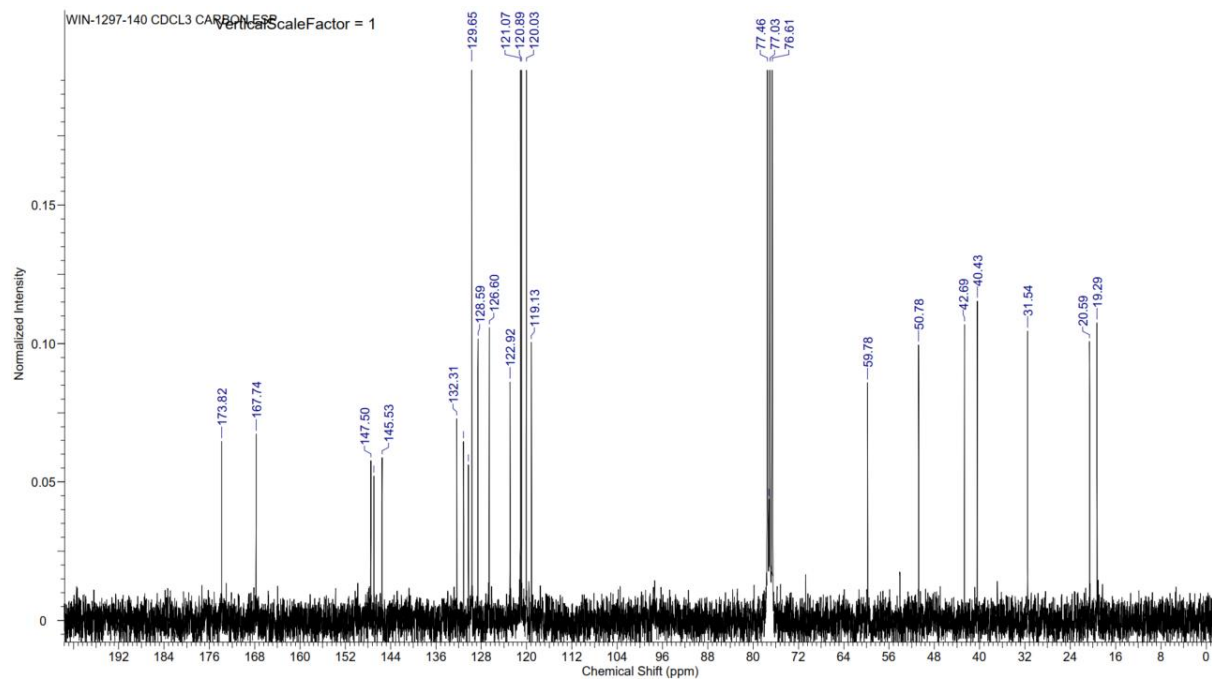
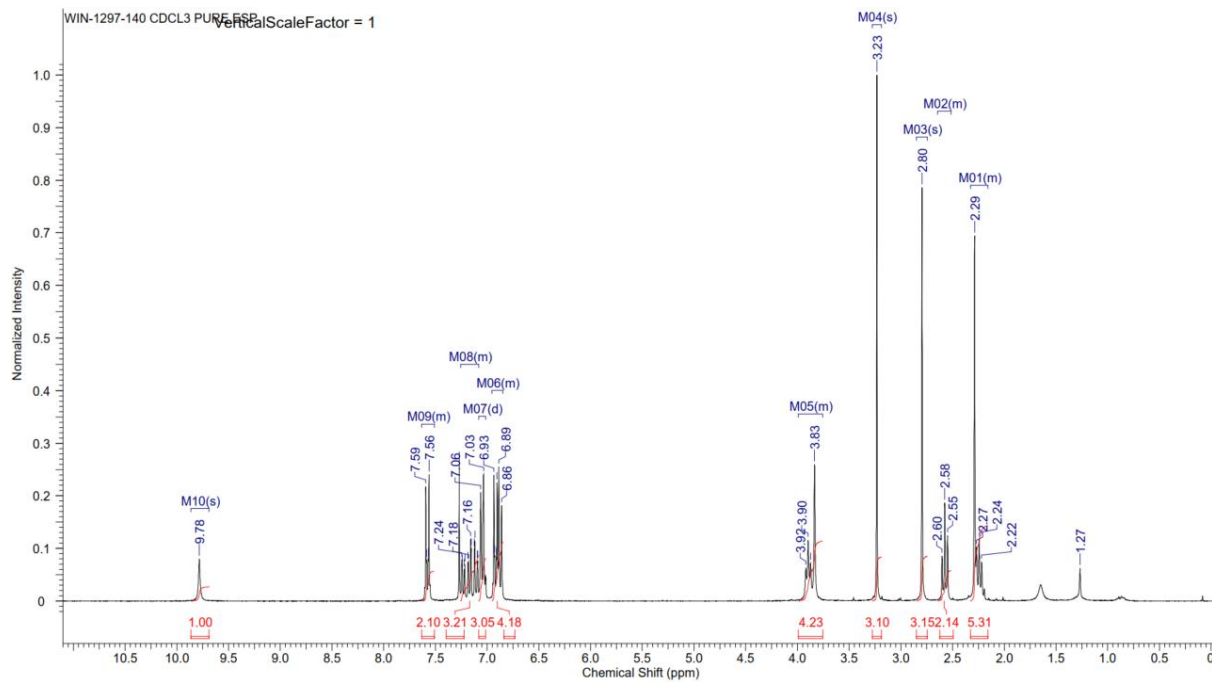
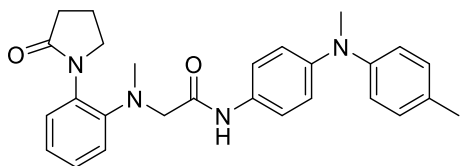
# Compound 24



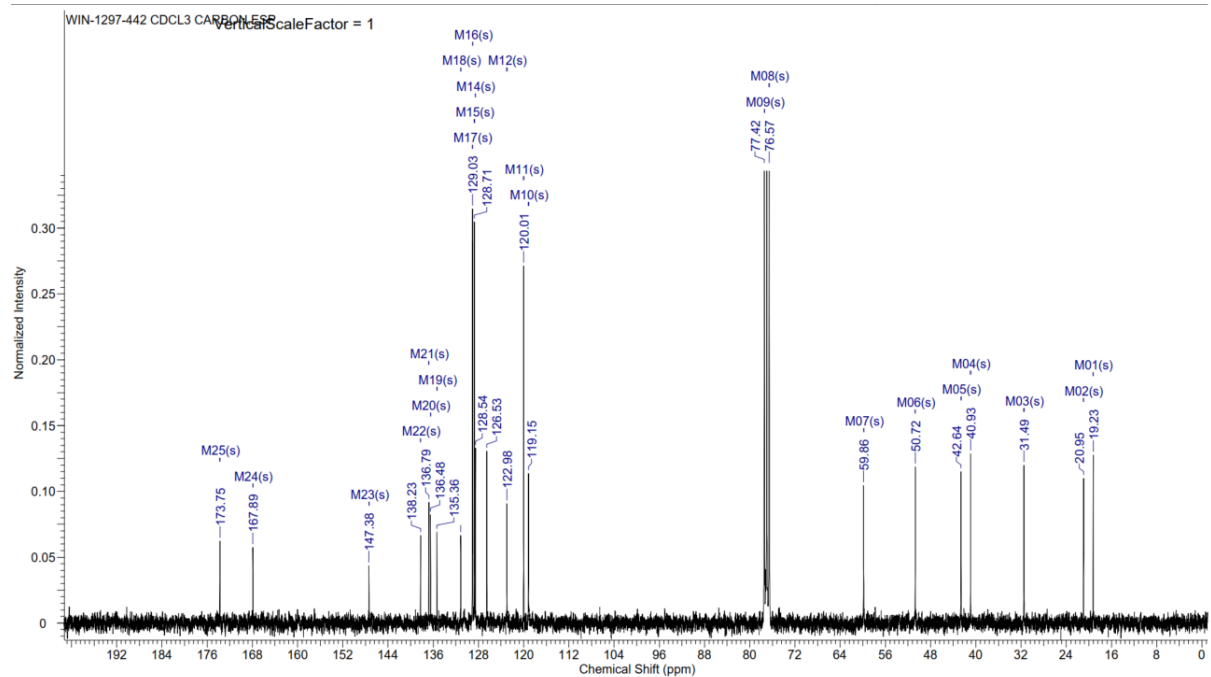
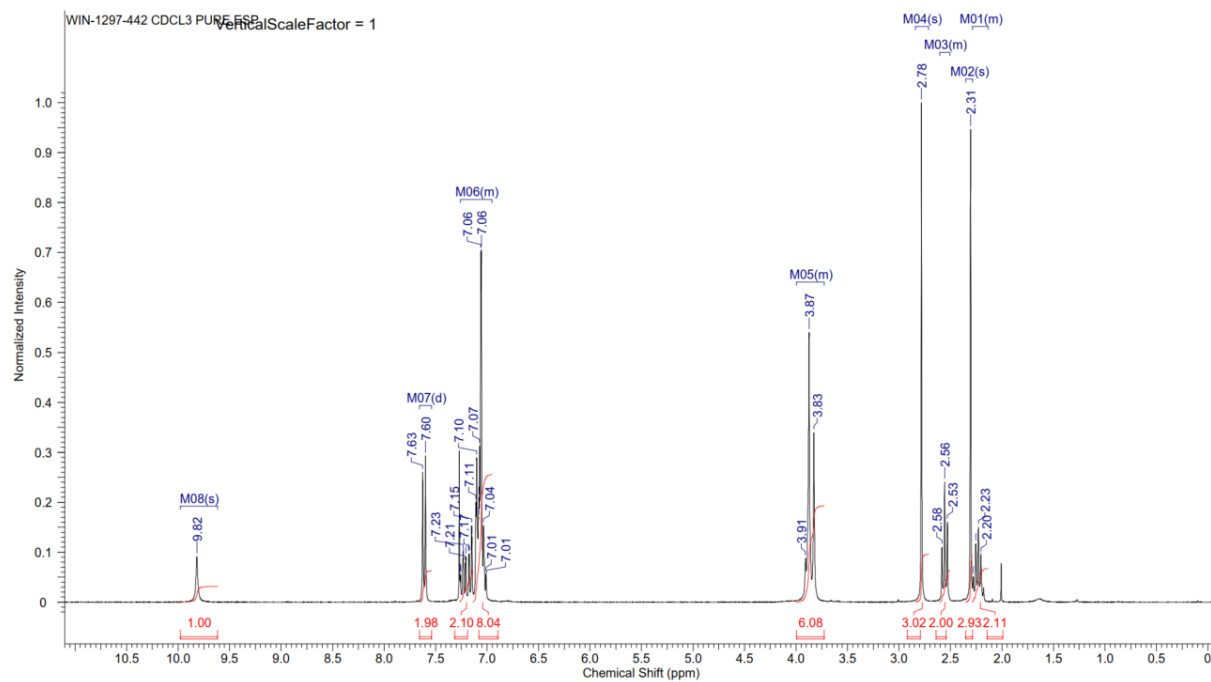
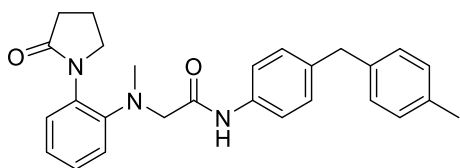
# Compound 25



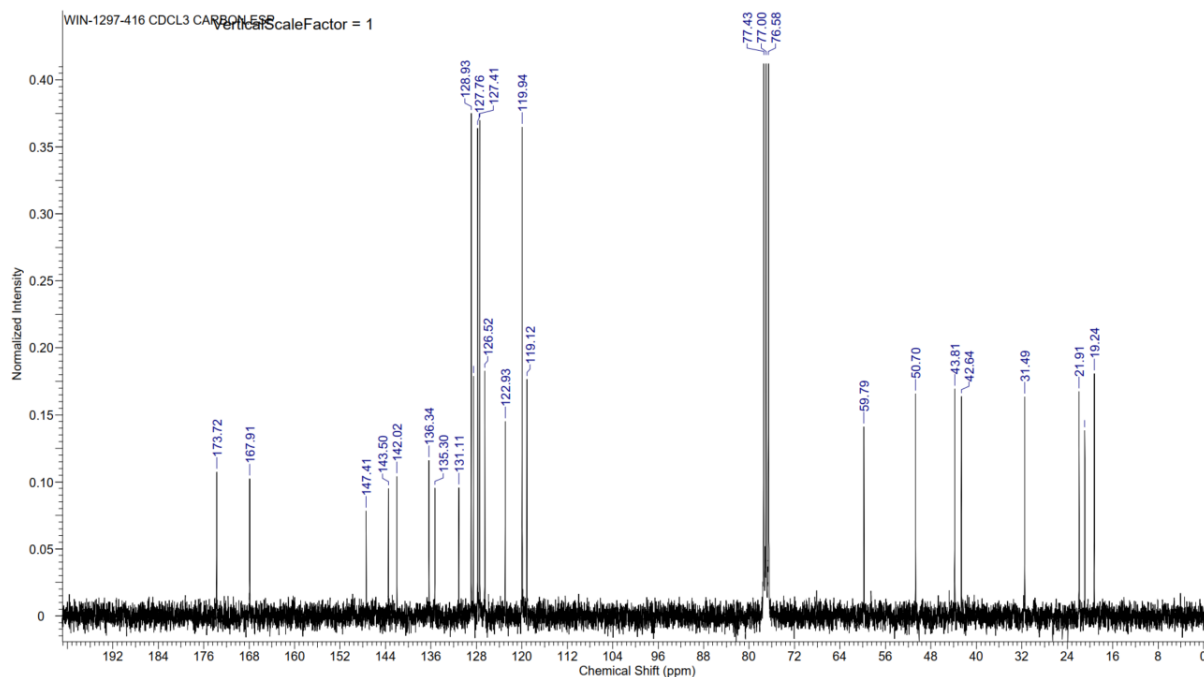
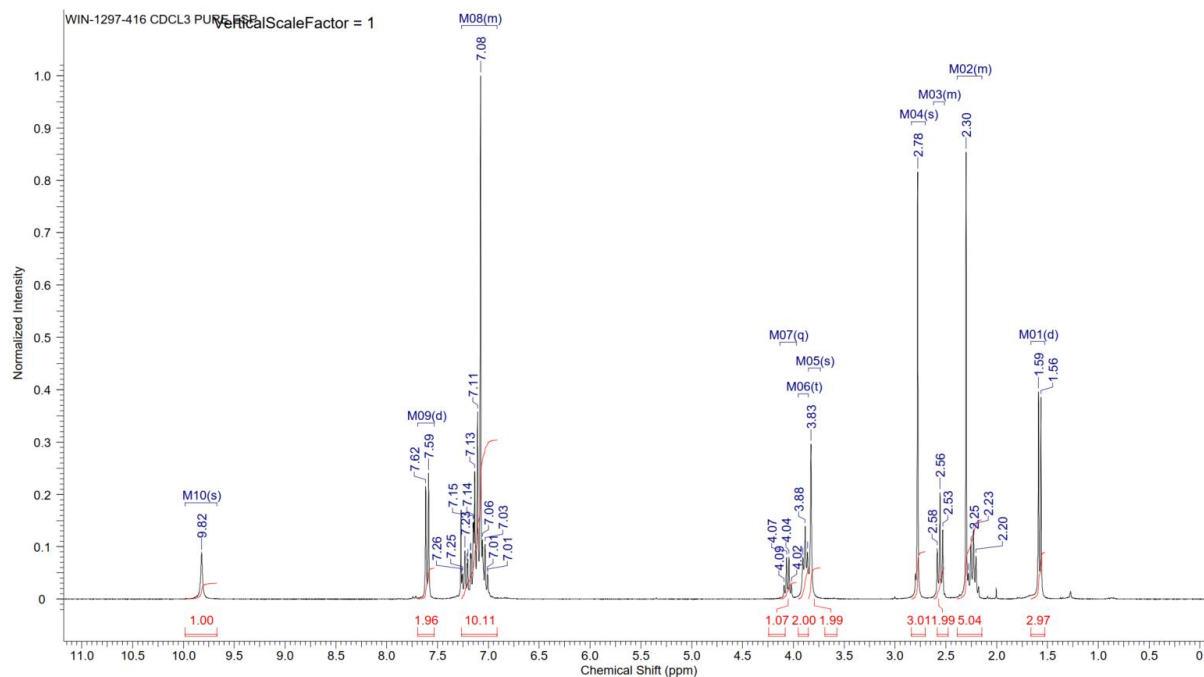
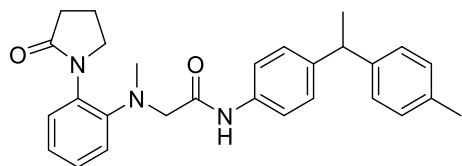
# Compound 26



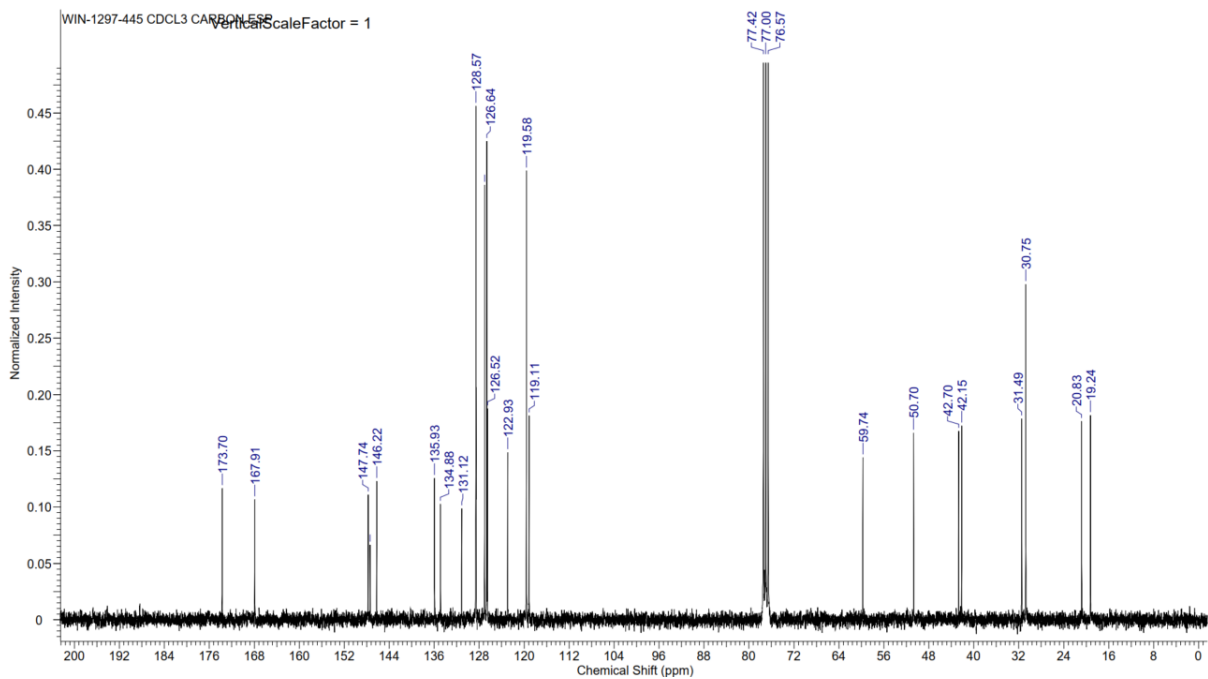
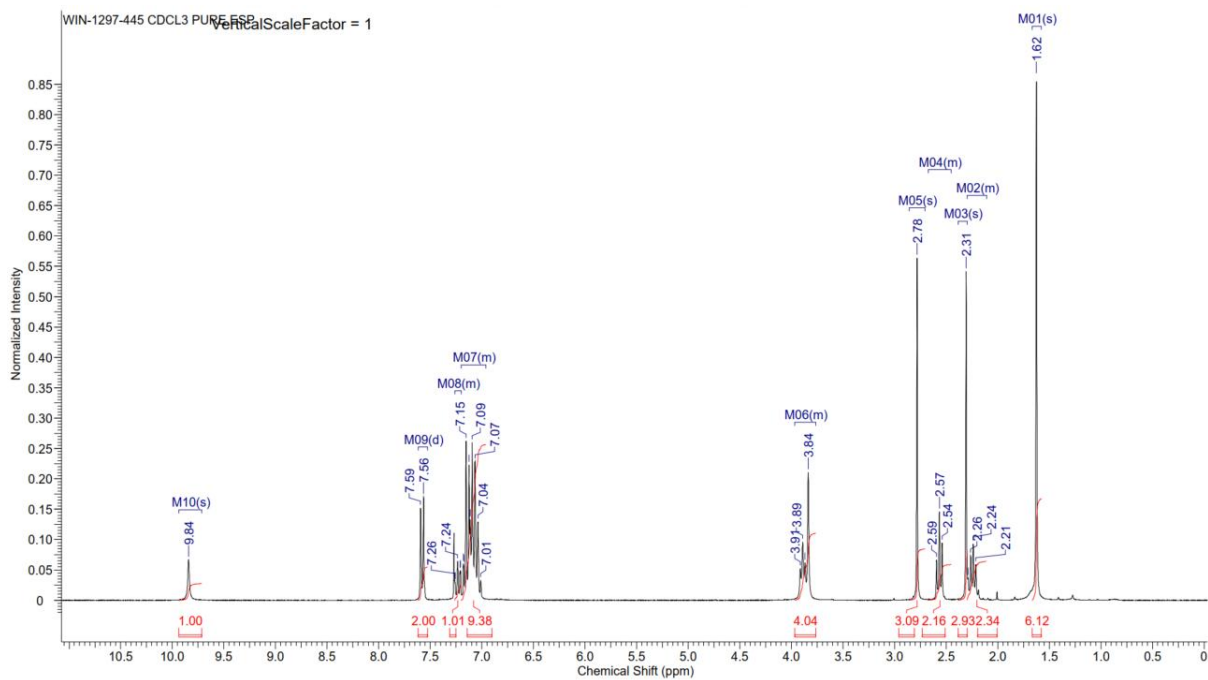
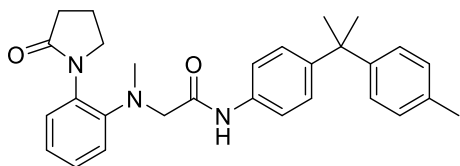
# Compound 27



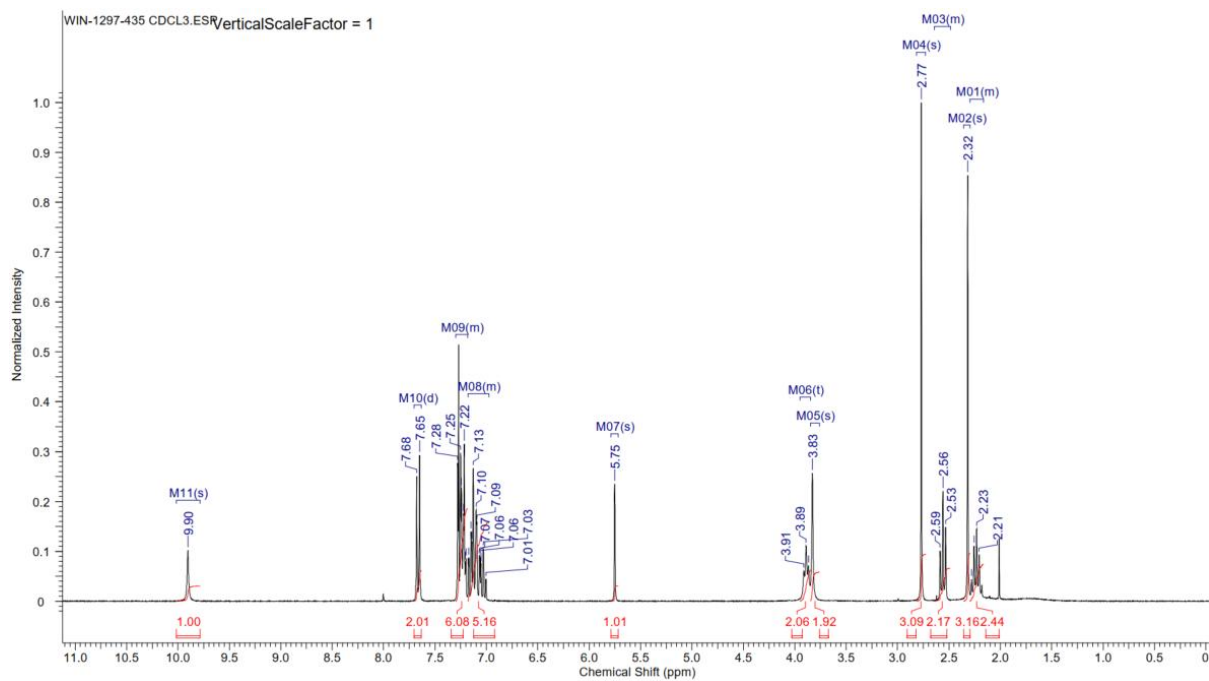
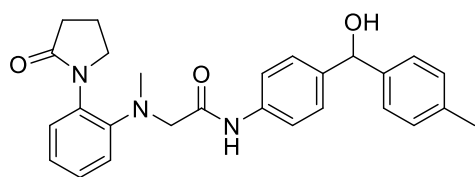
# Compound 28



# Compound 29

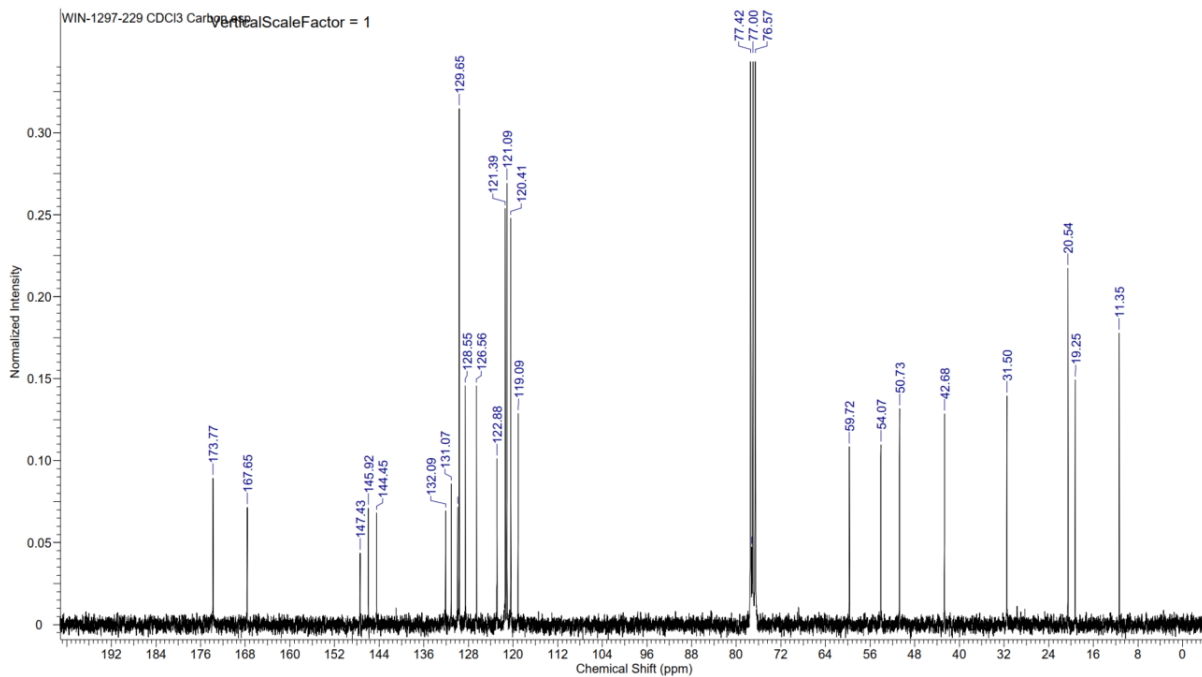
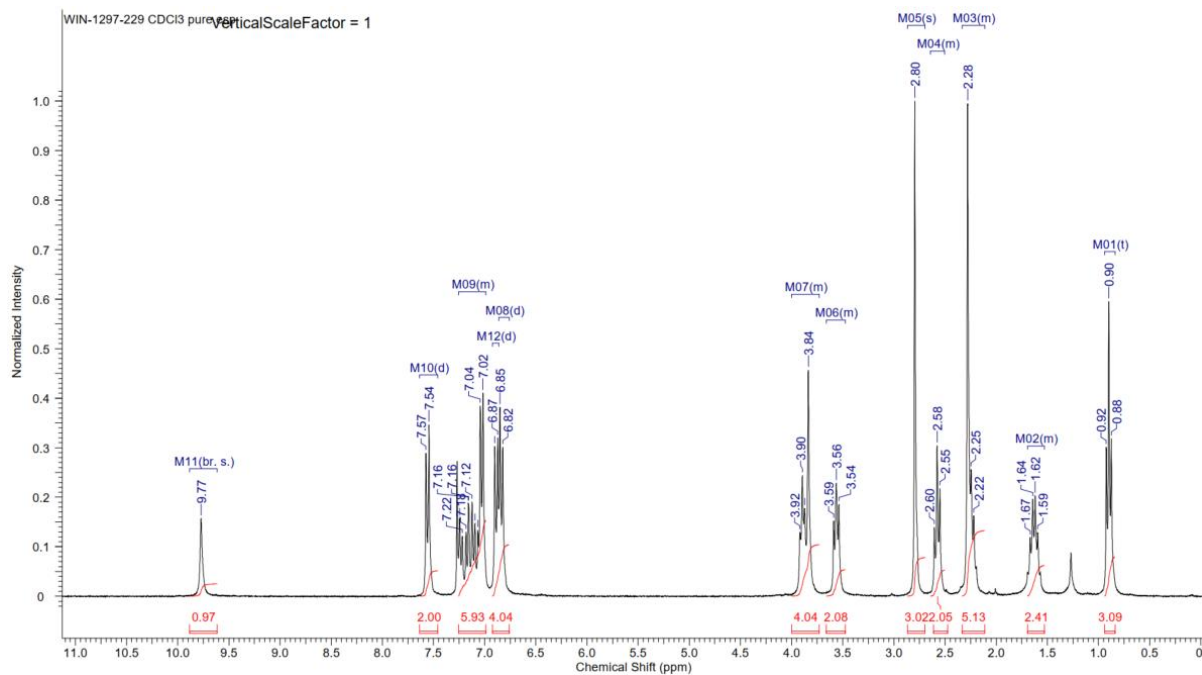
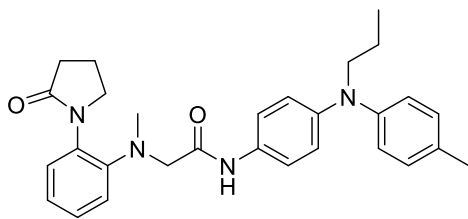


# Compound 30

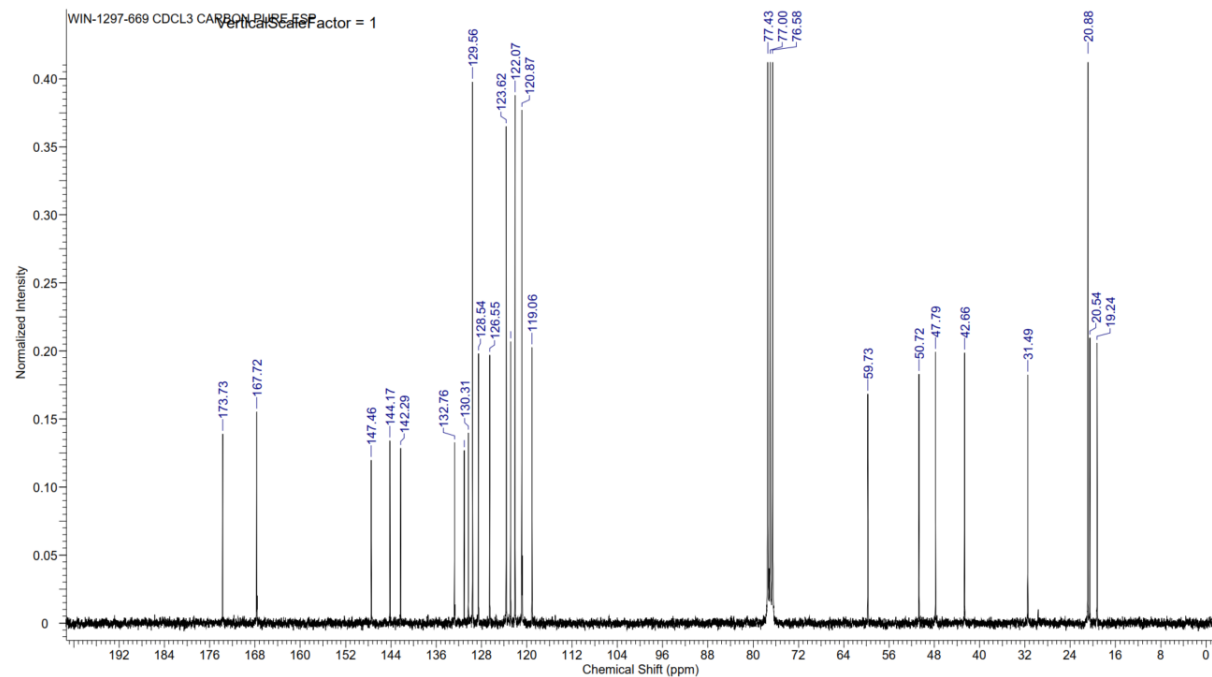
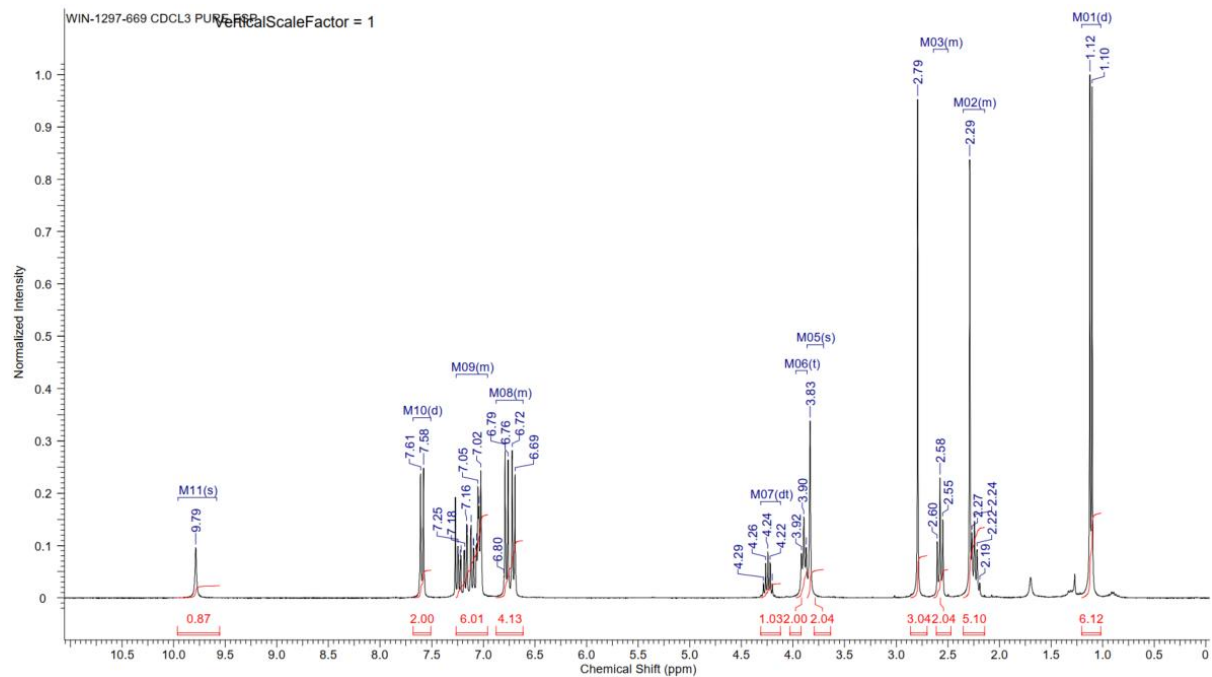
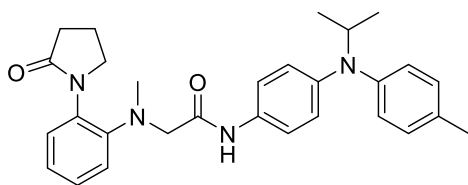




# Compound 32

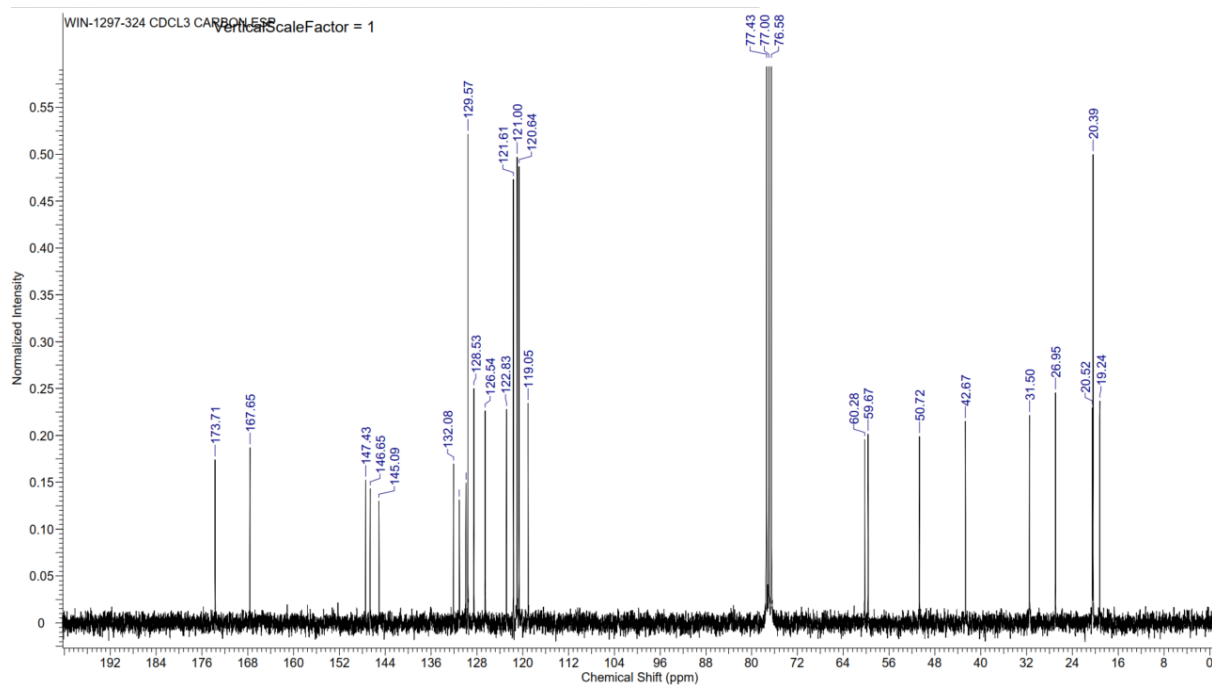
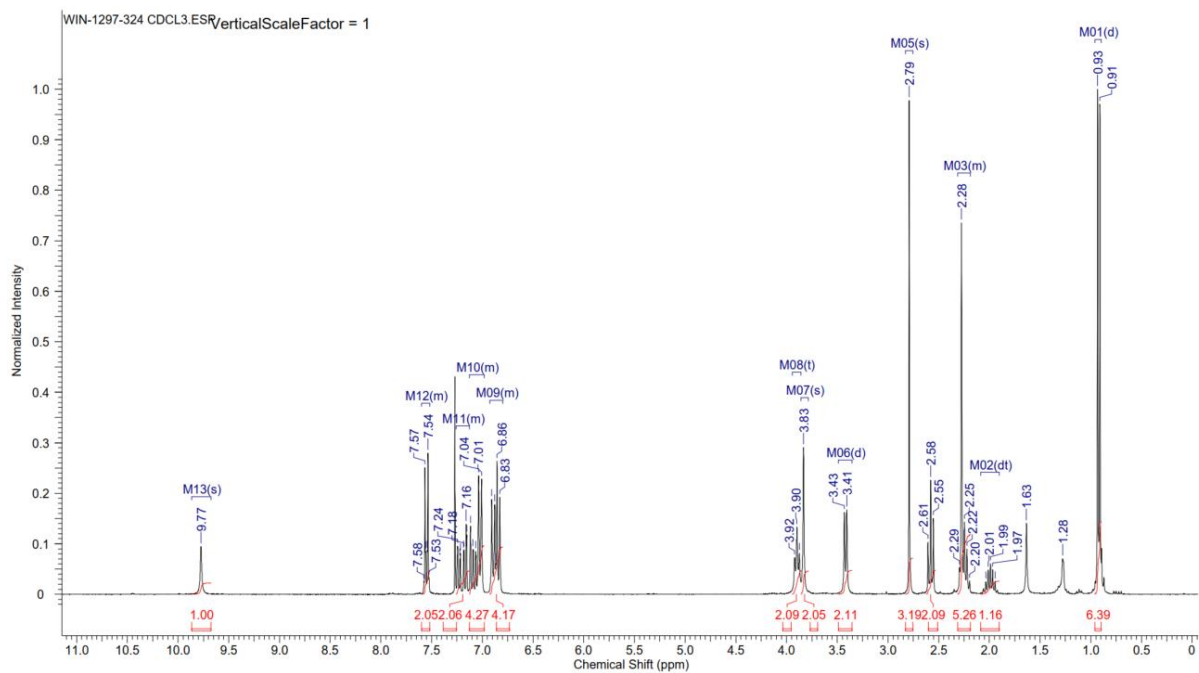
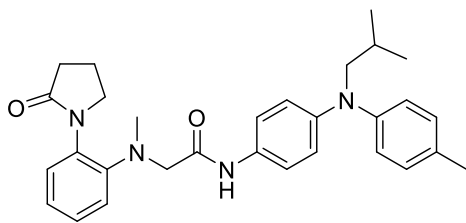


# Compound 33

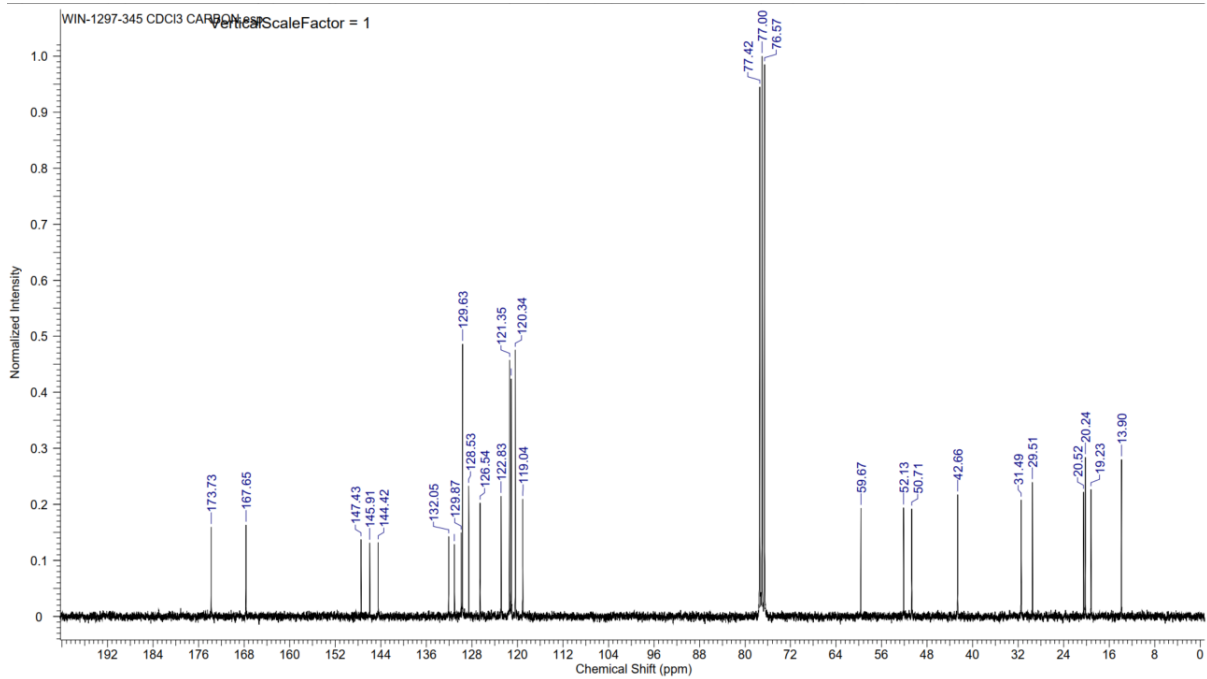
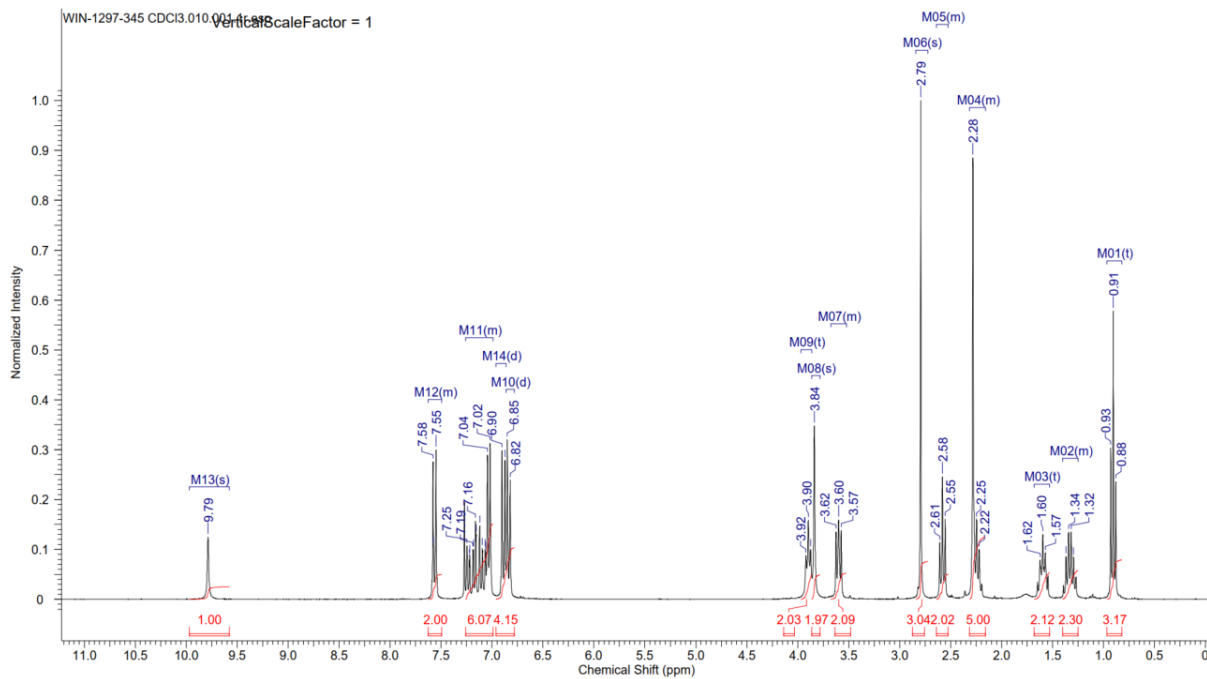
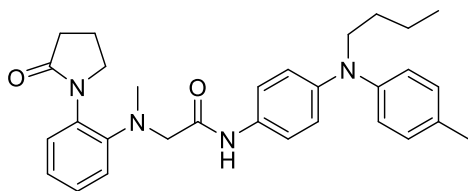




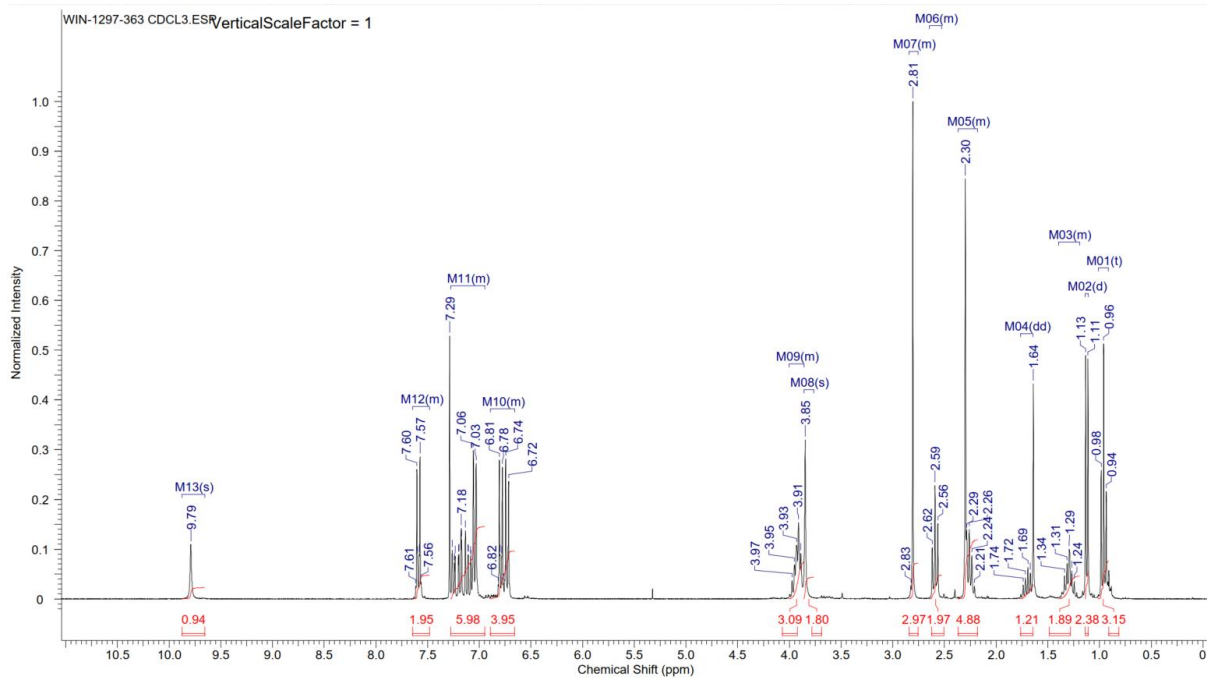
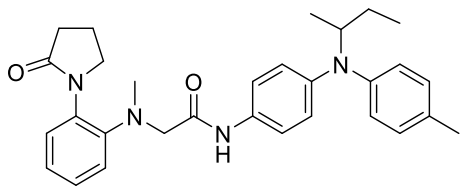
# Compound 35



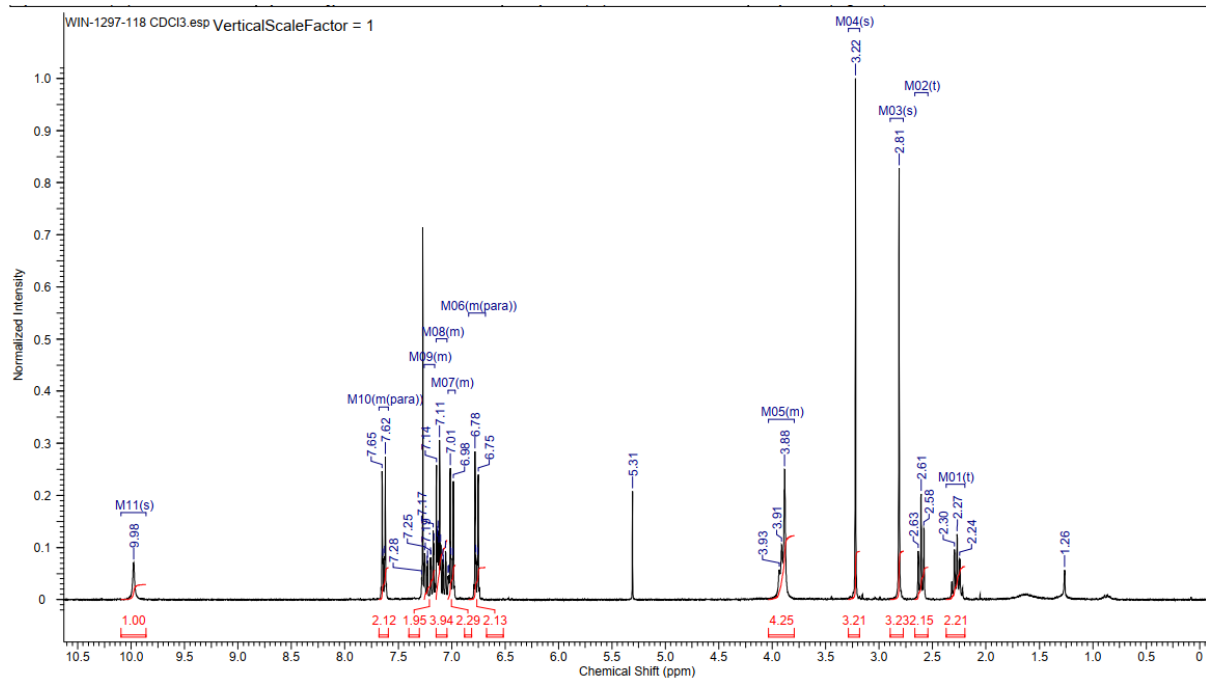
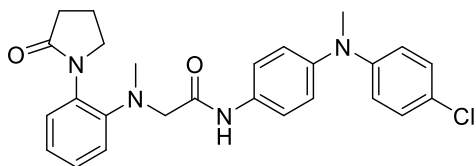
# Compound 36



# Compound 37

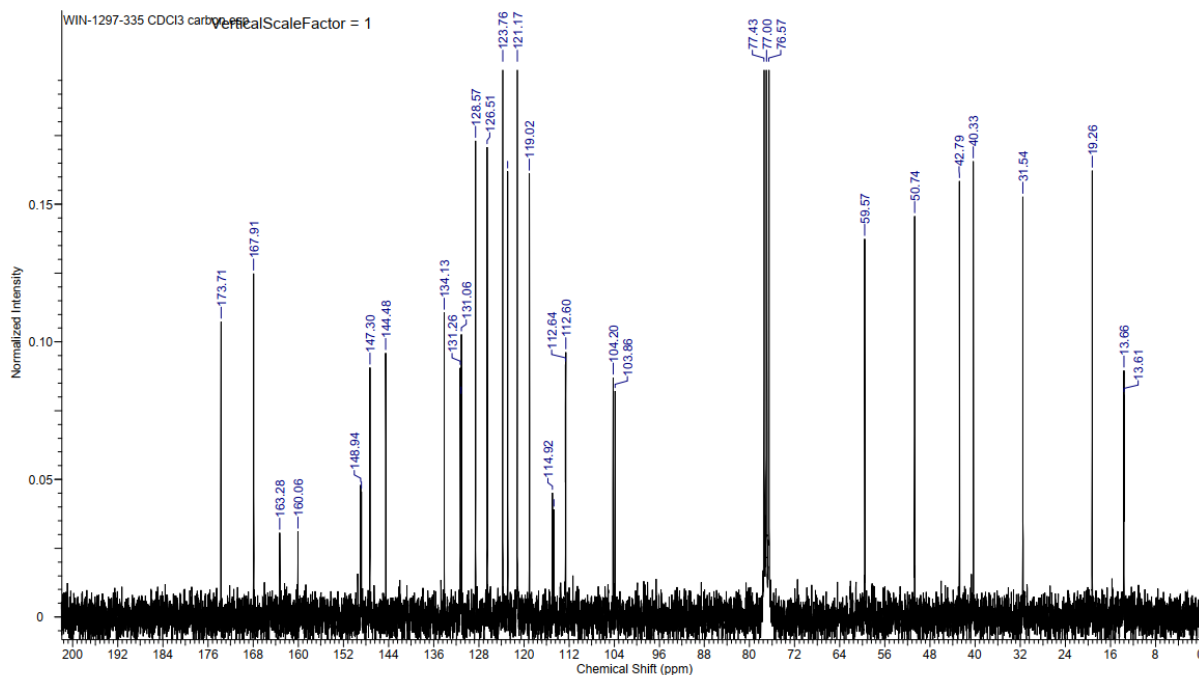
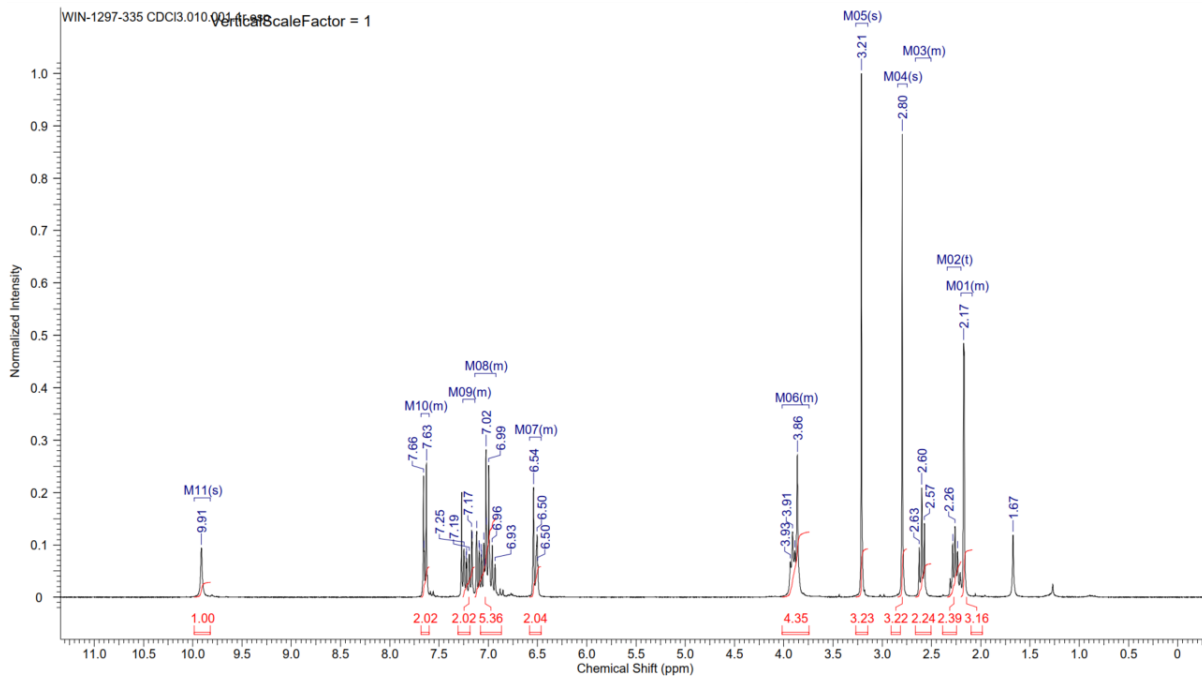
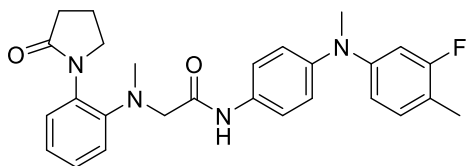


# Compound 38

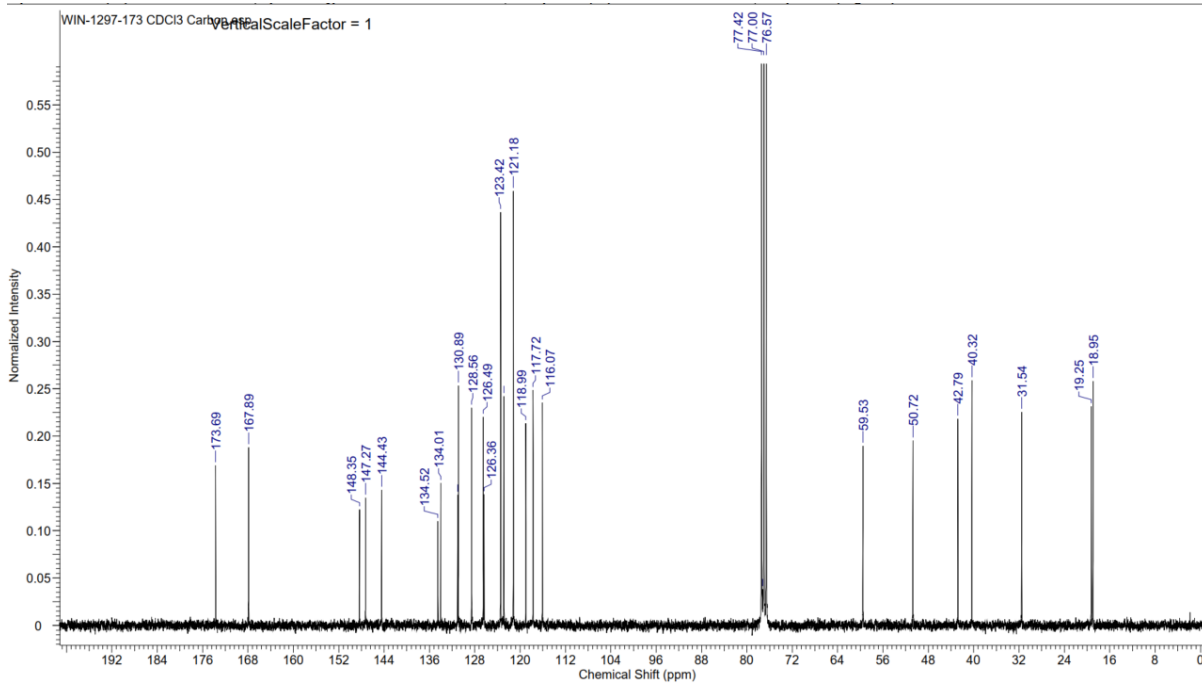
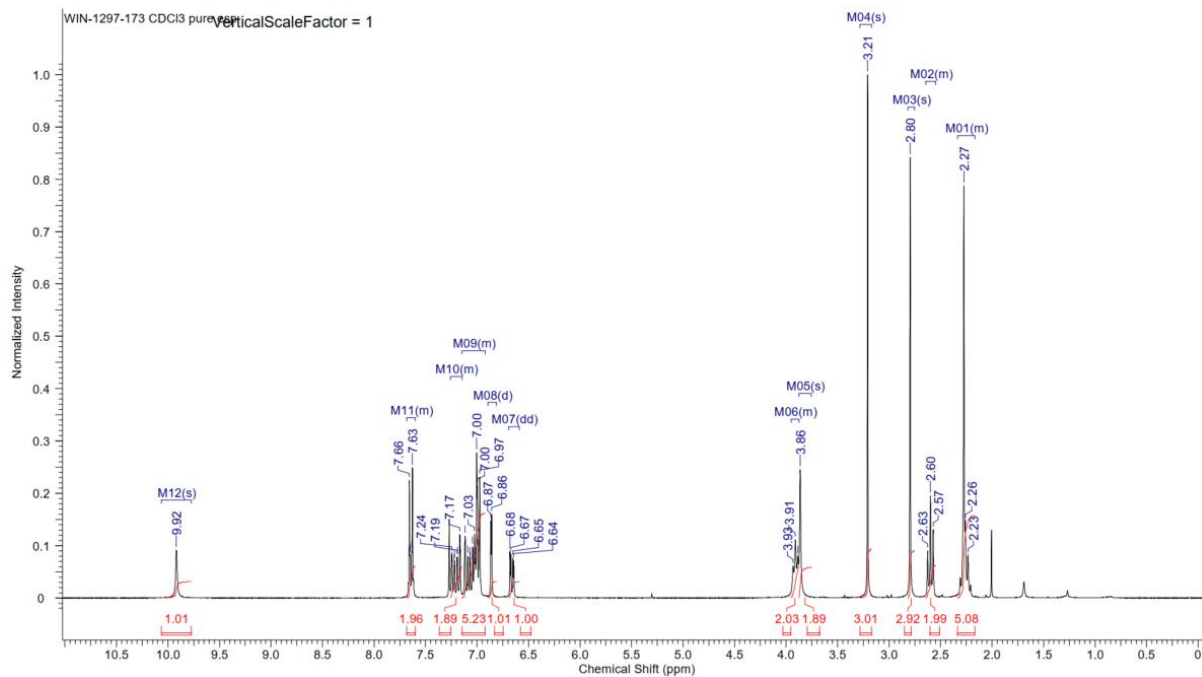
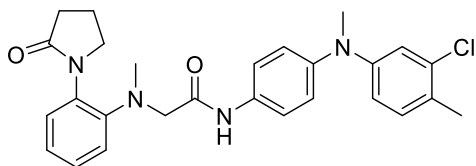




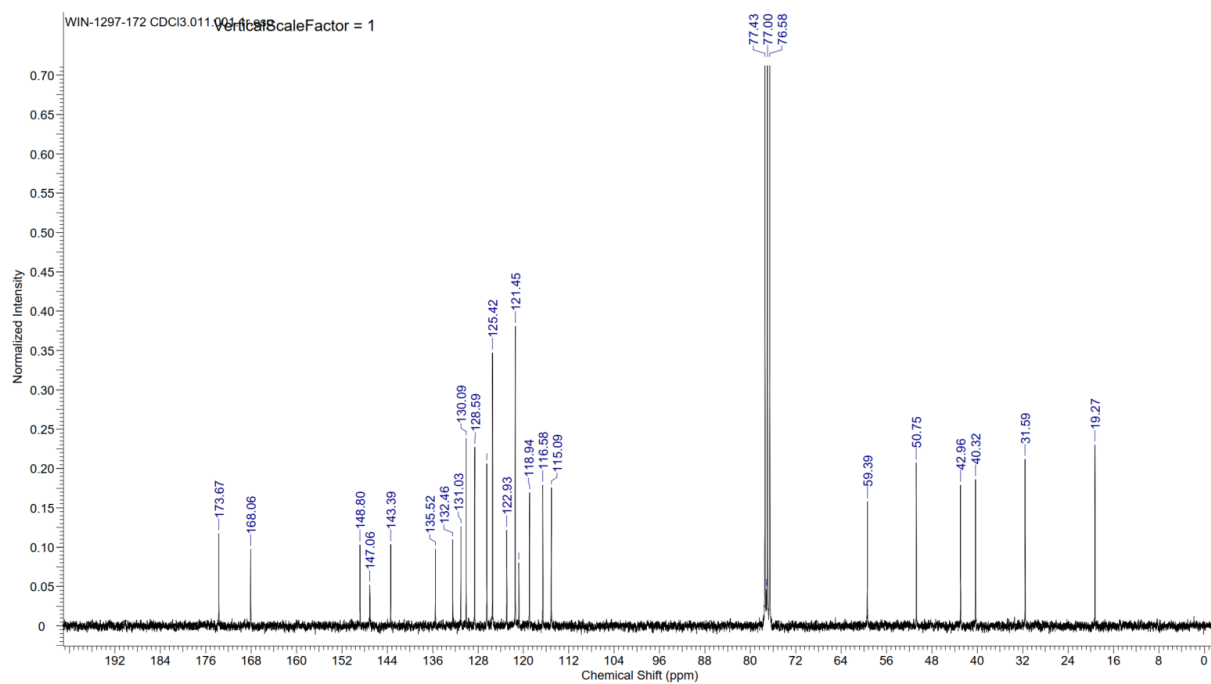
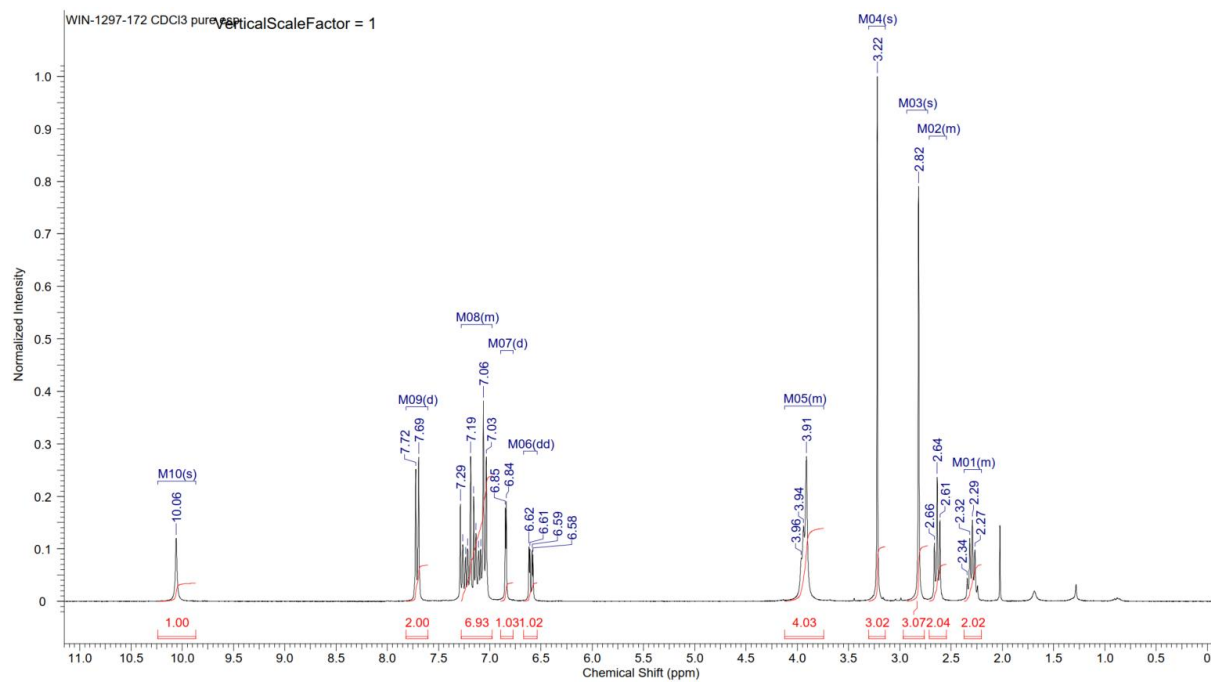
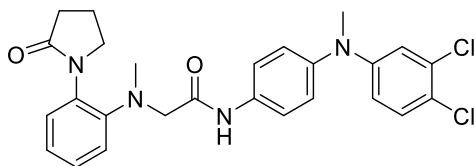
# Compound 40



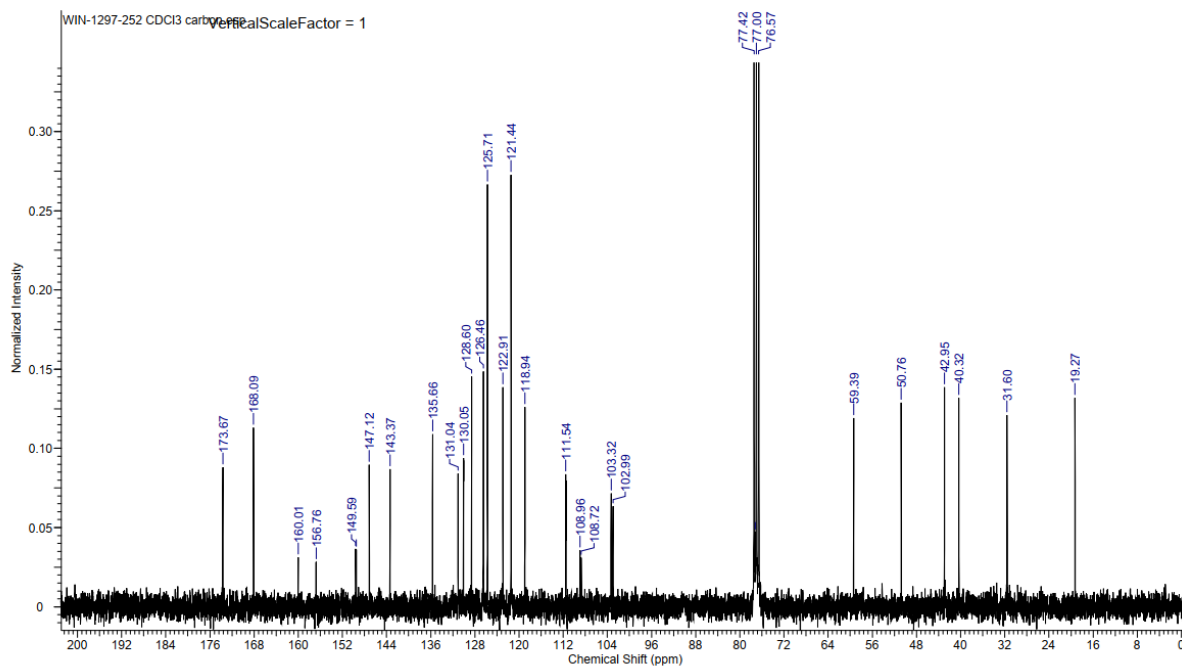
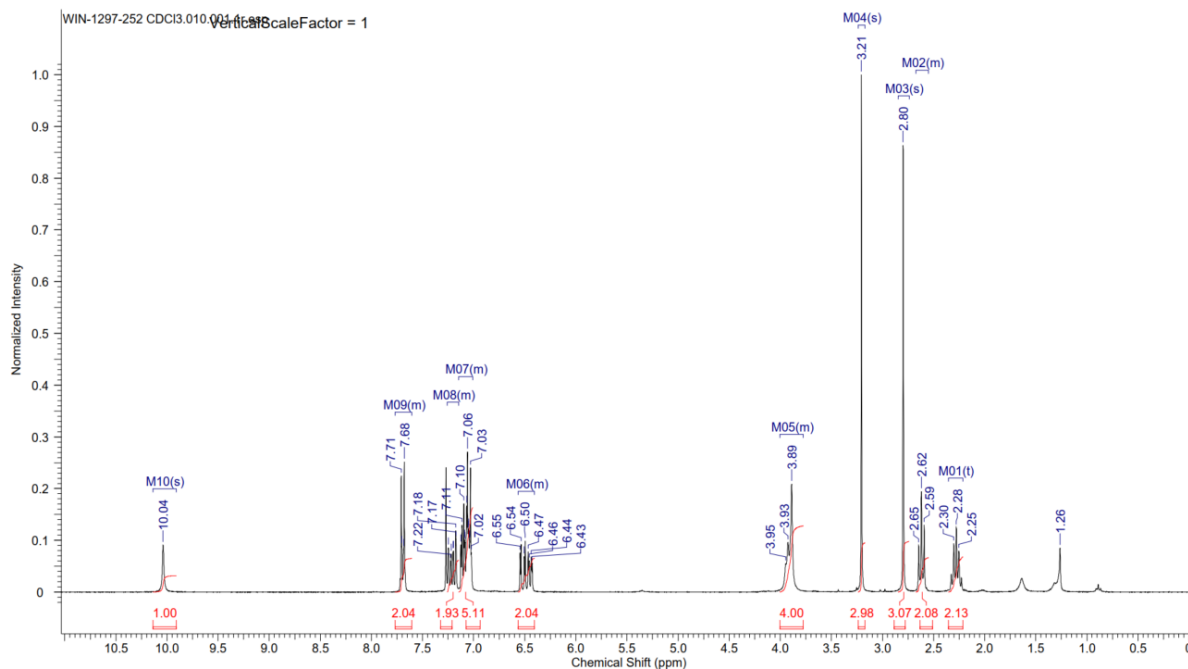
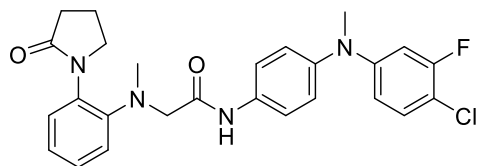
# Compound 41



# Compound 42

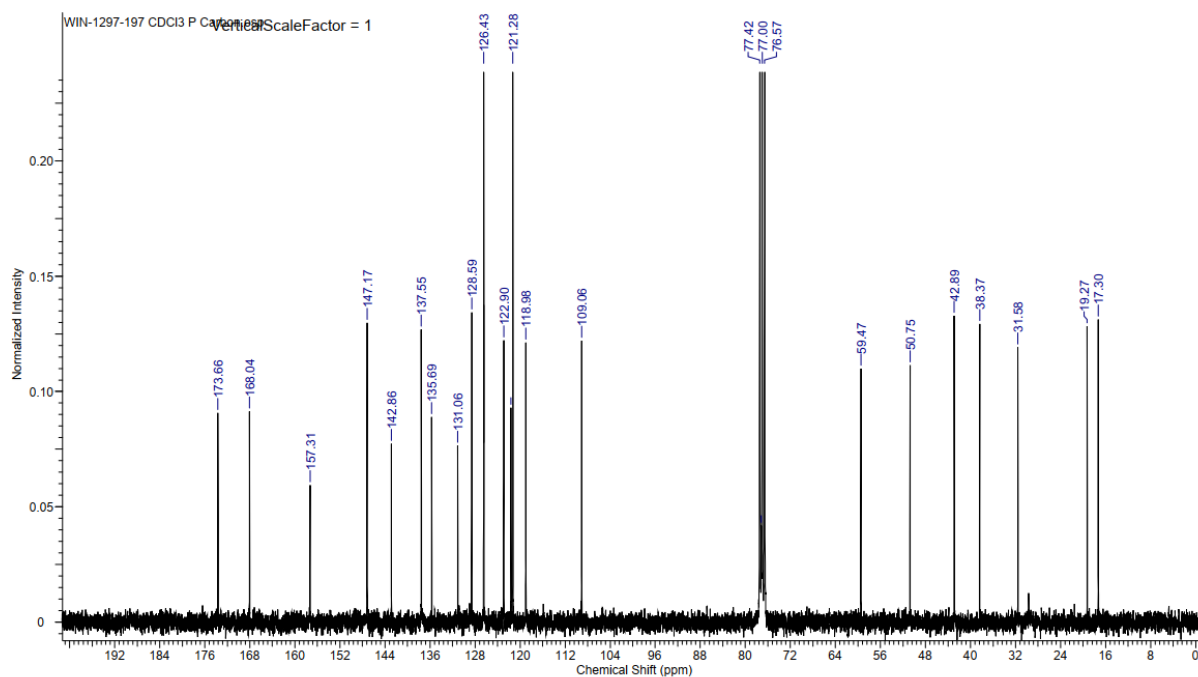
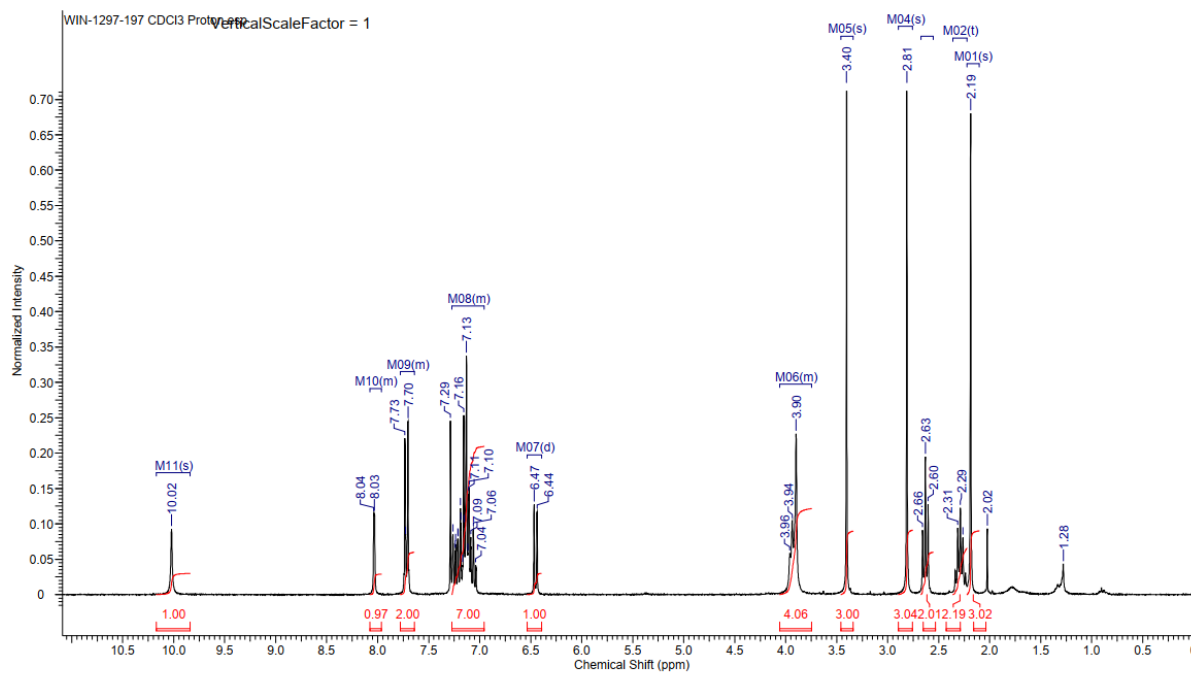
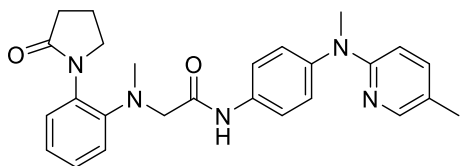


# Compound 43

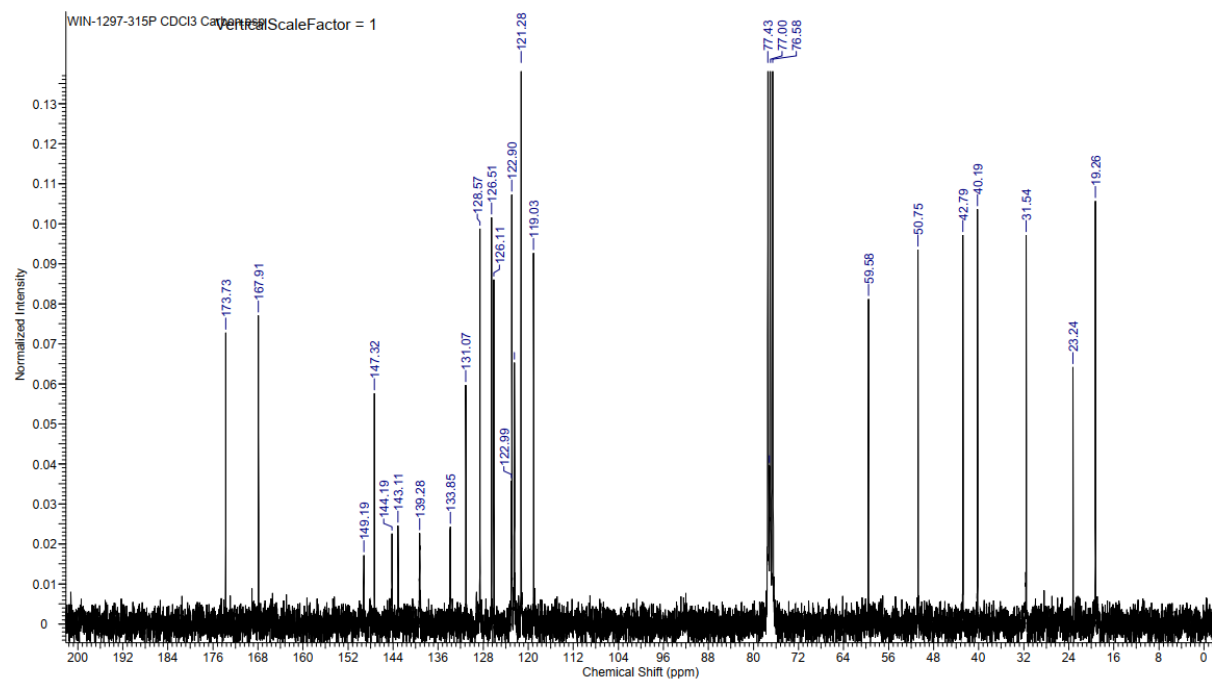
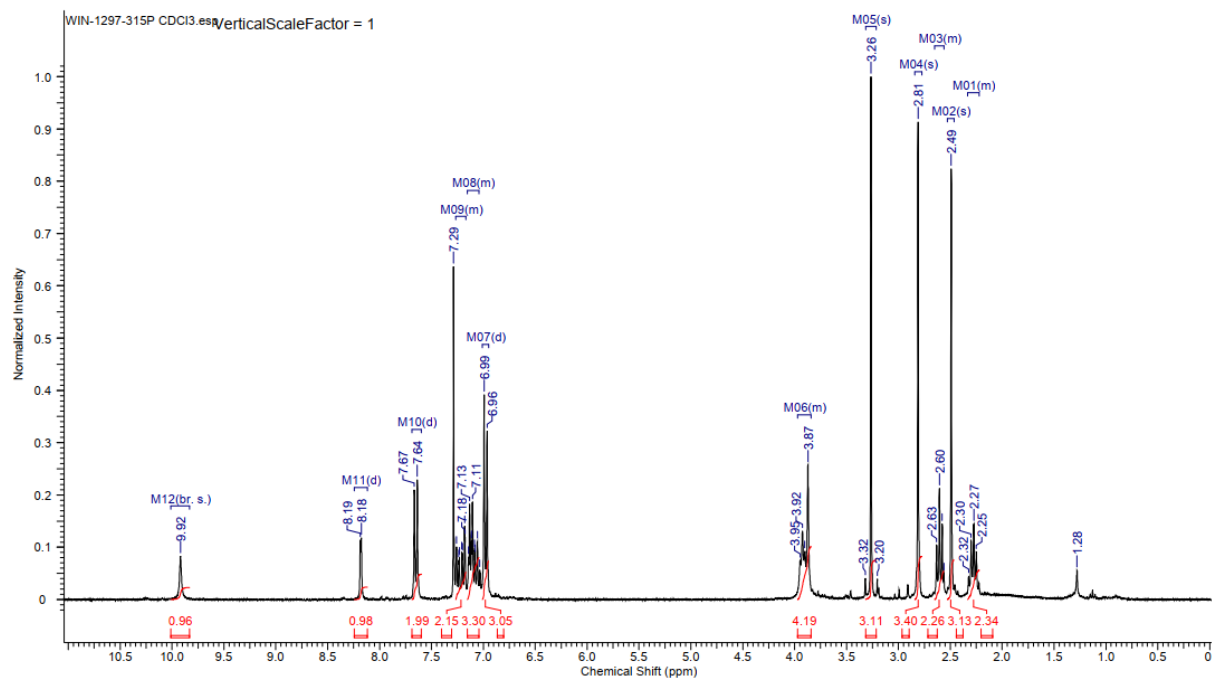
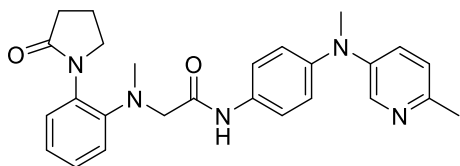




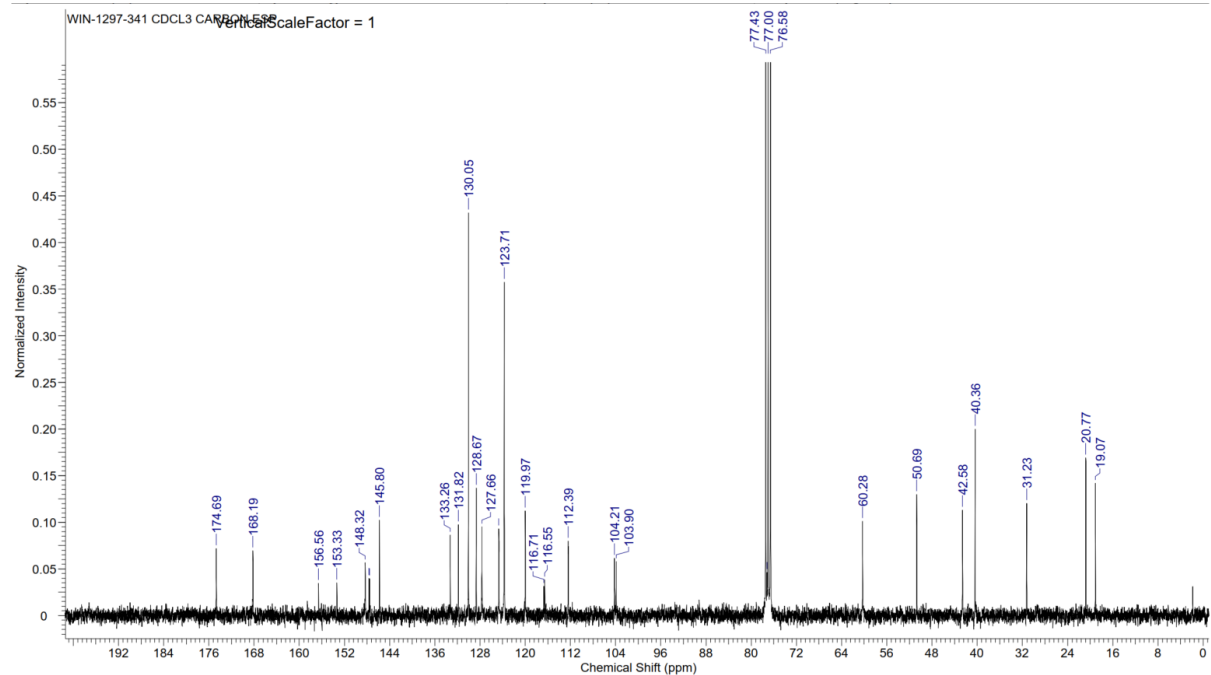
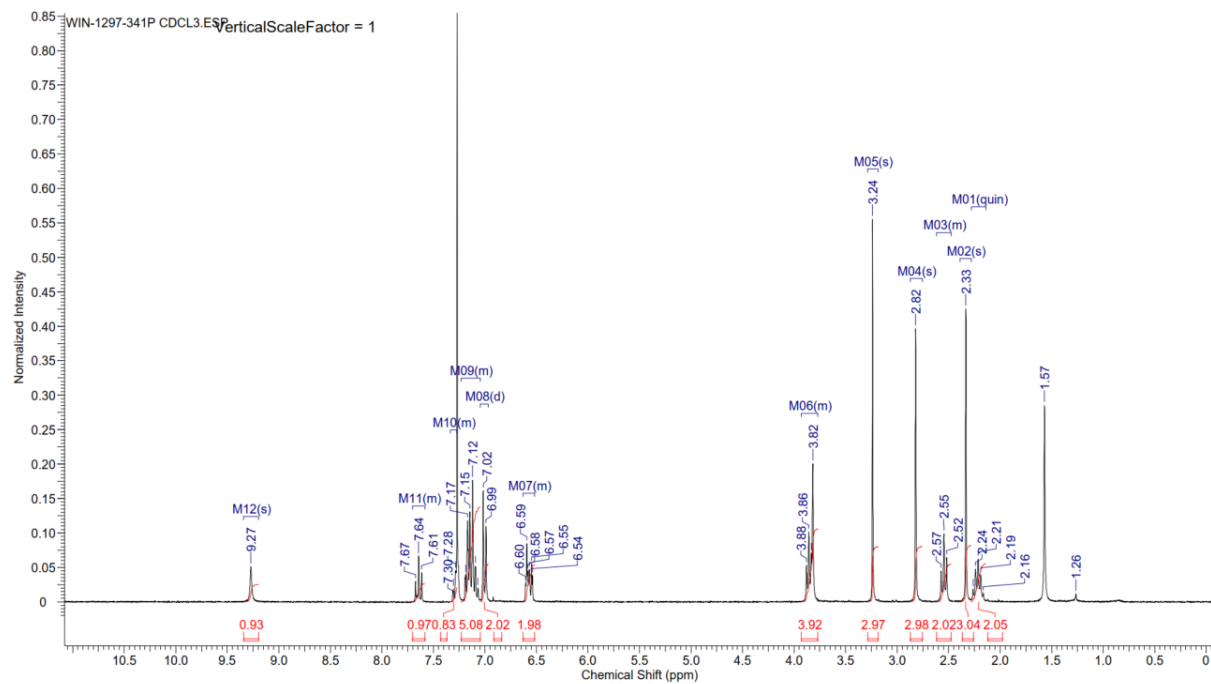
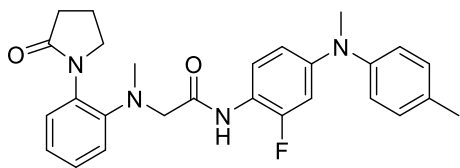
# Compound 45



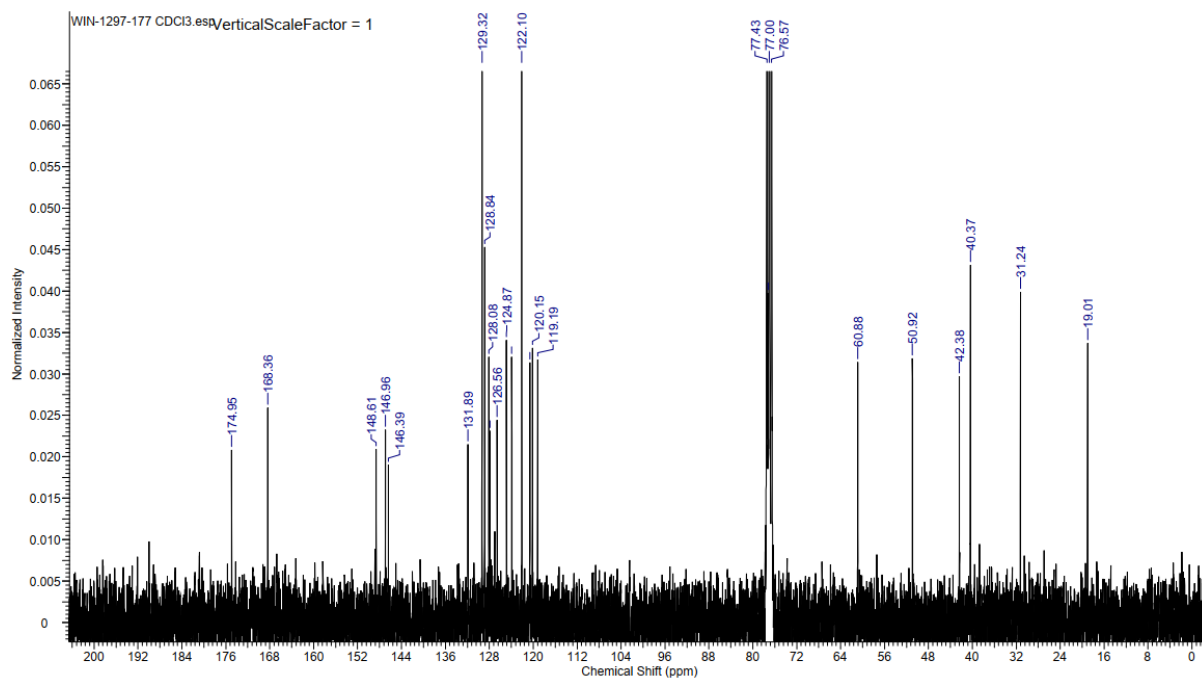
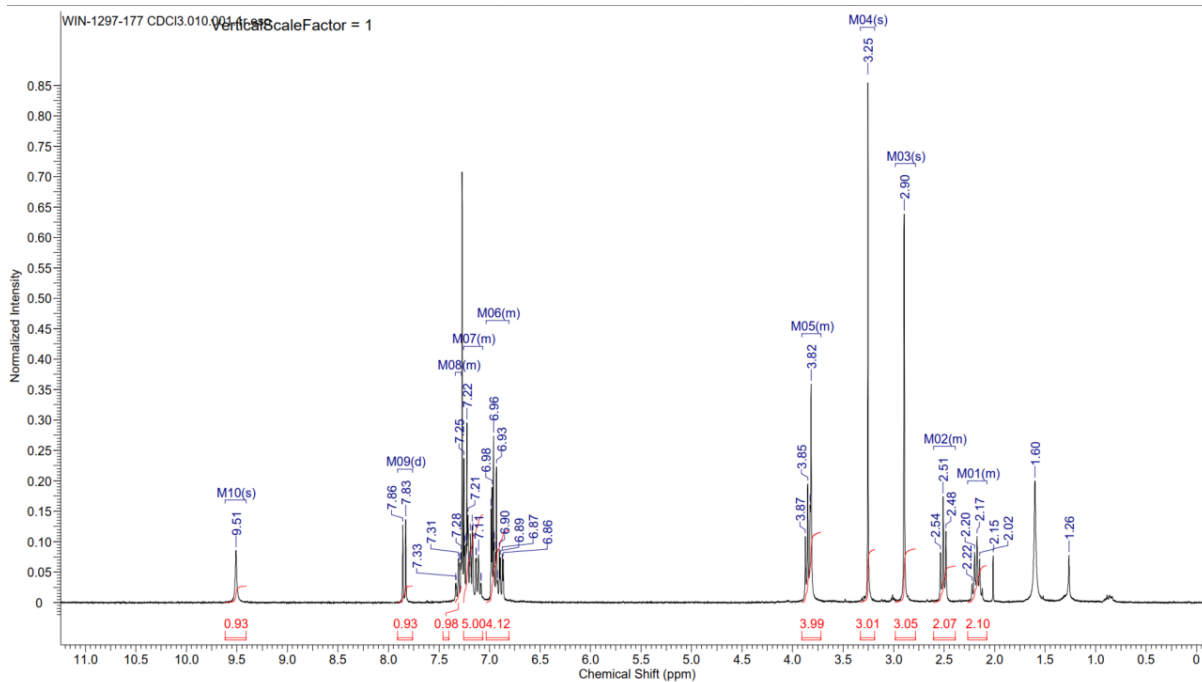
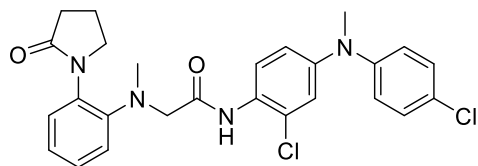
# Compound 46



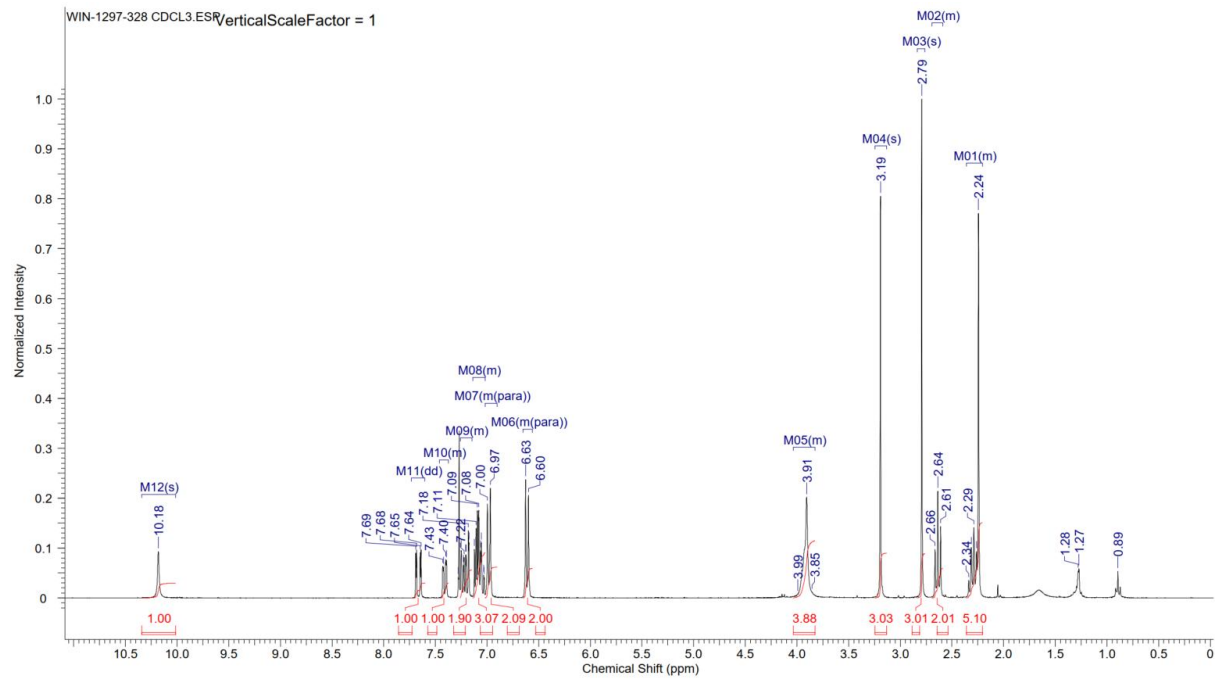
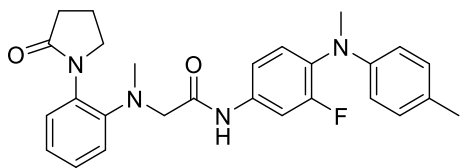
# Compound 47



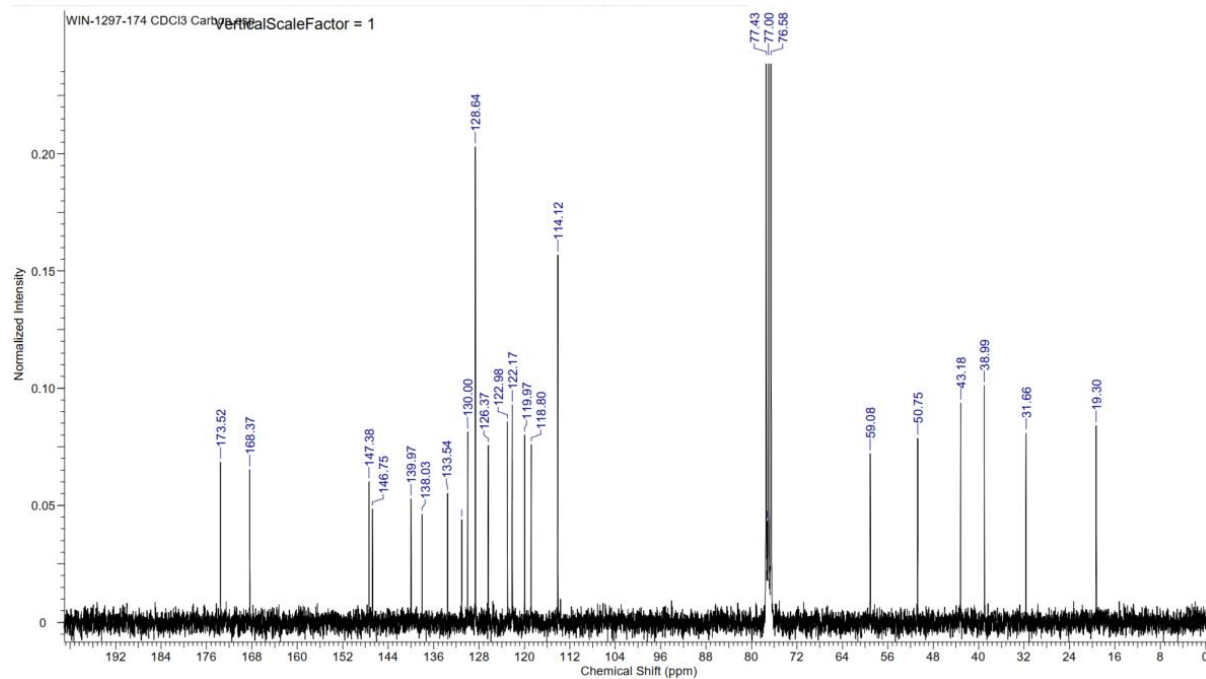
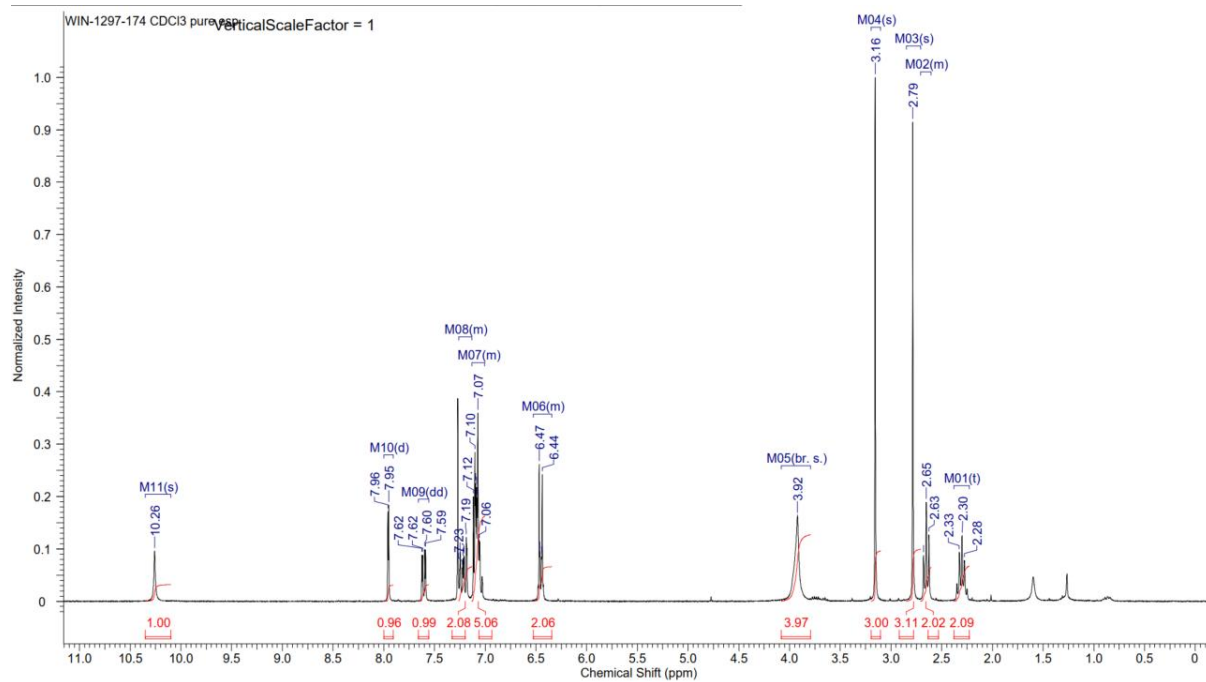
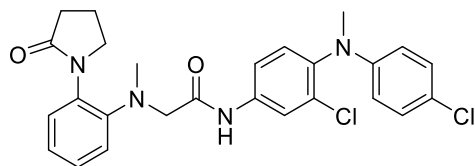
# Compound 48



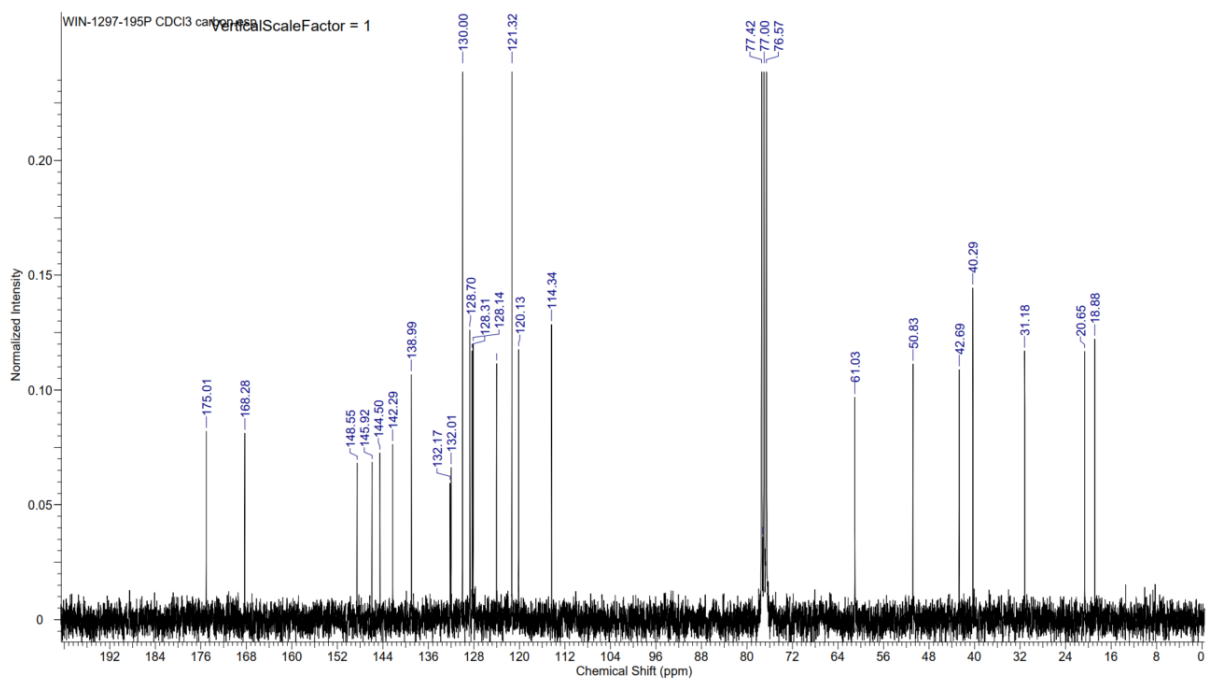
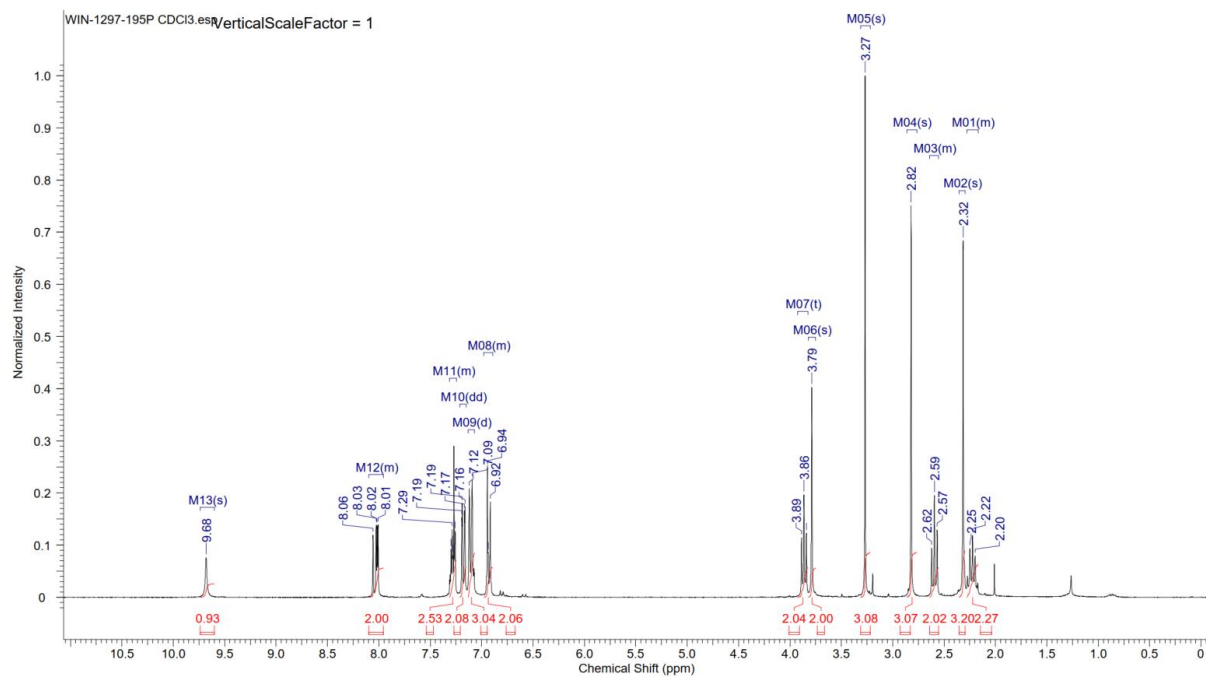
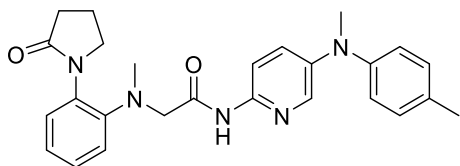
# Compound 49



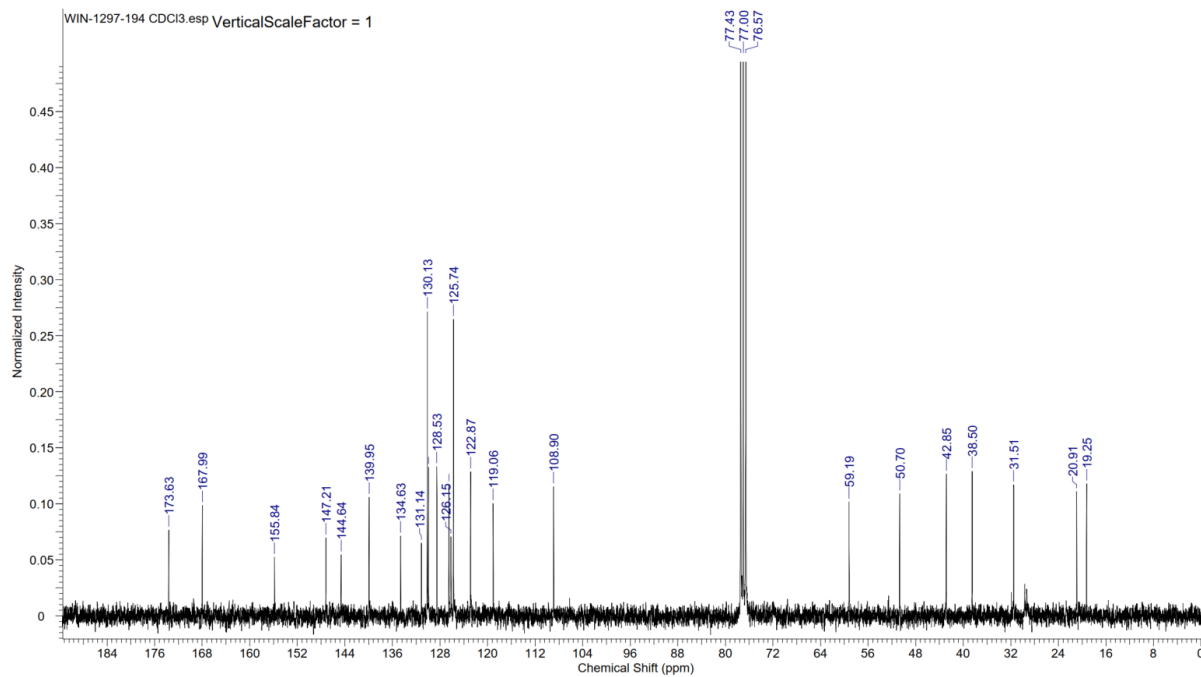
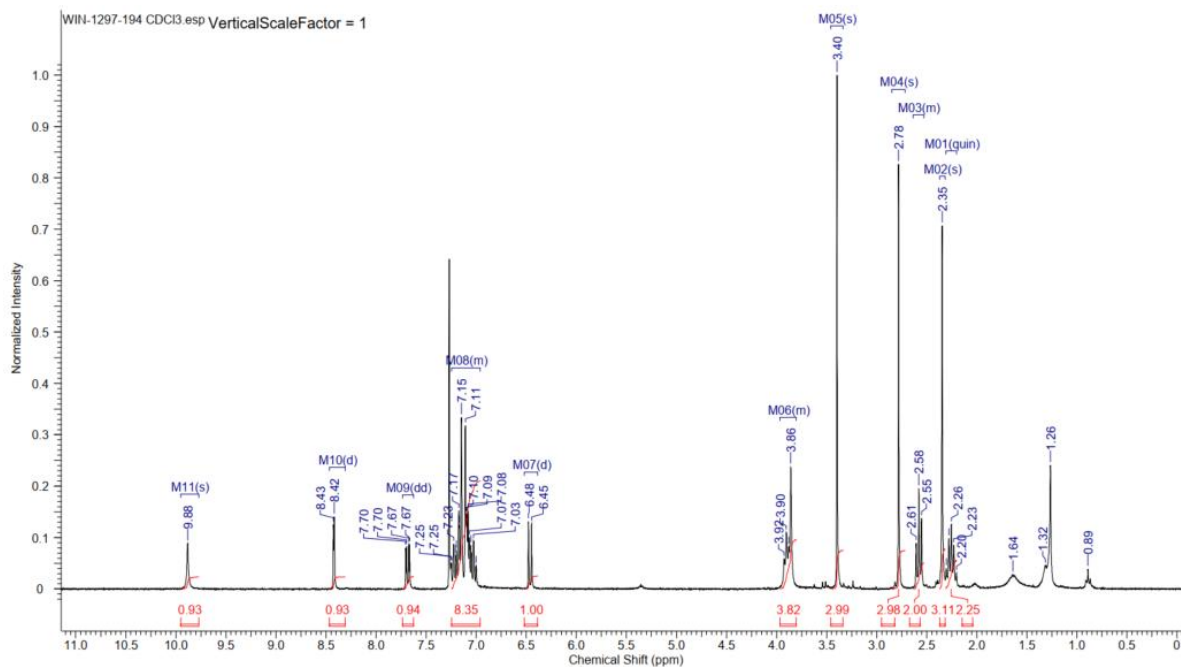
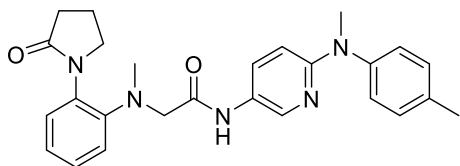
# Compound 50



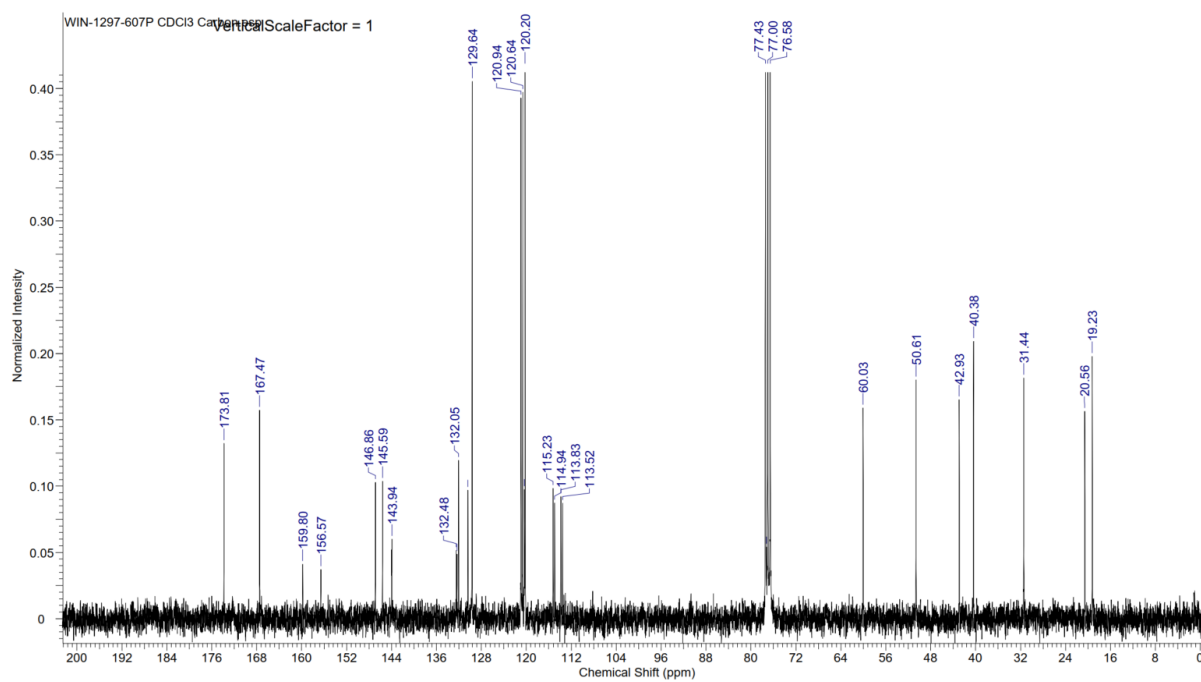
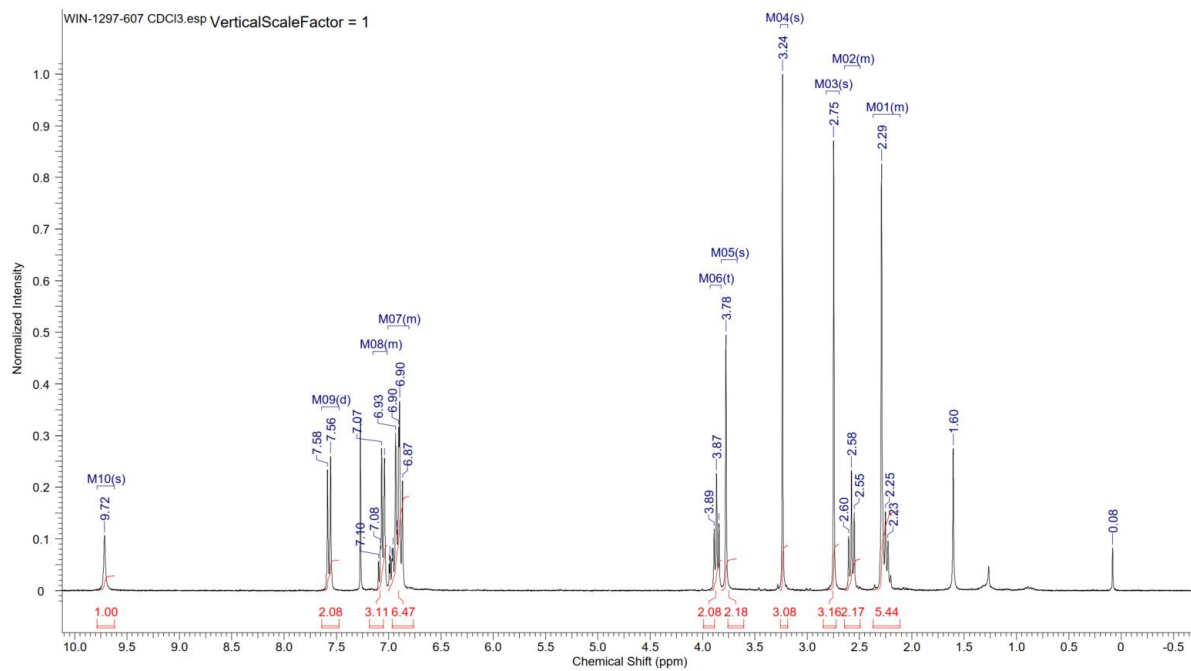
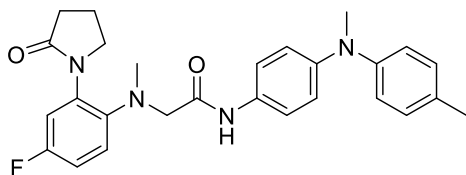
# Compound 51



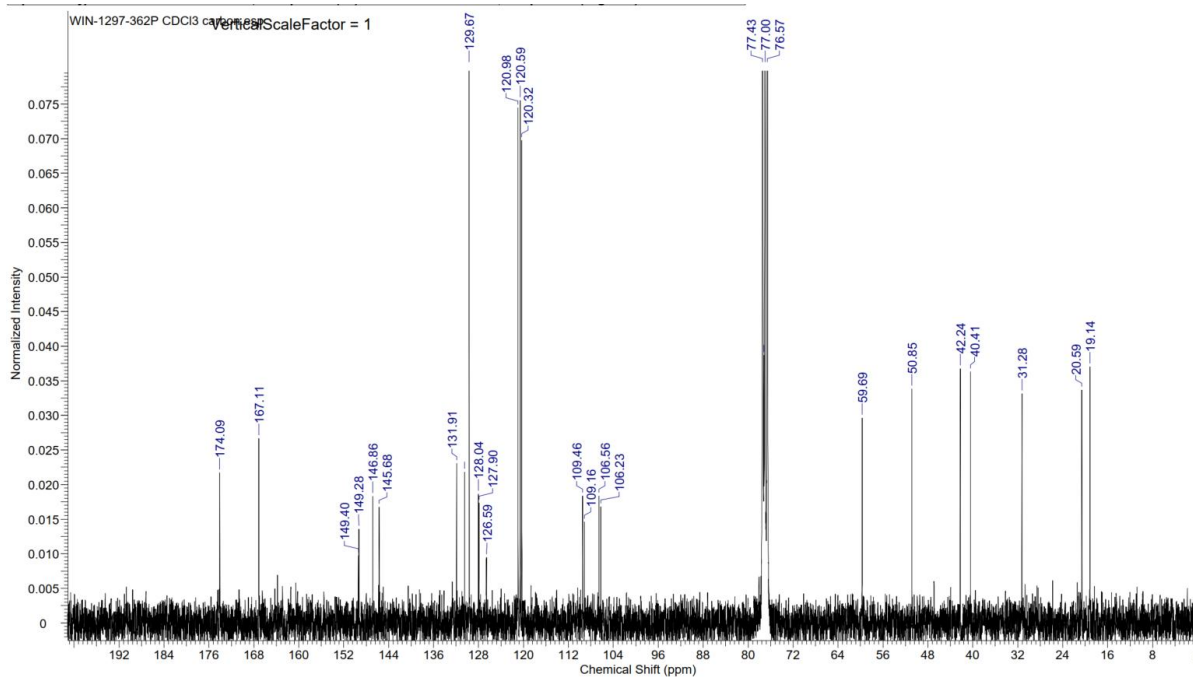
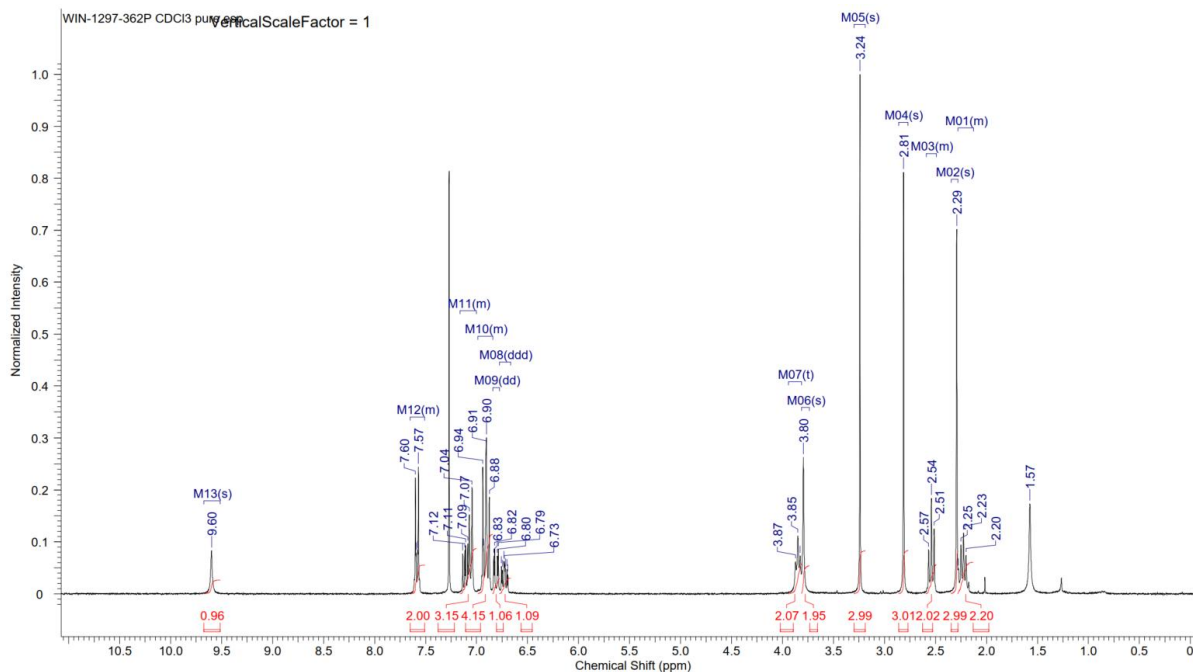
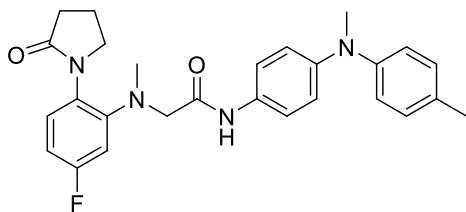
# Compound 52



# Compound 53

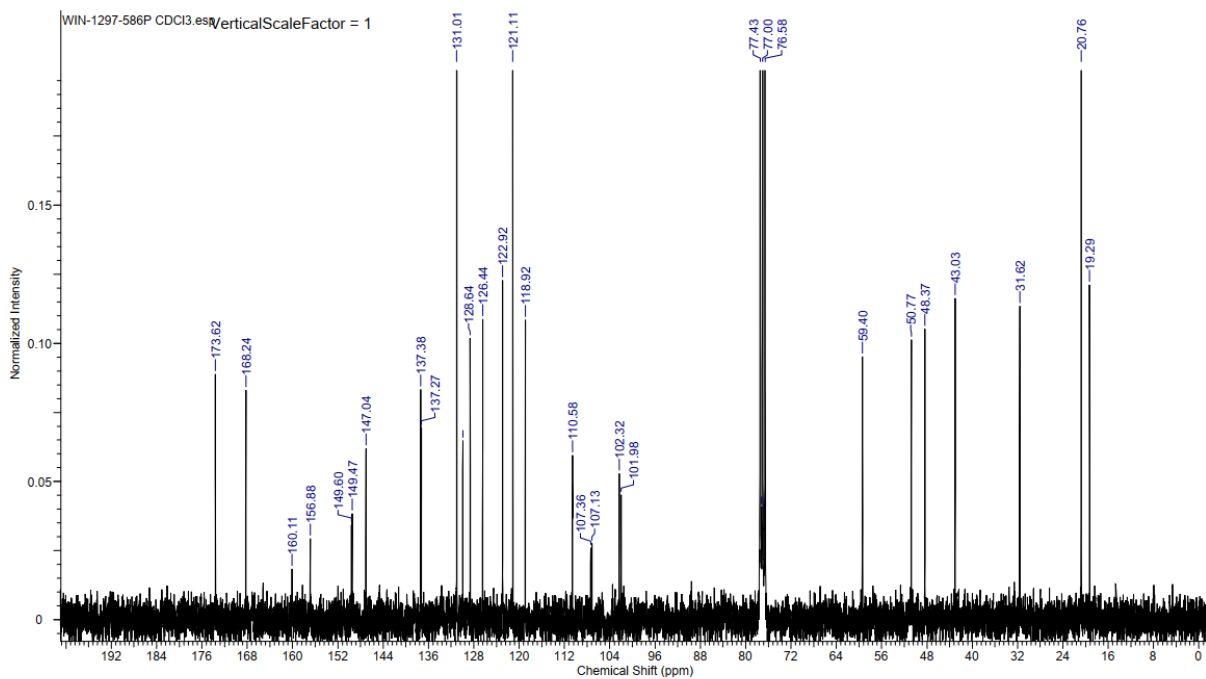
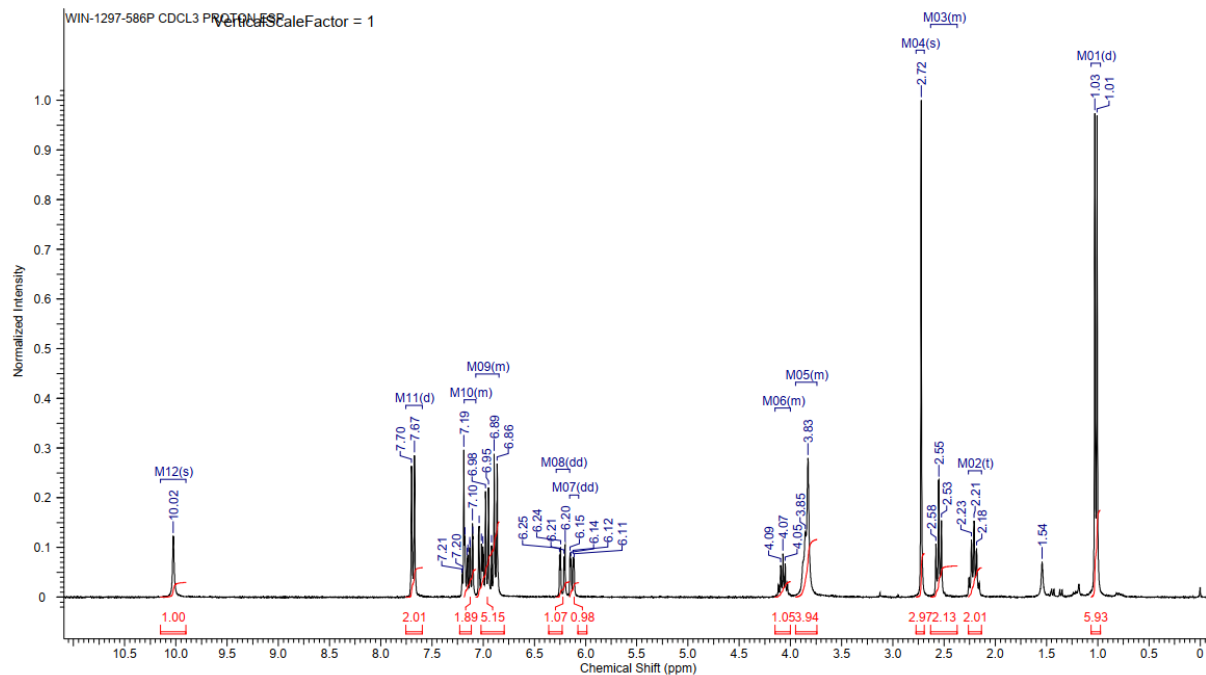
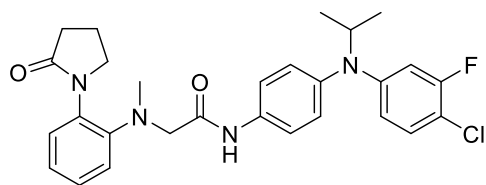


# Compound 54

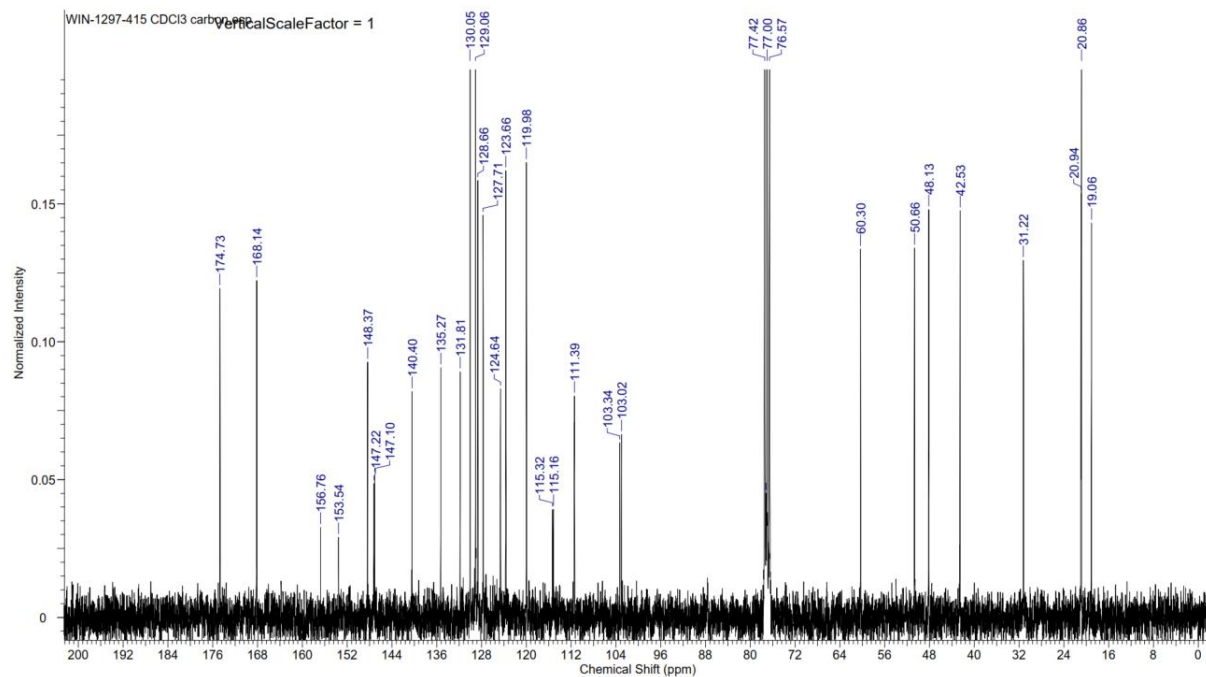
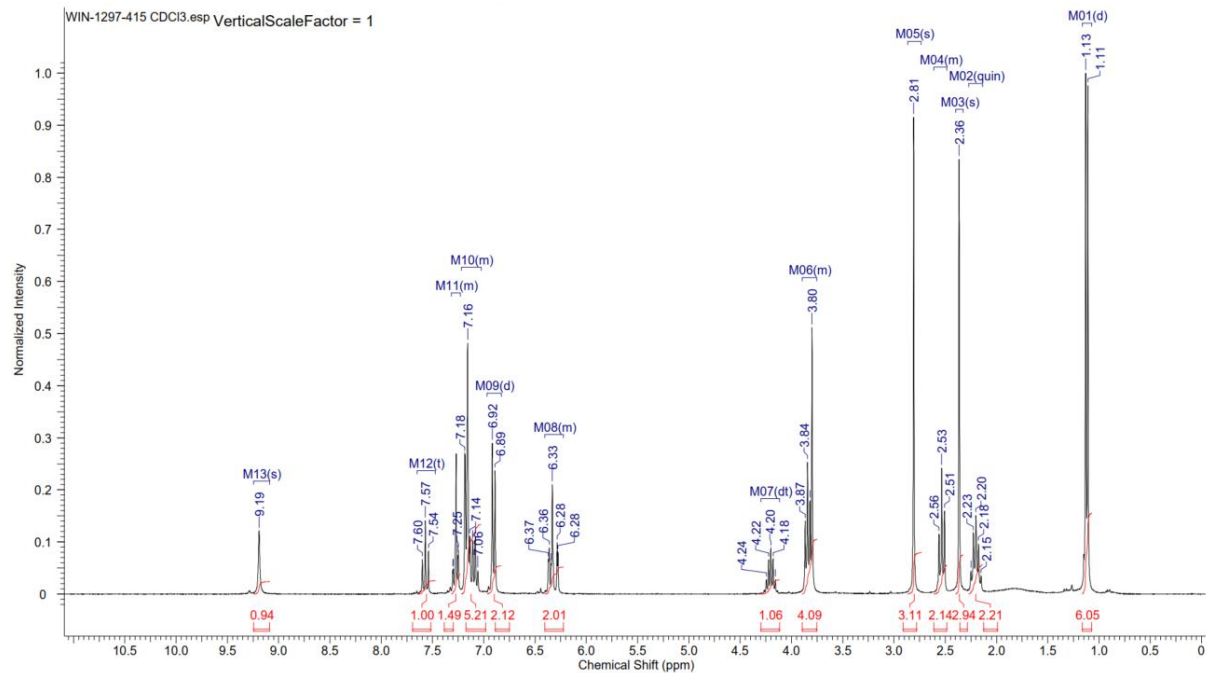
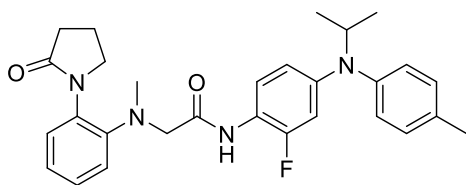




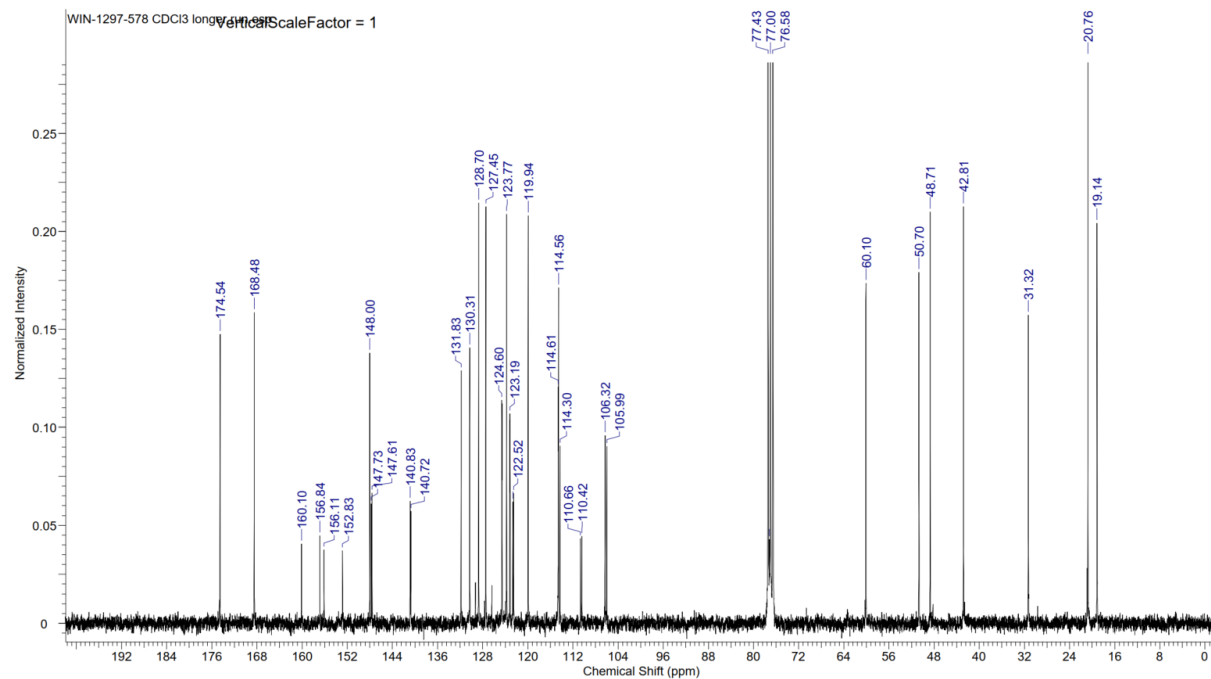
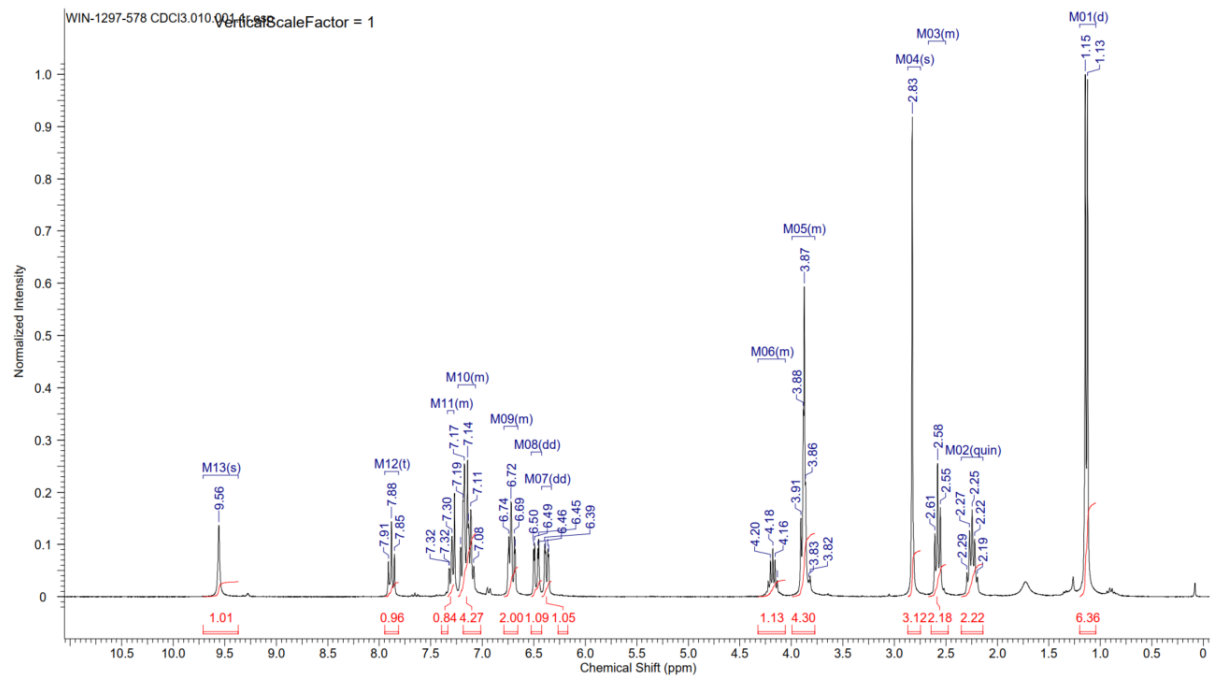
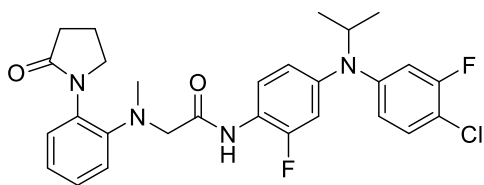
# Compound 56



# Compound 57

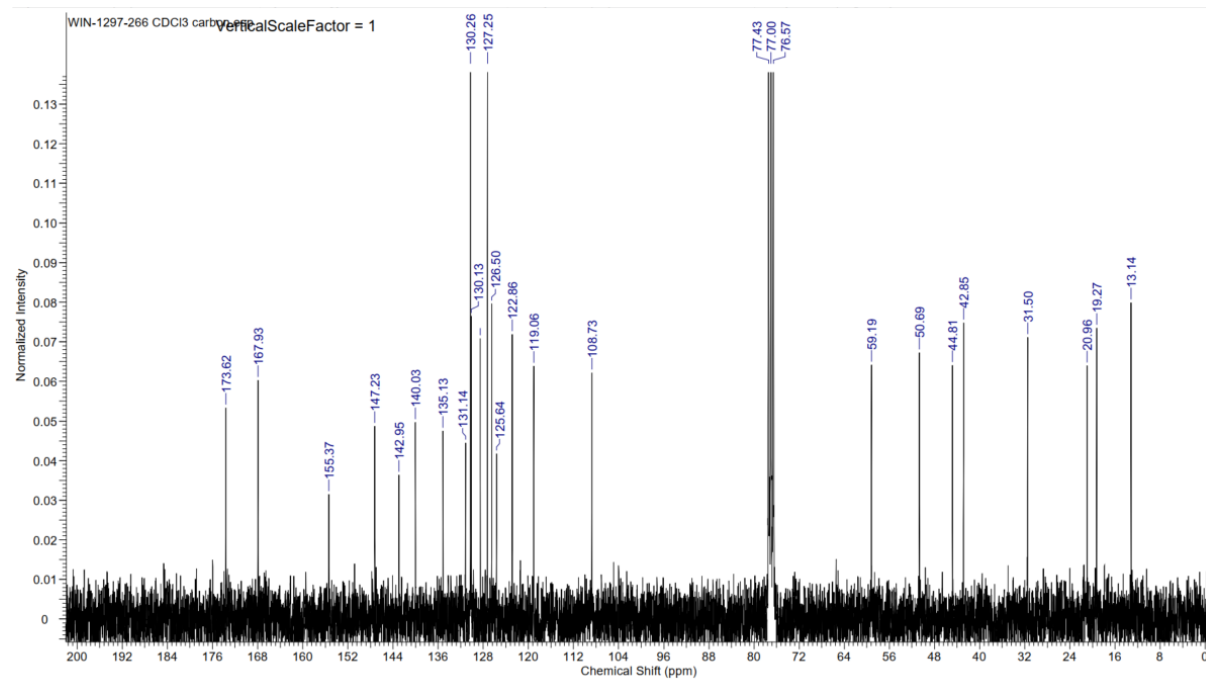
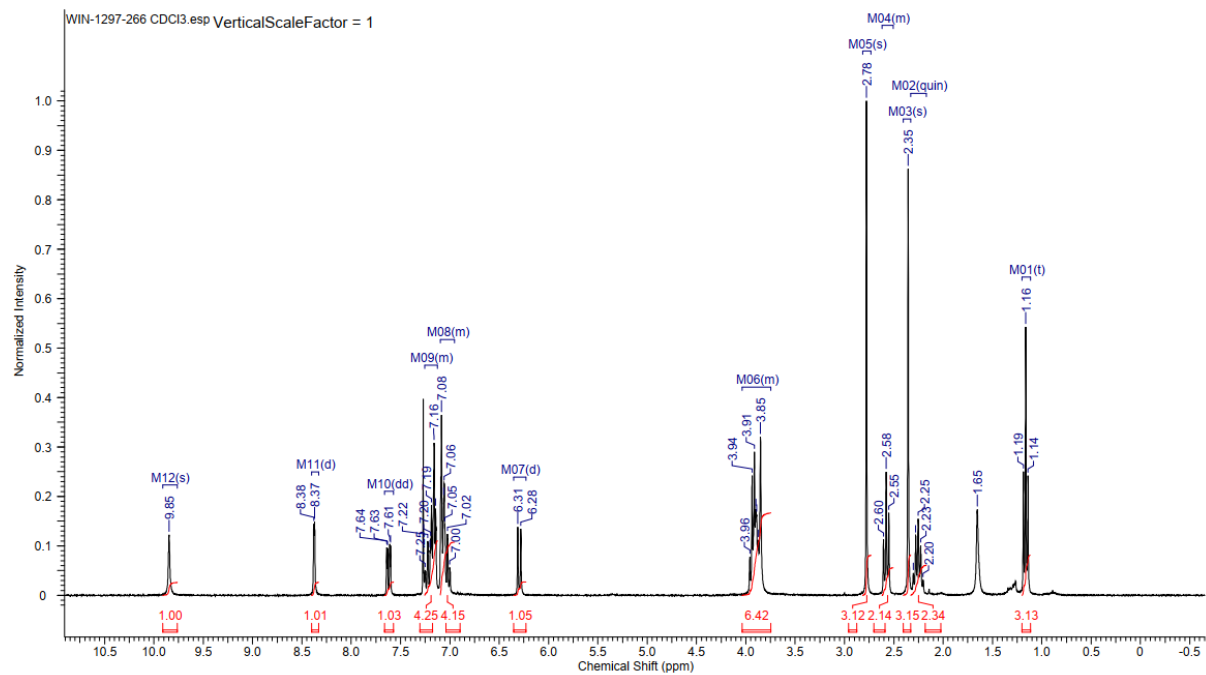
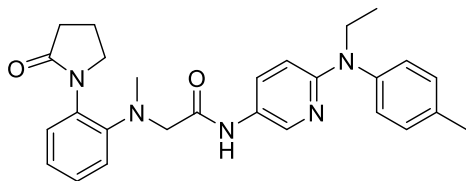


# Compound 58

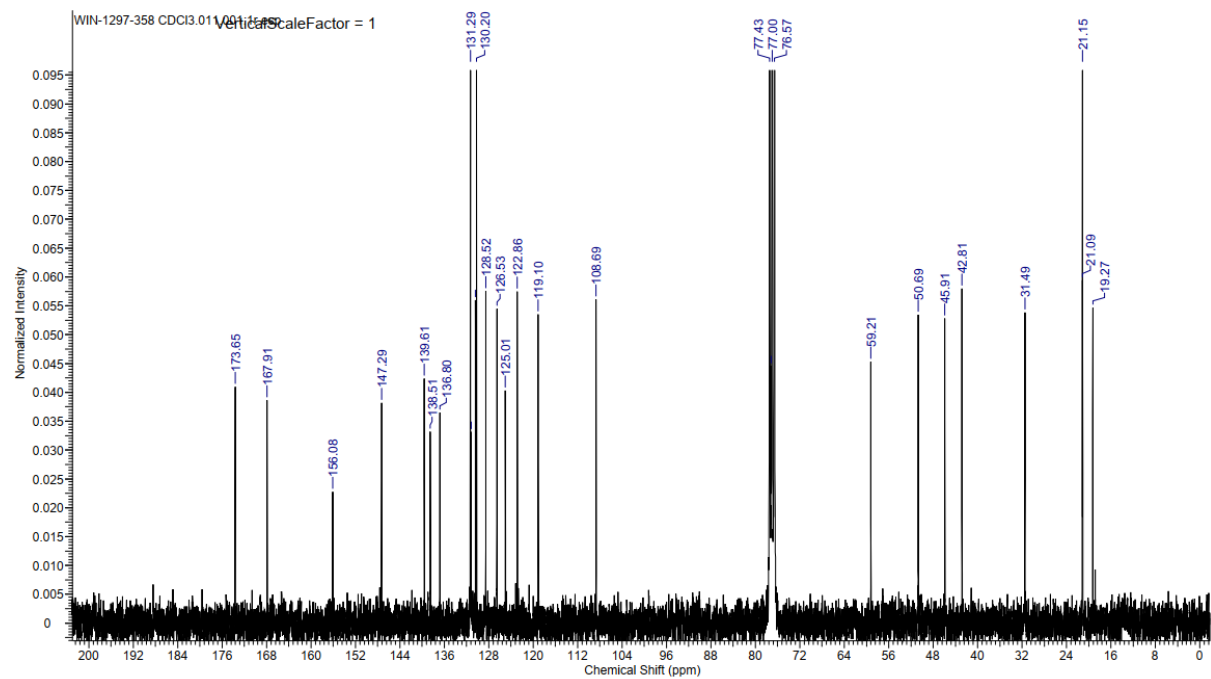
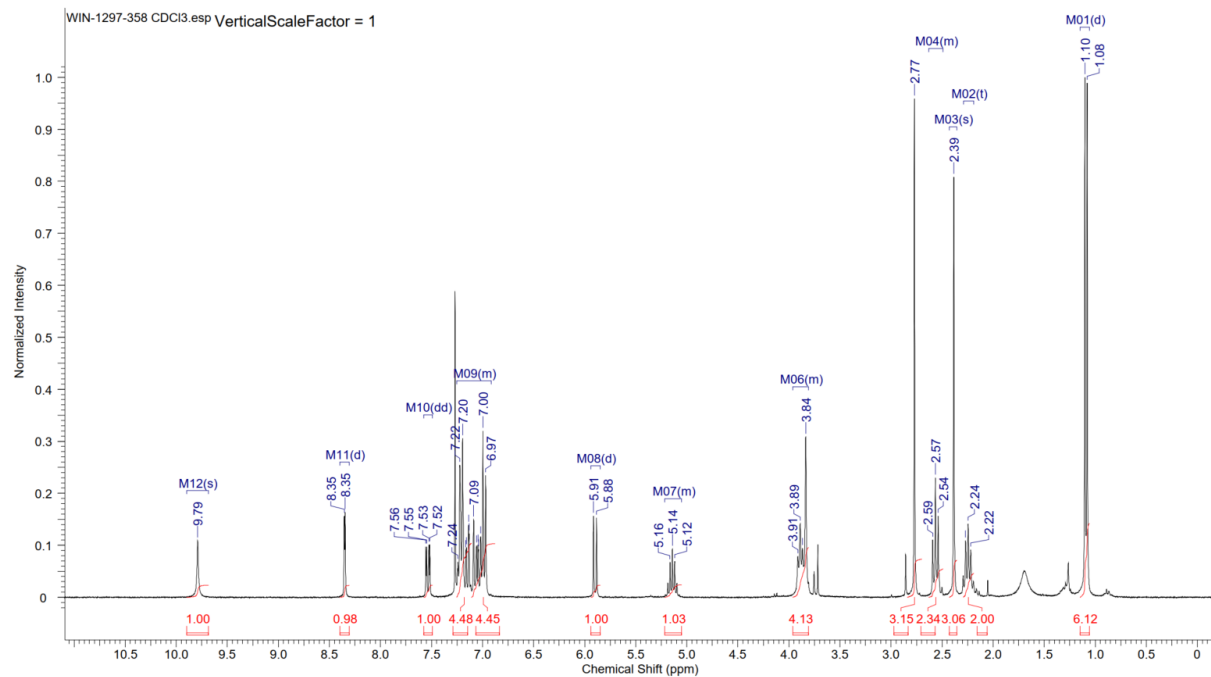
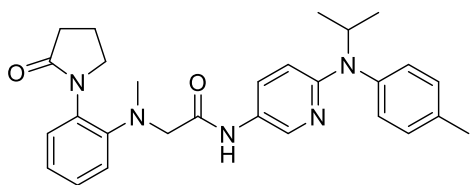




# Compound 60



# Compound 61



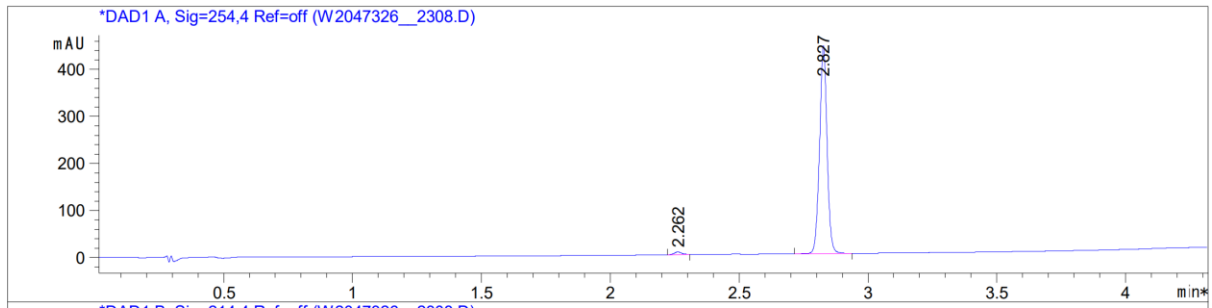




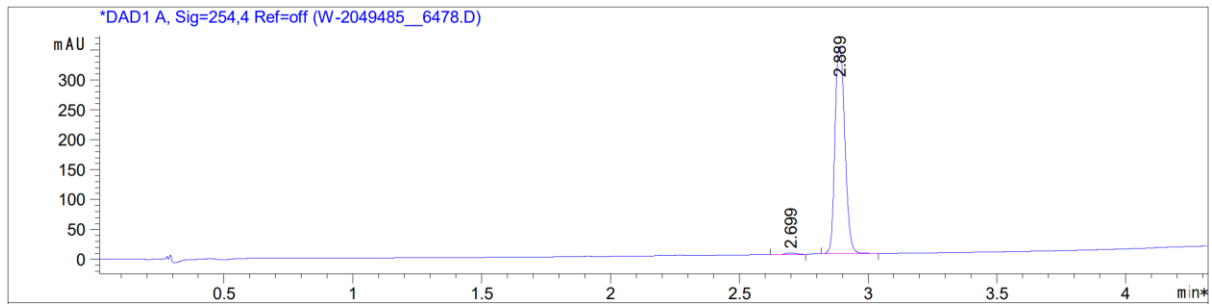


## HPLC trace of lead compounds

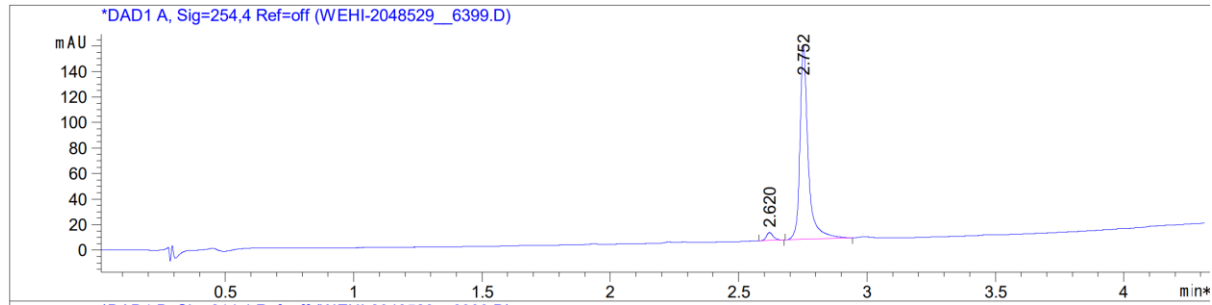
### Compound 77 (WEHI-326)



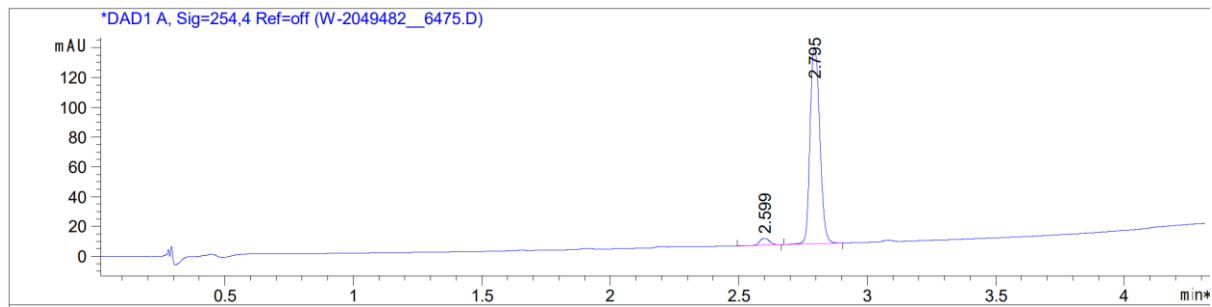
### Compound 56



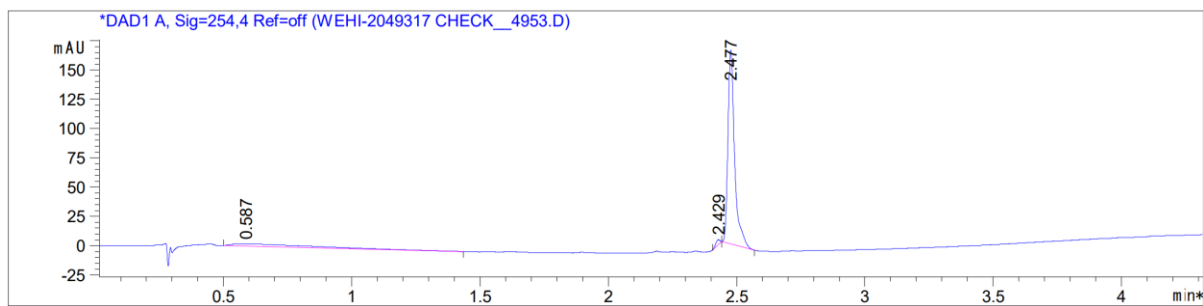
### Compound 57



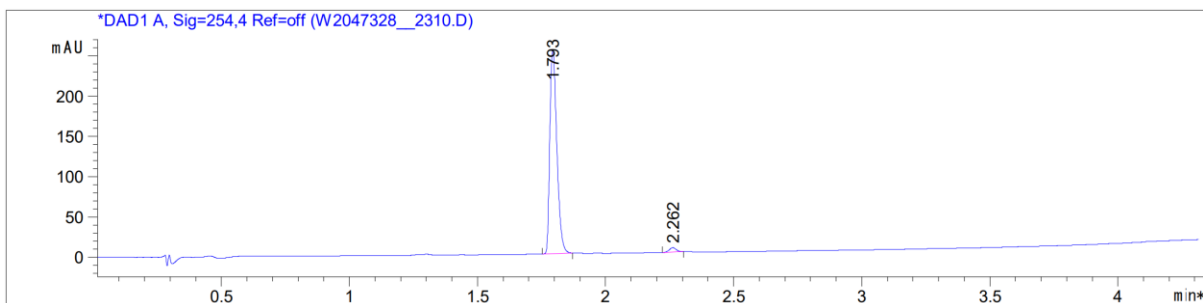
### Compound 58



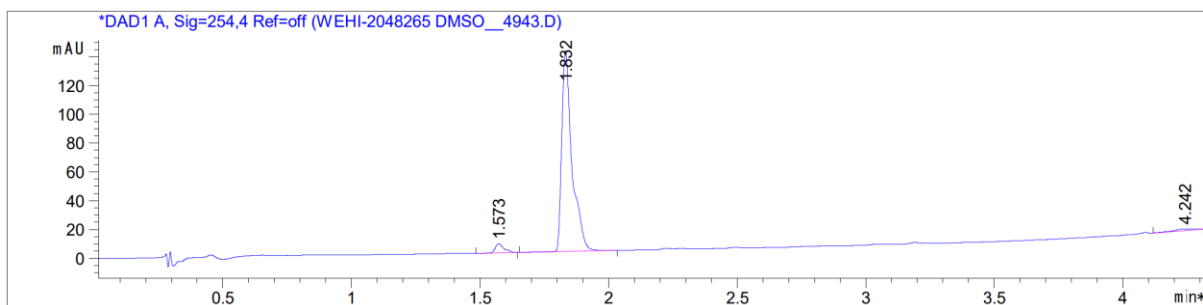
## Compound 59



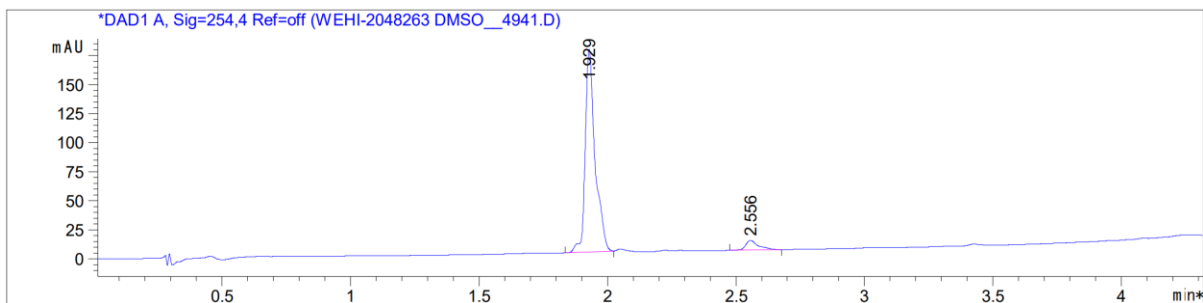
## Compound 60 (WEHI-328)



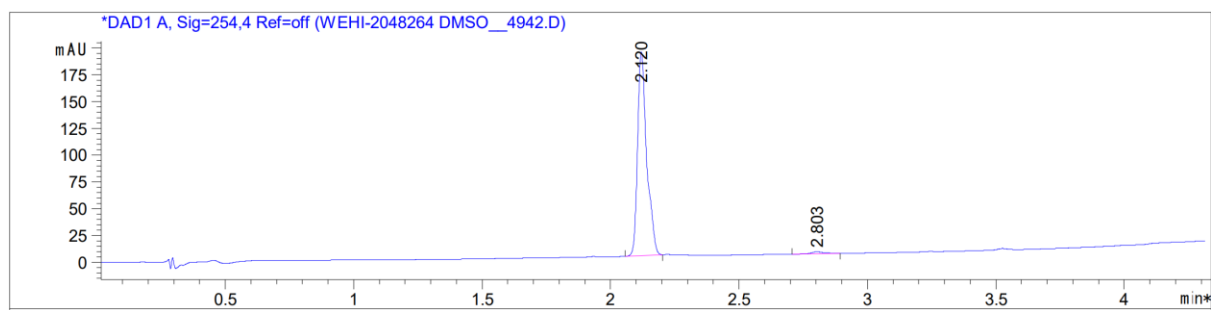
## Compound 61



## Compound 62



## Compound 63 (WEHI-264)



## Compound 64

